JOURNAL OF APPLIED PHYSICS

Physics Lib.

FEB 2 7 1946

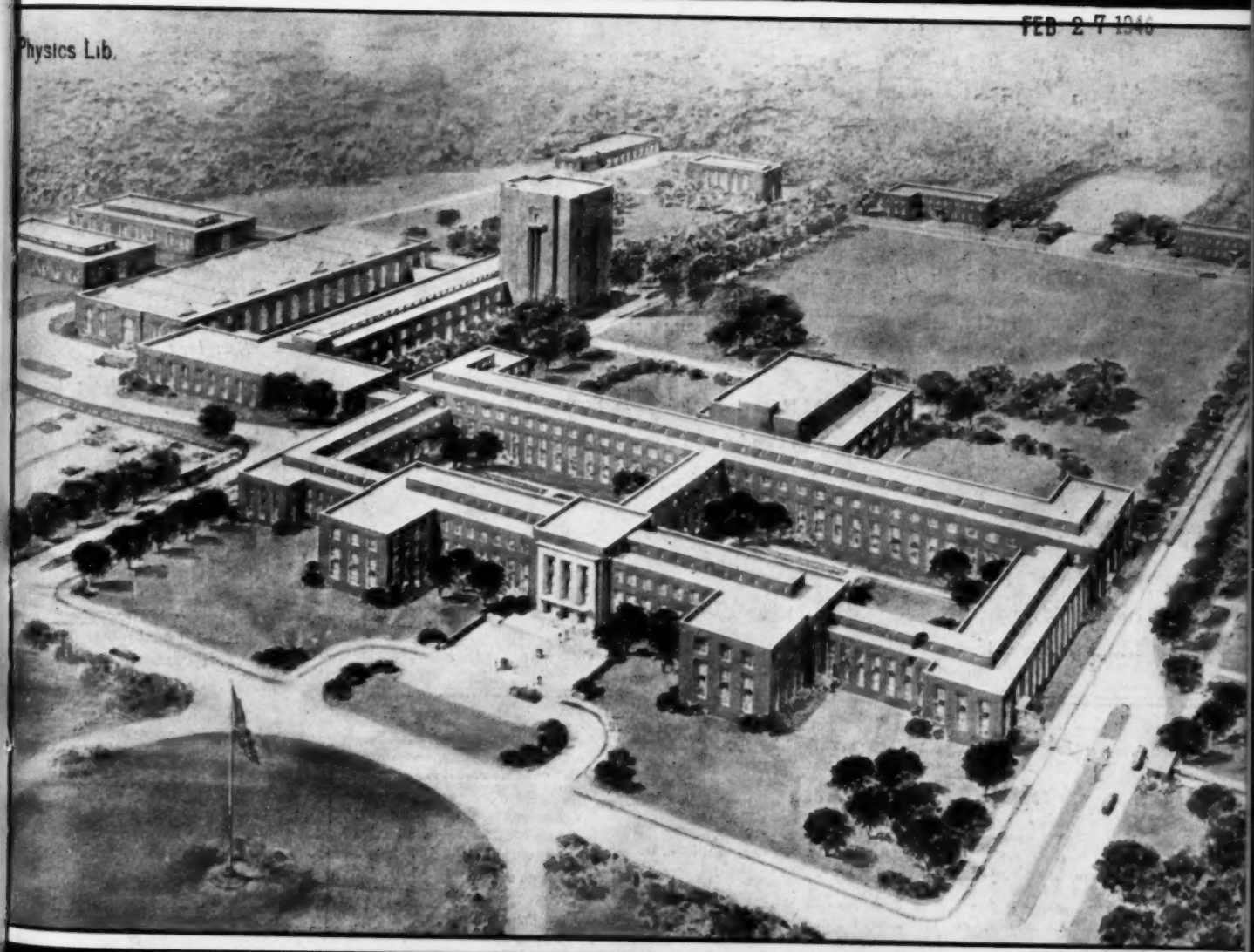

JOURNAL OF APPLIED PHYSICS

Vol. 17, No. 2 FEBRUARY, 1946

In This Issue

Page

Problems in Non-Elastic Deformation of Metals
CLARENCE ZENER AND J. H. HOLLOMON 69

Problems in Fracture of Metals
J. H. HOLLOMON AND C. ZENER 82

Some Integral Equations of Potential Theory H. BATEMAN 91

Federation of Atomic Scientists 108

Contributed Original Research

Calculation of the Output from Non-Linear Mixers
HARRY STOCKMAN 110

Filmless Sample Mounting for the Electron Microscope
JOHN H. L. WATSON 121

Investigation of Secondary Phases in Alloys by Electron Diffraction and the Electron Microscope
R. D. HEIDENREICH, L. STURKEY, AND H. L. WOODS 127

Errata:

On the Representation of Rigid Rotations H. SCHWERDTFEGER 109

On Maximum Gain-Band Width Product in Amplifiers
W. W. HANSEN 109

In Every Issue

Here and There 103

Calendar of Meetings 109

New Booklets 108

Index to Advertisers xxviii

BOARD OF EDITORS
ELMER HUTCHISSON, *Editor*
Associate Editors
R. BOWLING BARNES
OTTO BEECK
W. F. BUSSE
S. H. CALDWELL
CLARK GOODMAN
SELIG HECHT
W. JAMES LYONS
PAUL E. SABINE
FREDERICK SEITZ
J. R. TOWNSEND

Publication of the American Institute of Physics

ADMINISTRATIVE STAFF
HENRY A. BARTON, *Director*
MARGARET S. GRIFFIN *Publications Manager*
THEODORE VORBURGER, *Business Manager*
JOHN T. TATE, *Adviser on Publications*

GOVERNING BOARD
PAUL E. KLOPSTEG, *Chairman*
WALLACE WATERFALL, *Secretary*
GEORGE B. PEGRAM, *Treasurer*
T. D. COPE
R. B. DOW
L. A. DUBRIDGE
FLOYD A. FIRESTONE
HARVEY FLETCHER
R. C. GIBBS
K. S. GIBSON
HERMANN MARK
A. G. WORTHING
JOHN T. TATE
L. W. TAYLOR
N. W. TAYLOR

The JOURNAL OF APPLIED PHYSICS, published monthly at Prince and Lemon Sts., Lancaster, Pa., is devoted to physics in its role as the science basic to other natural sciences and to the arts and industries. Previous to 1937 this publication was known as PHYSICS. The JOURNAL OF APPLIED PHYSICS publishes editorials, news of physicists, and reviews, as well as technical papers of applied physics.

Manuscripts should be submitted to Elmer Hutchisson, Editor, Case School of Applied Science, Cleveland 6, Ohio.

Subscriptions and orders for back numbers should be addressed to Prince and Lemon Streets, Lancaster, Pa. or to the American Institute of Physics, 57 East 55 Street, New York 22, N. Y.

Subscription Price

	U. S. AND CANADA	ELSEWHERE
To members of scientific societies	$5.00	$5.70
To all others	7.00	7.70

Back Number Prices
Complete set: Vol. 1, July, 1931–Vol. 16, 1945—$101.50
Yearly back number rate: $7.70
Single copies: $0.70 each.

Changes of address and proofs should be addressed to the Publications Manager.

Advertising rates supplied on request. Orders, advertising copy, and cuts should be sent to the American Institute of Physics.

Entered as second class matter January 22, 1937, at the Post Office at Lancaster, Pennsylvania, under the Act of March 3, 1879
Accepted for mailing at the special rate of postage provided for in the Act of February 28, 1925, authorized May 2, 1932.

Copyright 1946, by the American Institute of Physics.

Journal
of
Applied Physics

Volume 17, Number 2 February, 1946

Problems in Non-Elastic Deformation of Metals*

BY CLARENCE ZENER** AND J. H. HOLLOMON

Research Division, Watertown Arsenal, Watertown, Massachusetts

In this article an attempt is made to examine the goals of current and of possible future types of research concerned with the non-elastic deformation of metals. It is found that an understanding of non-elastic deformation would be enhanced by research upon the following topics: 1. The anelasticity associated with the viscous behavior of grain boundaries and the at least temporary viscous behavior of slip bands. 2. The mechanics of the initiation and growth of twin bands. 3. The mechanics of the initiation and growth of slip bands, including the drop in resistance to deformation which accompanies the initial slip bands. 4. The mechanics of the segregation of solute atoms in solid solution, such as of carbon and nitrogen in iron. 5. The conditions under which strain hardening is not removed by recovery or by recrystallization, and hence under which a mechanical equation of state exists, i.e., under which a relation exists between strain rate, strain, stress, and temperature. 6. Variation of the heat of activation for plastic strain rate upon stress and upon the microstructure. 7. Anisotropy introduced by deformation.

IN all fields of investigation it is advisable now and then to assess the potentialities of the various paths along which further research may profitably proceed. Such an assessment should be particularly valuable in the fields of plastic deformation and fracture of metals, because of the large number of variables involved in the types of experiments which may be performed and in the types of materials to be investigated. In this and an accompanying report, attempts are made to examine the goals of current and possible future types of research concerned with the non-elastic deformation and fracture of metals.

I. INTRODUCTION

In an idealized metal the stress-strain relation consists of two parts, elastic and plastic. The essential feature of the first part is that of reversibility, i.e., the uniqueness of the relation. This relation is usually, but is not necessarily, regarded as linear. The essential feature of the second part is the presence of a permanent set. Thus in Fig. 1 the path ABB' is traced in loading, $B'A'$ is traced in unloading, while the permanent set AA' remains. The slope of the stress-strain relation in the plastic region is usually, but is not necessarily, positive.

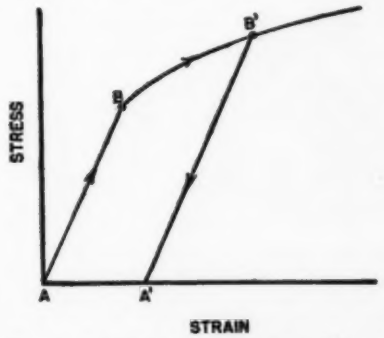

FIG. 1. Idealized stress-strain relation.

* The statements or opinions in this article are those of the authors and do not necessarily express the views of the Ordnance Department.

** Now at the Institute for the Study of Metals, University of Chicago, Chicago, Illinois.

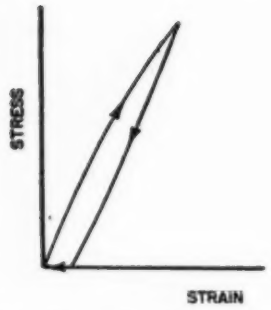

FIG. 2. Typical stress-strain relation of an actual metal in the pre-plastic region.

No real metal possesses an ideally elastic region. Even though a definite yield stress may exist below which no permanent set occurs, the strain is a function of the past history of the stress as well as of its instantaneous value. A stress-strain curve in the pre-plastic region may thus be like that represented in Fig. 2; the recovery takes place gradually after the removal of the load. If the observations cease before the hysteresis loop is essentially complete, the observer will deduce that the metal has acquired a permanent set, and has thus behaved plastically. That property of a solid in virtue of which stress and strain are not uniquely related in the pre-plastic range has been called anelasticity. An appreciation of anelastic phenomena is therefore essential to a complete understanding of plastic deformation.

The plastic part of the stress-strain curve in Fig. 1 is idealized in two respects. Firstly, in the case of alloys the curve as observed is often jagged, consisting of "serrations." Secondly, the curve for a real metal approximates that in Fig. 1 only if certain parameters are maintained constant during the test, such as strain rate and temperature, parameters which under many conditions of strain do not remain constant.

No intrinsic difficulties prevent one from deducing the elastic part of the idealized stress-strain curve under any stress pattern from the simple tensile test, provided Poisson's ratio is also measured. Similarly, one may predict the plastic portion of the idealized stress-strain curve for an arbitrary stress pattern from data obtained in simple tension, upon taking Poisson's ratio equal to $\frac{1}{2}$. Such predictions are not however as successful as in the elastic case.

From the above brief introduction it is clear that the non-elastic behavior of metals cannot be described in simple terms except under very special conditions. In order to understand the multitudinous ways a metal may respond to the application of stress, it will be necessary first to understand the details of deformation on a microscopic scale.

The physical origins of anelasticity have recently been reviewed by one of the authors.[1] The origins are of two general types. The first type is associated with some sort of diffusion induced by applied stresses, e.g., thermal diffusion, atomic diffusion, magnetic flux diffusion. The second type is associated with isolated regions which behave in a viscous manner. Whatever the origin of the anelasticity, Boltzmann[2] has shown how one may predict the behavior of the speci-

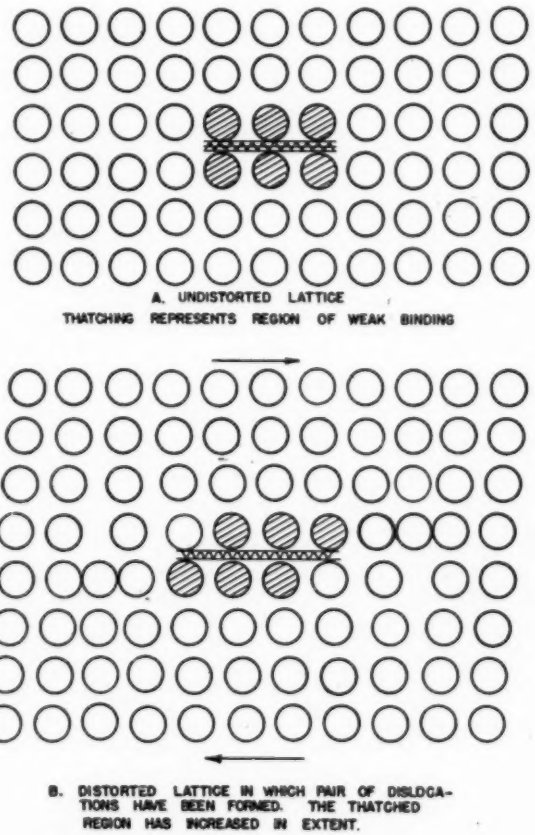
A. UNDISTORTED LATTICE
THATCHING REPRESENTS REGION OF WEAK BINDING
B. DISTORTED LATTICE IN WHICH PAIR OF DISLOCATIONS HAVE BEEN FORMED. THE THATCHED REGION HAS INCREASED IN EXTENT.

FIG. 3. Illustration of initiation of dislocations.

[1] C. Zener, "Anelasticity of metals," Trans. A. I. M. E. (in press).

[2] L. Boltzmann, "Zur Theorie der elastische Nachwirkung," Ann. d. Physik **7**, 624 (1876); also Sitz. Wien Akad. [2] **70**, 275 (1874).

men under any conditions of loading from observations made upon the response when a fixed load is suddenly applied.

A detailed description of one microscopic mechanism for plastic deformation in crystal lattices was first given by Orowan[3] based upon suggestions of Polanyi. According to this description, plastic deformation takes place in two stages. In the first stage lattice distortions of a particular type are produced in the vicinity of a region of low shear resistance. These distortions are known as dislocations. Their mode of generation is illustrated in Fig. 3. In the second stage the dislocations are propagated through the lattice. This propagation is hindered by any type of lattice disturbance, such as other dislocations (which hindrance gives rise to strain hardening), precipitates, grain boundaries, etc.

A second possible mechanism of plastic deformation is by the formation of twins. No satisfactory dynamic theory has yet been advanced as to how such twin formation occurs.

If these four mechanisms, diffusion, viscous flow in isolated regions, dislocations, and twinning, are the only mechanisms for non-elastic behavior of metals, it must be possible to interpret all observed types of non-elastic behavior, and the influence thereon of microstructure, in terms of one or other of these mechanisms.

II. ANELASTICITY

Viscous flow in isolated regions may, on the other hand, cause deviations of more than 100 percent from perfect elasticity. Viscous flow may be expected in regions where the atoms are arranged in an amorphous, or non-crystalline, manner. Thus the atoms on the two sides of grain boundaries cannot be aligned with one another, and so such boundaries might be expected to behave in a viscous manner. The profound effects of viscous slip upon the stress-strain relation may be seen from Fig. 4. This figure has been constructed from the recent work[4] of W. A. West of this laboratory. One practical problem of great importance in which viscous slip at grain boundaries may play a dominant

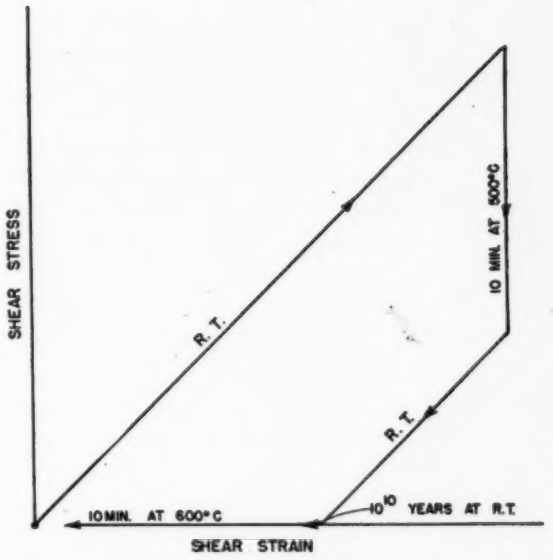

FIG. 4. Anelastic behavior of an iron wire due to viscous flow at grain boundaries, after experiments of West (reference 4).

role is stress relaxation at elevated temperatures. Thus in the example of Fig. 4, 60 percent of the stress was relaxed by a recoverable anelastic deformation associated with grain boundary slip, not more than 6 percent by plastic deformation. Another problem of even greater practical importance in which viscous slip at grain boundaries may play a dominant role is creep at elevated temperatures when close tolerances must be maintained. Thus with the iron specimen from which the data of Fig. 4 were taken, ten minutes at 500°C would more than double the strain under conditions of constant stress. At least 95 percent of this additional strain would be of the recoverable anelastic type associated with grain boundary slip.

Rosenhain[5] recognized the importance of viscous grain boundary slip in the 1910's, and performed many experiments demonstrating the existence of such slip. In spite of the above-mentioned practical importance of this phenomenon, no experiments have been performed during the intervening 30 years to measure in any metal the relation between rate of slip across the grain boundary and the stress which causes such slip. This complete absence of experimental data is

[3] E. Orowan, "Zur Kristallplastizität," Zeits. f. Physik **89**, 605, 614, 634 (1934).

[4] W. A. West, "Elastic after-effects in iron wires from 20°C to 550°C," communicated to A. I. M. E.

[5] W. Rosenhain and D. Ewen, "Intercrystalline cohesion in metals," J. Inst. Metals [2], **8**, 149 (1912); also *Introduction to Physical Metallurgy* (Constable and Company, London, 1915), pp. 255–264.

due to the fact that nearly all physical testing of metals, especially in this country, has been, and is still being, done with an entire disregard of the microstructure of the metal. This procedure is a reflection of the lack of faith in the ability of physical science to predict the gross mechanical behavior of metals in terms of the mechanical behavior of the individual constituents, a faith to which the present authors adhere.

Until an atomistic interpretation of all nonelastic effects is forthcoming, it will be useful to have certain phenomenological concepts regarding the mechanical behavior of microscopic elements larger than atomic dimensions. Such a concept is, for example, that of viscous grain boundaries. Another concept which may prove of value is that of viscous slip bands, a concept which may be studied by anelastic measurements.

It was recognized as early as 1900 that plastic deformation was confined to slip bands,[6] that such deformation introduced anelastic phenomena, such as mechanical hysteresis, and that this anelasticity was removed[7] by annealing at temperatures as low as 100°C. Rosenhain[8] pointed out in 1905 that these effects of plastic deformation indicated that the material in freshly formed slip bands behaved as if it were disorganized, i.e., in a viscous manner, and that upon aging this material gradually assumed the order of the surrounding matrix. During the intervening 40 years no experiments have been performed for the purpose of further elucidating the mechanical behavior of freshly formed slip bands. Many observations have been made upon special aspects of the anelasticity introduced by plastic deformation. These have been reviewed in reference 1. It is not to be expected, however, that such observations can contribute to an understanding of the mechanics of deformation until they are interpreted in terms of the mechanical properties of the constituent slip bands.

[6] J. A. Ewing and W. Rosenhain, "Experiments in micrometallurgy—effects of strain," Phil. Trans. Roy. Soc. **193**, A353 (1900).
[7] J. Muir, "Recovery of iron from overstrain," Phil. Trans. Roy. Soc. **193**, A1 (1900).
[8] W. Rosenhain, "Deformation and fracture in iron and steel," J. Iron and Steel [2] **70**, 189 (1906).

III. MECHANISM OF PLASTIC DEFORMATION

Plastic deformation in metals, that is, permanent deformation, may occur by two distinct mechanisms: deformation by twinning and deformation by slip. In any particular case deformation may proceed by any combination of these two types.

Two adjacent parts of a crystal separated by a plane are said to be twins when their crystallographic axes are different but are so related that each part is the mirror image of the other part with respect to their common plane. The crystallographic relations between known twins are given by Schmid and Boas[9] and by Barrett.[10] Twinning is deformation through the formation of twins. The final configuration may be thought of as having been attained by a homogeneous simple shear parallel to the common plane. Twinning is not associated with any lattice distortion.

Deformation by slip is said to occur whenever strain is confined to narrow bands which are not twins of the adjacent region. The orientation of the slip bands, as well as the direction of slip, are observed to have certain crystallographic relations with the parent lattice. These relations are given by Schmid and Boas[11] and by Barrett.[12] The material within the slip band has in general the same orientation as the parent lattice, but suffers considerable fluctuation from region to region.

Temperature and rate of strain are the primary factors which determine in what manner a crystalline material will deform. As the temperature increases, or the rate of deformation decreases, the resistance to deformation by slip decreases rapidly, resistance to deformation by twinning decreases less rapidly, if indeed it decreases at all. Stress gradient is another factor which has some influence in determining the manner in which deformation will occur. A macroscopic deformation may be thought of as the superposition of many small deformations, the smallest possible deformation being called an

[9] E. Schmid and W. Boas, *Kristallplastizität* (Verlagsbuchhandlung Julius Springer, Berlin, 1935), p. 100.
[10] C. S. Barrett, *Structure of Metals* (McGraw-Hill Book Company, Inc., New York, 1943), p. 312.
[11] Reference 10, p. 90.
[12] Reference 10, p. 289.

elementary deformation. Each elementary deformation is essentially confined to a limited region. To a first approximation only the average of the stress throughout the region is important in determining whether an elementary deformation will occur. In deformation by twinning and by slip the lateral dimensions of the region are comparable to the crystal size. Whether stress localization favors slip over twinning, or *vice versa*, is not at present known. Composition is another factor which has some influence over the type of deformation which occurs. Thus the addition of silicon to iron raises the resistance to deformation by slip relative to the resistance to deformation by twinning.[13] Whether this effect of silicon is common to all solid solutions is not known at present, nor is the relative effect of insoluble precipitates known.

A. Twinning

As was probably first observed by Chalmers[14] in his experiments upon tin, deformation by twinning is a discontinuous process on a macroscopic scale, in other words, the region of an elementary deformation is of macroscopic dimensions. It would be antipicated that under conditions of a uniform stress a critical shear stress would exist for the initiation of a twin. Actually, however, the conditions for the initiation of a twin appear to be so structure sensitive that in no case has a reproducible resolved critical shear stress for twin formation been obtained in work upon single crystals. Unlike deformation by slip, deformation by twinning may start in a local region of high stress concentration and propagate for a long distance through regions which were under no stress prior to deformation. (See Fig. 47 of Schmid and Boas.) One might suspect that this ability of twins to be set off by local stress concentrations would render the critical resolved shearing stress for twin initiation sensitive to surface irregularities. This possible effect of surface irregularities has not been investigated.

Once a twin band has been formed, the band may grow continuously by the propagation of the twin interfaces. Thus the twin bands of recrystallized alpha-brass grow broader as the grains grow. No studies have been made upon the dependence of the velocity of these interfaces with the various parameters, such as with stress and temperature.

Phase transformations by lattice shear have many features in common with twinning. Examples are the formation of martensite in steel and of martensite-like structures in beta-brass. Any progress in understanding the mechanics of one phenomenon will aid in the understanding of the other.

B. Slipping

As a first approximation, deformation by slip may be regarded merely as the slipping of one set of planes upon another. This picture is sufficiently accurate to predict the planes and directions of slip. If one plane be regarded as uniformly slipping over another plane, the potential energy of the system will undergo a periodic fluctuation. The amplitude of the fluctuation will be least for planes of closest packing, both because the atoms are closest together in these planes and because these planes are the furthest apart. Similarly, the fluctuation will be least along those directions in which the atoms are most closely packed. Thus the picture of simple slip interprets satisfactorily the observation that the planes of easiest slip are the planes of closest packing, and that the direction of slip is the direction along which the atoms are closest.

The concept of a homogeneous slip of one plane of atoms over another cannot however be correct. Such slip would require for an unalloyed crystal a shearing stress several orders of magnitude larger than is actually observed. Polanyi[15] was apparently the first to realize how this difficulty could be resolved through the introduction of a certain type of lattice distortion, known in English as "dislocations." These dislocations will move through the lattice, and thereby result in a net macroscopic strain, under a considerably smaller stress than would be necessary to cause two planes to slip over one another in a homogeneous manner. The full effectiveness of dis-

[13] C. S. Barrett, C. Ansel and R. F. Mehl, "Slip, twinning and cleavage in iron and silicon ferrite," Trans. Am. Soc. Metals **25**, 702 (1937).

[14] B. Chalmers, "Twinning of single crystals of tin," Proc. Phys. Soc. (London) **47**, 733 (1935).

[15] M. Polanyi, "Über eine Arte Gitterstorung, die einen Kristall plastisch machen konnte," Zeits. f. Physik **89**, 660 (1934).

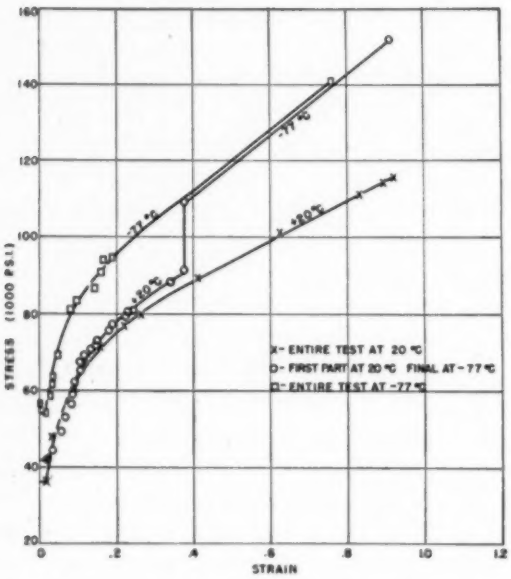

FIG. 5. Example of validity of mechanical equation of state for a plain carbon steel at low temperatures. (Tensile tests.)

locations in reducing the resistance to slip can be appreciated only by a consideration of the thermal energy of the lattice. The fluctuations in the thermal energy will, given time, give rise to a unit slip when the stress by itself is not sufficient to cause slip. Such fluctuations in thermal energy would not aid one plane of atoms to slip homogeneously over another plane, for the probability of a large enough fluctuation would be too small. Thus suppose E is the directed kinetic energy which the system must have in order to aid the stress in producing a unit slip. The probability that at any given time the system possesses directed kinetic energy equal or greater than this amount varies as $\exp(-E/kT)$. The thermal fluctuations can therefore be of significance only when E is not many orders of magnitude greater than kT, therefore only when a unit slip occurs in a comparatively small volume, as in the case of dislocations.

If the only effect of temperature upon plastic deformation is through the introduction of energy fluctuations, it must follow that at a constant stress the strain rate will be higher the higher the temperature, or, conversely, the stress necessary to produce a given strain rate will be lower the higher the temperature. At sufficiently high temperatures additional effects occur, such as grain growth, spheroidization of precipitates, etc., and, if the prior deformation is sufficiently large, recovery with or without recrystallization. At lower temperatures when such additional effects do not occur it might be expected, as was pointed out by Ludwik,[16] that a mechanical equation of state exists which relates stress s, strain ϵ, strain rate $\dot{\epsilon}$, and temperature T. Such an equation may be written symbolically as

$$S = S(\epsilon, \dot{\epsilon}, T), \tag{1}$$

or as

$$\dot{\epsilon} = \dot{\epsilon}(\epsilon, S, T). \tag{2}$$

The existence of a mechanical equation of state would imply that the stress necessary to produce a given strain rate at a given temperature depends only upon the strain and not upon the temperature or strain rate at which the prior strain occurred. According to Taylor's concept,[17] a discontinuous change in temperature would not produce a discontinuous change in stress, only a discontinuous change in rate of increase of stress with strain. In order to determine whether a mechanical equation of state exists, experiments have been performed in this laboratory in which the temperature was suddenly changed during the determination of a stress-strain curve. The results, presented as Fig. 5, show that the stress is independent of the temperature at which prior deformation occurred, and therefore indicate that a mechanical equation of state does in fact exist (at least at low temperature), and therefore that, at the temperature of the test, the only influence of temperature is through the introduction of fluctuations in thermal energy.

Both deformation by twinning and by slip are processes characteristic of crystals. Hence any kind of disturbance of the crystalline structure would be expected to raise the resistance to deformation by twinning and by slip. This is indeed the case. Such disturbance may be due to prior plastic deformation, to grain boundaries, to soluble impurities, to insoluble impurities, etc. The increase in resistance to plastic deformation by prior deformation has been investigated theoretically by Taylor[17] using the concept of

[16] P. Ludwik, *Elemente der technologischen Mechanik* (Verlagsbuchhandlung Julius Springer, Berlin, 1909).
[17] G. I. Taylor, "Mechanism of plastic deformation of crystals, Part One," Proc. Roy. Soc. **145A**, 362 (1934).

dislocations. Although Taylor's theory must be regarded as a milestone on the road leading to understanding strain hardening, it was based upon assumptions too naive to allow it to pass the test every physical theory should meet, the prediction of new phenomena. No more recent analysis has eliminated the undesirable assumptions, e.g., the assumptions of inpenetrable barriers and of parallel dislocations of indefinite length. The increase in resistance to plastic deformation caused by grain boundaries has likewise been investigated theoretically by Taylor.[18] While his analysis reproduces precisely the difference between the stress-strain curves of aluminum single crystals and of aluminum polycrystalline specimens, it does not provide an explanation of the frequently observed variation[19,20] of resistance to deformation with grain size in polycrystalline material. Taylor assumed in essence that the effect of the restraints imposed by adjacent grains extended uniformly through the grains, while the above-mentioned observations indicate that the effect of the restraints is confined more or less to the vicinity of the grain boundaries. No modifications have as yet been made of Taylor's theory to take account of the localization of the effects of the restraints. A correlation has been found by Gensamer[21] of the increase in resistance to plastic deformation introduced by solute atoms and the difference in size of the solute and solvent atoms. A correlation has been found by Gensamer and his collaborators[22] of the increase in resistance to plastic deformation introduced by insoluble precipitates and the mean free path between these precipitates. As yet no satisfactory theory has interpreted these two types of correlations.

Although, on the whole, deformation raises the resistance with respect to further deformation, the same cannot be said of each element of deformation. A slight deformation may in fact momentarily lower the resistance with respect to further deformation. Thus a lower stress is required to propagate a slip band than to initiate it. Further, in many cases a lower stress is required to initiate a slip band adjacent to one already formed than to initiate the original band. This momentary lowering of resistance to further deformation by a small deformation gives rise to a diversity of phenomena. Thus when a constant stress is applied to the specimen, elongation may occur in a step-wise fashion. On the other hand, when the over-all strain rate is maintained constant, the stress may undergo a series of discontinuous jumps. Whether each jump is associated with a single slip line, or with a series as in the case of Duralumin, depends to a great extent upon the elasticity of the system. Thus the elastic strain in the specimen and test machine may be only sufficient to produce a single slip band, or it may be sufficient to produce a whole series of slip bands. In spite of a large number of experiments in which discontinuous yielding has been observed and studied,* no satisfactory theory has been presented which accounts for the momentary drop in resistance upon yielding, and the attendant phenomena. The ideas advanced by Orowan[3] concerning the origin of dislocations may form the basis for such a theory. According to these ideas, the dislocations originate in some weak region of the lattice, represented by the thatched area in Fig. 3. As may be seen in illustration *b* of this figure,

[18] G. I. Taylor, "Plastic strain in metals," J. Inst. Metals **62**, 307 (1938).

[19] C. A. Edwards and L. B. Pfeil, "Tensile properties of single iron crystals and the influence of crystal size upon the tensile properties of iron," J. Iron and Steel Inst. **112**, 79 (1925).

[20] W. A. Wood, "X-ray studies of grain size in steels of different hardness values," Phil. Mag. **10**, 1073 (1930).

[21] M. Gensamer and C. E. Lacy, Trans. A. S. M. E. **32**, 88 (1944).

[22] M. Gensamer, E. B. Pearsall, W. S. Pellini, and J. R. Low, "Tensile properties of pearlite, bainite and spheroidite," Trans. Am. Soc. Metals **30**, 983 (1942).

* *Drop in Load on Yielding in Mild Steel:* J. H. Wicksteed, Proc. Inst. Mech. Eng., p. 26 (1886). *Serrations in Mild Steel:* A. Le Chatelier, Revue de Metallurgie **6**, 914 (1909). *Discontinuous Yielding in Copper:* Andrade, Proc. Roy. Soc. **84**, 1 (1916). *Serrations in Duralumin:* A. Portevin and F. Le Chatelier, Trans. A. S. Steel Treat. **5**, 457 (1924); R. Anderson, Proc. A. S. T. M. [2] **26**, 349 (1926); N. Dawidenkow, Zeits. f. Physik **61**, 46 (1930). *Discontinuous Yielding in Alpha Brass:* G. Sachs and H. Shoji, Zeits. f. Physik **45**, 776 (1921); W. Köster, Zeits. f. Metallkunde **19**, 309 (1927); M. Classen-Nekludowa, J. d. Russ. Phys. Ges. **60** (1928). *Discontinuous Yielding in Rock Salt:* M. Classen-Nekludowa, J. d. Russ. Phys. Ges. **59** (1927); Obreimow and Schubnikoff, Zeits. f. Physik **41**, 907 (1927); A. Joffè, *The Physics of Crystals* (McGraw-Hill Book Company, Inc., New York, 1928); M. Classen-Nekludowa, Zeits. f. Physik **55**, 555 (1929); N. Dawidenkow, *ibid.* **61**, 46 (1930). *Discontinuus Yielding in Zinc and Cadmium Crystals:* E. Schmid and Valouch, Zeits. f. Physik **75**, 513 (1932); R. Becker and E. Orowan, *ibid.* **79**, 566 (1932); E. Orowan, *ibid.* **89**, 605 (1934).

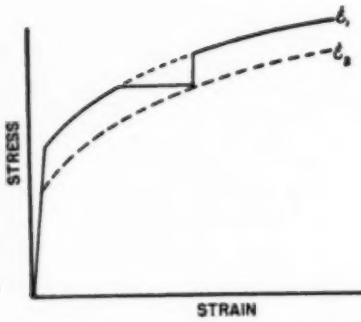

FIG. 6. Example of stress-strain relation when stress is temporarily maintained constant.

after one pair of dislocations has been formed and has propagated away from its origin, the weak region has become extended. A smaller stress will now be required to form a new pair of dislocations. The formation of dislocations thus becomes a cataclysmic phenomenon.

Discontinuous yielding is especially marked in mild steel and in dural. In each case the phenomenon may be related to a state of supersaturation, in iron with carbon and/or nitrogen, in aluminum with copper or zinc. Thus the discontinuous phenomenon disappears when all the carbon and nitrogen are removed from the iron, and becomes much less marked in aluminum after aging. It looks as if in these cases the phenomenon is associated with the presence of flake-like regions in which the solute atoms have either become especially highly concentrated, or have precipitated. Such flake-like regions appear commonly to precede visible precipitation, and presumably arise from the circumstance that such a distribution decreases the strain energy of the system.[23] These flakes will act as restraints with respect to the passage of dislocations. Once a dislocation has crossed a flake, thereby separating it into two halves, the flake offers no further resistance to dislocations along the same plane. Many problems relating to this phenomenon remain to be solved. For example, the phenomenon does not occur in single crystals of iron, but it does in single crystals of aluminum alloys. Again, the theory of the formation of concentration flakes has not yet been developed.

[23] N. F. Mott and F. R. N. Nabarro, Proc. Phys. Soc. (London) **52**, 86 (1940).

IV. GROSS FEATURES OF PLASTIC DEFORMATION

A. Mechanical Equation of State

The assumption of a mechanical equation of state leads to many interesting qualitative predictions. As an example, suppose a specimen is strained isothermally at a constant rate until a strain ϵ_0 is reached; the stress is then maintained constant for a long interval of time, and straining is then resumed at the initial rate. A plot of the observed stress-strain curve obtained under such conditions is given in Fig. 6. While the stress is maintained constant the strain is increasing at a rate given by Eq. (2), and hence the stress necessary to resume straining at the original rate is also increasing in accordance with Eq. (1). Stress-strain curves of this type have in fact been observed by Hanson and Wheeler.[24] As a second example, we shall consider that the load rather than the stress is maintained constant, an example which has been discussed in detail by Ludwik. As may be seen from Fig. 7, the sudden application of a load will give rise to an initially large strain rate, a strain rate which gradually decreases, reaches a minimum at a strain E_0, and thereafter increases. The diagram of strain *vs.* time will therefore look as depicted in Fig. 7, the inflection in the curve corresponding to the initiation of necking.

The strain *vs.* time relation depicted in Fig. 7 is precisely of the type encountered in creep tests. In spite of the fact that Ludwik's work was published over 40 years ago, the universal interpretation of the constant creep rate portion of the creep curves is that it represents a balance between the rate of strain-hardening and of softening by recovery or by recrystallization. A decision as to which interpretation of creep curves is correct could be reached by experiments in which the temperature was varied during the test, e.g., by straining 1 percent at room temperature, heating to the temperature at which creep tests are made, cooling back to room temperature, and finally determining if the hardening introduced by the initial small strain has been reduced. It is to be particularly em-

[24] D. Hanson and M. A. Wheeler, "Deformation of metals under prolonged loading. Part I. Flow and fracture of aluminum," J. Inst. Metals **45**, 1 (1931).

phasized that the determination of a stress function $S_T(\epsilon, \dot{\epsilon})$ at a series of temperatures by experiments performed at constant strain rates, as discussed by Nadai,[25] does not establish the existence of a mechanical equation of state. In order that such a function represent a mechanical equation of state it is necessary for the additional observation to be made that the stress required for further deformation is not lowered with time as the strain is maintained constant.

Two approaches have been followed in an attempt to establish the form of the mechanical equation of state for metals. Since neither approach has been entirely successful, it will be of profit to examine them in some detail in order to discern along what path further research may be successful.

The first approach was indicated by Becker[26] in 1926, and was further elucidated by Orowan[3] in 1936. Here attention is focused upon the shearing stress which an elementary region must possess in order that it undergo plastic deformation. Suppose S_0 is the net shearing stress necessary for deformation, and S is the macroscopic shearing stress. Then thermal fluctuations must provide the additional stress (S_0-S). If V is the minimum volume in which the stress S_0 must exist in order that deformation occur, then the strain rate will be given by

$$\dot{\epsilon}=f_0 \exp\left[-V(S_0-S)^2/2GkT\right]. \qquad (3)$$

The second factor is the probability that a given region will at any time have a thermal shear stress of magnitude greater than S_0-S. The first factor f_0 may be thought of as being composed of the following factors

$$f_0=n\epsilon_0/\tau, \qquad (4)$$

where n is the number of effective regions of volume V per unit volume, ϵ_0 is the mean strain induced by a unit plastic deformation in one region per unit volume, and τ is the mean time an elementary region must possess the shearing stress S_0 before a shear deformation occurs therein. In his discussion of Becker's mechanical equation of state, Orowan has pointed out that

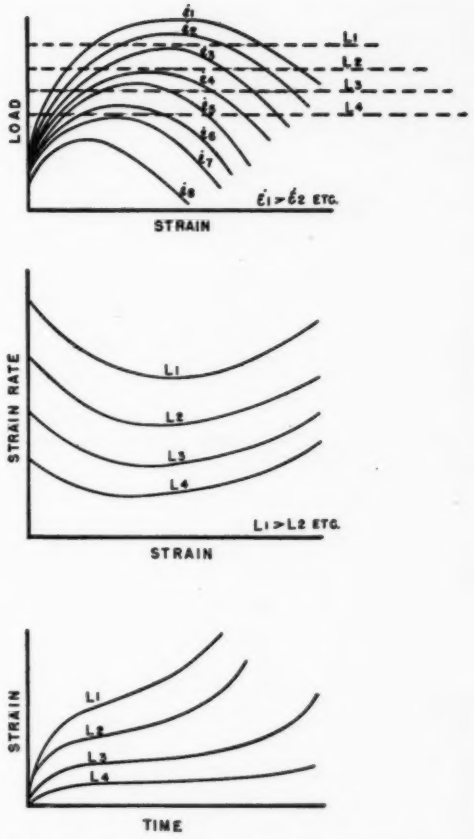

FIG. 7. Derivation of strain-time curves according to concept of mechanical equation of state.

S_0 is of the same order of magnitude as the macroscopic shear stress needed to induce deformation at room temperature. From this observation Orowan concluded that deformation was confined, at any one instant, to locales of high stress concentration.

The second approach was initiated by Condon[27] in 1938, and expanded by Kauzmann[28] and by Dushman[29] and collaborators. Here attention is focused upon the activation energy necessary for an elementary slip process. If Q_0 is the activation energy in the absence of an externally applied stress, when a stress S is applied, the activation energy is assumed to be lowered by an amount proportional to S, thus

$$Q(S)=Q_0-VS.$$

[25] A. Nadai, *Plasticity* (McGraw-Hill Book Company, Inc., New York, 1931), Chap. 39.
[26] R. Becker, "Über Plastizität, Verfestigung und Rekrystallisation," Zeits. f. tech. Physik **7**, 547 (1926).
[27] E. U. Condon, Trans. A. I. M. E. **131**, 410 (1938).
[28] W. Kauzmann, "Flow of metals from the standpoint of the chemical-rate theory," Trans. A. I. M. E. **143**, 57 (1941).
[29] S. Dushman, L. W. Dunbar, and H. Huthsteiner, "Creep of metals," J. App. Phys. **15**, 108 (1944).

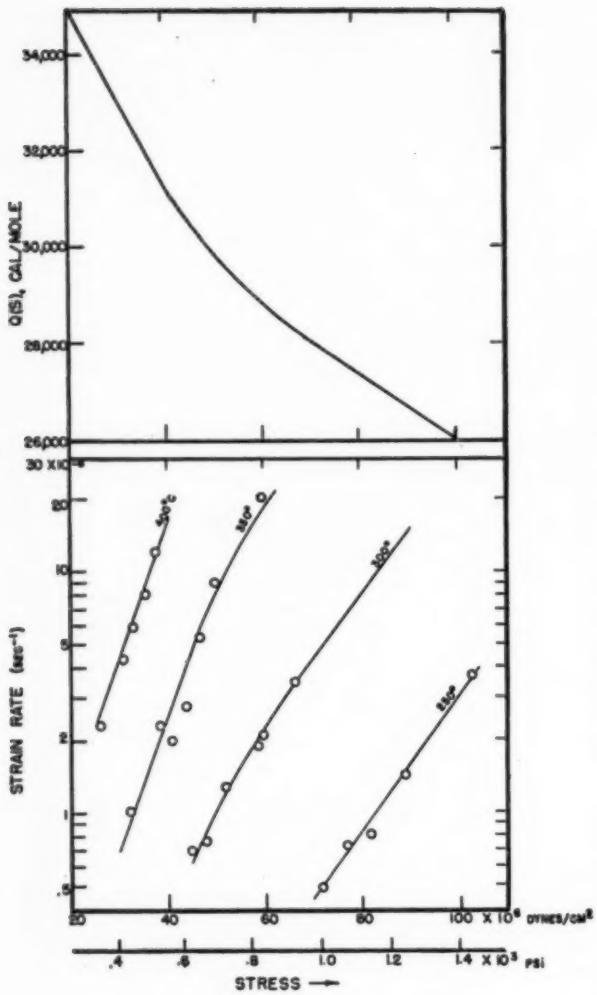

FIG. 8. Application of mechanical equation of state to pure aluminum $f_0=2.2\times10^6$. (Data after Dushman *et al.* (reference 28).)

The corresponding mechanical equation of state is therefore

$$\dot{\epsilon}=f_0 \exp\left[-(Q_0-VS)/kT\right], \qquad (5)$$

where the two factors have the same interpretation as in Becker's equation.

Equations (3) and (5) are equivalent only when $S\ll S_0$, i.e., only when the stress necessary to produce deformation is much less than that necessary to produce deformation at the absolute zero temperature. Orowan has pointed out that S and S_0 are of the same order of magnitude, therefore the two equations cannot be regarded as equivalent. A closer analysis into the details of an elementary slip process shows that both equations can only be approximations of the more general equation

$$\dot{\epsilon}=f_0 \exp\left[-Q(S)/RT\right]. \qquad (6)$$

In the Becker approach the assumption is implicitly made that the probability that the thermal stress attain a certain value in a locale is independent of the stress due to external forces. In view of Orowan's concept that the external forces produce very high stresses in the locales susceptible to slip, the strict validity of this assumption is questionable. In the Condon-Kauzmann-Dushman approach the assumption is explicitly made that the activation energy may be regarded as a linear function of the stress. Again in view of Orowan's concept, this assumption is questionable. Thus a linear correction to the heat of activation does not take into consideration that the stress changes the positions of the potential valleys and peaks as well as their heights.

In their application of Eq. (5) to experimental data, Kauzmann and Dushman found it necessary to assume that V varied with temperature, a variation for which no satisfactory interpretation was evident. As evidence of the validity of Eq. (6), Figs. 8–9 are presented, the data for which were taken from Dushman.

In their recent investigations upon the influence of changes in strain rate and in temperature on the strength properties of steels, the authors[30] concluded that the stress at a given strain depended upon strain rate and temperature only through the single parameter P defined by

$$P=(\dot{\epsilon}/f_0)e^{-Q/RT}. \qquad (7)$$

It is of interest to determine under what conditions this conclusion is compatible with the general mechanical equation of state. Suppose one is interested in a range of strain rates and in a range of temperature in which the stress level is near S_0. Upon letting ΔS represent the difference between S and S_0, one obtains from

[30] C. Zener and J. H. Hollomon, "Effect of strain rate upon plastic flow of steel," J. App. Phys. **15**, 22 (1944).

Eq. (6)

$$\Delta S = RT/Q'(S_0)\{\ln (f_0/\dot{\epsilon}) - Q(S_0)/RT\}. \quad (8)$$

In the range of strain rates and temperature in which the stress level is near S_0, the second factor contains two large terms which nearly cancel each other. A given change in temperature will hence produce a much greater relative change in the second factor than in the first factor. The effect of changes in strain rate and in temperature therefore enters primarily through the parameter P of Eq. (7) with Q taken at S_0.

In spite of the vast amount of experimental work upon creep which has been carried out, and is still being carried out, especially in this country, no attempts have been made other than by Dushman to establish mechanical equations of state. No experimental evidence therefore exists regarding the influence upon the constant f_0 and upon the activation energy function $Q(S)$ of the various metallurgical variables, such as dissolved elements, precipitates, grain size, etc. Further, no theoretical considerations have been advanced since the early work of Orowan which gives a more detailed picture of the mechanism of plastic deformation and of the influence of thermal energy thereon.

A mechanical equation of state can exist only under conditions where the metal does not undergo significant changes with time at zero strain rate. Thus it must not soften through recovery or through recrystallization. The smaller the prior strain the higher is the temperature needed to reduce the strain hardening. The agreement of the experimental observations reproduced in Figs. 8 and 9 with the predictions of an equation of state indicate that for the metals used strain hardening was not significantly reduced by recovery or by recrystallization under the conditions of the experiment. An understanding of the conditions under which a mechanical equation of state is applicable will require the development of a theory of recovery and of recrystallization.

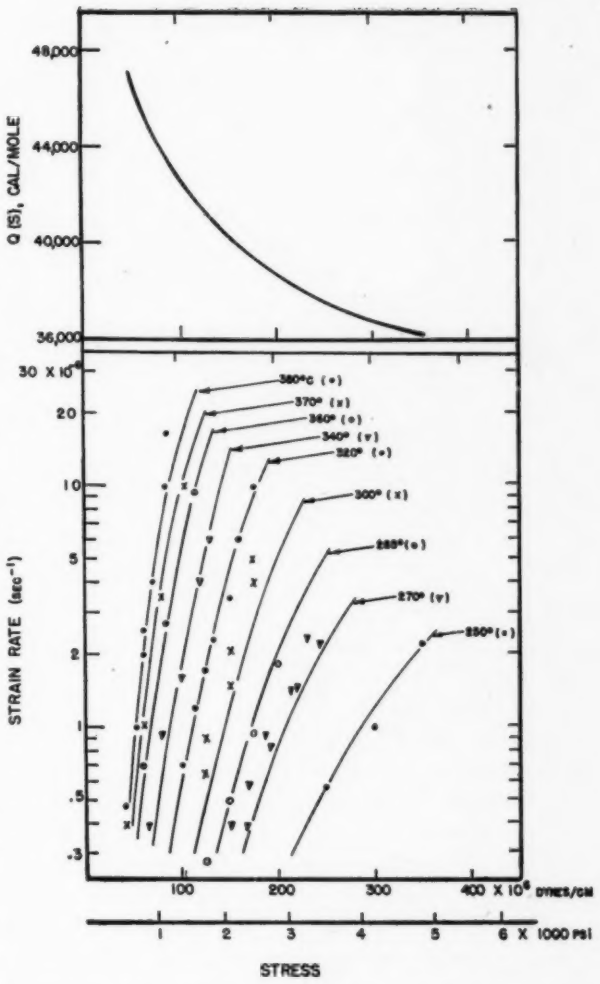

FIG. 9. Application of mechanical equation of state to an aluminum alloy with 2 percent magnesium. $f_0 = 2.5 \times 10^9$. (Data after Dushman *et al.* (reference 28).)

B. Strain Hardening

As has been previously mentioned, resistance to deformation usually increases with deformation. Thus in Eq. (1), the stress S increases with the strain E. The precise manner in which the tensile stress increases with the tensile strain, at constant strain rate and temperature, has been discussed in a recent paper.[31] It appears that, in the absence of discontinuous yielding, the stress may be represented as a power function of the strain up to strains as large as 0.4. Thus

$$S = S_0 \cdot (\epsilon/\epsilon_0)^m$$

where S_0 is the stress at some arbitrary strain ϵ_0.

[31] J. H. Hollomon, "Tensile deformation," Metals Tech. (June, 1945).

The variation of the constants S_0 and m upon the metallurgical variables has been rather exhaustively studied in the case of iron and steel. Thus in the absence of precipitates, the addition of soluble alloys[32] raises S_0 without essentially altering the strain hardening exponent m. On the other hand, in steels where the strength arises primarily from insoluble carbides, the strain hardening exponent is inversely proportional to S_0 for any given carbon content. It is not known at present whether similar relations are true for other metals.

C. Generalized Stress and Strain

In the previous part of this paper it has been implicitly assumed that stress and strain referred to uniaxial tensile conditions. A discussion will now be given of the problems which arise when the stress system is of a more complex type.

Von Mises[33] has indicated the path along which the laws for uniaxial tension may be generalized to include the most general type of stress system. A certain invariant function S_I of the stresses plays the same role in determining the rate of strain as does the tensile stress in the case of uniaxial tension. This function is so defined that S_I^2 is proportional to the elastic shear strain energy. Thus

$$S_I^2=\tfrac{1}{2}\{(Y_y-Z_z)^2+(Z_z-X_x)^2+(X_x-Y_y)^2\}+3(Y_z^2+Z_x^2+X_y^2). \quad (9)$$

The type of strain due to a generalized stress system is of the same type as if the specimen were amorphous, thus

$$\dot{\epsilon}_{xx}=\lambda\{X_x-(Y_y+Z_z)/2\},$$

with analogous equations for $\dot{\epsilon}_{yy}$ and $\dot{\epsilon}_{zz}$ having the same factor λ, and

$$\dot{\epsilon}_{yz}=3\lambda Y_z,$$

with analogous equations for $\dot{\epsilon}_{zx}$ and $\dot{\epsilon}_{xy}$. The generalized mechanical equation of state may therefore be written in the following manner:

$$\dot{\epsilon}_{xx}=\{X_x-(Y_y+Z_z)/2\}S_I^{-1}f_0\times\exp[-Q(S_I)/RT], \quad (10)$$

with analogous equations for $\dot{\epsilon}_{yz}$ and $\dot{\epsilon}_{zx}$, and

$$\dot{\epsilon}_{yz}=3X_{yz}S_I^{-1}f_0\exp[-Q(S_I)/RT],$$

with analogous equations for $\dot{\epsilon}_{zx}$ and $\dot{\epsilon}_{xy}$.

In the case of uniaxial tension it was seen that strain hardening could be taken into account by regarding f_0 and Q as functions of the strain. The same procedure may be followed in the case of a general type of stress. Before this can be done, however, it is necessary to have a measure of strain in a general type of deformation. In obtaining this measure, two steps must be taken. Firstly, the method must be determined of combining strain increments associated with increments of deformation. Secondly, strain increments must be defined in terms of increments of deformation. The first question has been answered by following a suggestion of Ludwik[16] that the strain increment associated with a given increment of deformation be computed using as a reference configuration the configuration of the system before that particular increment of deformation. Thus if during an increment of deformation in uniaxial tension the length changes from l to $l+dl$, the strain increment associated therewith is dl/l, irrespective as to what prior deformation the specimen had undergone. Ludwik pointed out that the total strain is then simply the sum of all the strain increments. Thus if the gauge length changes, during a uniaxial tension, from l_1 to l_2, the total strain associated therewith is $\ln(l_2/l_1)$. A satisfactory measure of a strain increment is an invariant function of the strain components which is proportional to S_I in an isotropic elastic medium. Such a function, $d\epsilon_I$, is defined by

$$d\epsilon_I^2=\tfrac{1}{2}\{(d\epsilon_{yy}-d\epsilon_{zz})^2+(d\epsilon_{zz}-d\epsilon_{xx})^2+(d\epsilon_{xx}-d\epsilon_{yy})^2\}+\tfrac{3}{4}(d\epsilon_{yz}^2+d\epsilon_{zx}^2+d\epsilon_{xy}^2). \quad (11)$$

From the previous equations in this section it may be verified that the strain defined in this manner satisfies the following equation

$$\dot{\epsilon}_I=f_0\exp[-Q(S_I)/RT]. \quad (12)$$

[32] C. E. Lacy and M. Gensamer, "Tensile properties of alloyed ferrites," Trans. Am. Soc. Metals **32**, 88 (1944).

[33] R. von Mises, "Mechanik der Festen Korper in plastischdeformablen Zustand," Nachr. Gesellsch. Wissensch. zur Göttingen, Math-Phys. Klasse, 1913.

The quantities f_0 and Q are to be regarded as functions of the strain ϵ_I.

Equations (10) to (12) form a self-consistent scheme of a general mechanical equation of state. The outstanding problems relate to how well this scheme represents the behavior of actual metals, and to what deviations therefrom are to be ascribed.

One consequence of the general equation of state is that when the temperature and the strain rate are held constant a general strain hardening function exists of the type

$$S_I = S_I(\epsilon_I). \tag{13}$$

Nadai and Davis[34] have performed experiments designed to check this equation. Thus they measured the stress S_I as a function of strain ϵ_I under various types of stress pattern. They found that at small strains below 0.2, this equation was in fact satisfied, but that at larger strains deviations became appreciable.

In the establishment of the general mechanical equation of state in terms of the invariant functions ϵ_I and S_I, it was implicitly assumed that the material was initially, and remained, isotropic. It is to be expected that anisotropy will be introduced by plastic deformation, and that this anisotropy will be greater, the greater the deformation. The amount of anisotropy introduced by a given deformation will, however, very likely depend upon the microstructure. As an example, logarithmic strain hardening curves taken in tension and in torsion are compared for steels of two types of microstructure in Figs. 10 and 11. As might be expected, the steel which has the greatest anisotropy of structure, pearlite,

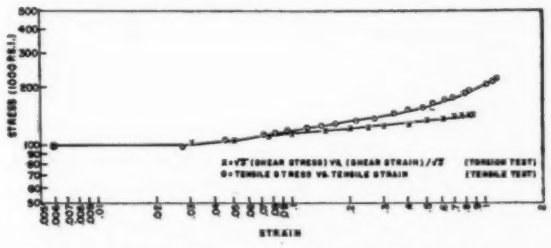

FIG. 10. Correlation of tensile and torsional tests by means of concept of generalized stress and strain (tempered martensitic steel).

[34] A. Nadai and E. Davis, "Plastic behavior of metals in the strain hardening range," J. App. Phys. **8**, 205 (1937).

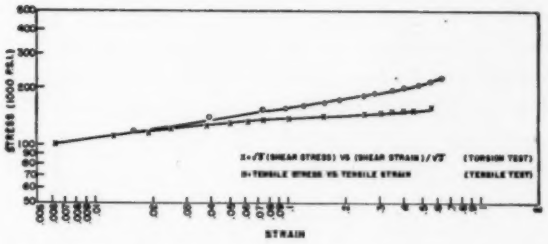

FIG. 11. Correlation of tensile and torsional tests by means of concept of generalized stress and strain (pearlitic steel).

shows the greatest apparent strain anisotropy. A further understanding of plastic deformation under general types of stress pattern must therefore involve an evaluation of the anisotropy introduced by deformation, and of the modification of the mechanical equation of state by this anisotropy.

It has been implicitly assumed that the strain and strain components in the above equation refer only to the plastic, i.e., permanent, deformation. The elastic strain components are deducible from the elastic equation, thus

$$(\dot{\epsilon}_{xx})_{\text{elastic}} = E^{-1}\{\dot{X}_x - \sigma(\dot{Y}_y + \dot{Z}_z)\}. \tag{14}$$

The total strain components are therefore the sum of the elastic and plastic components, thus

$$(\dot{\epsilon}_{xx})_{\text{total}} = (\dot{\epsilon}_{xx})_{\text{elastic}} + \dot{\epsilon}_{xx}. \tag{15}$$

One could therefore obtain a set of equations for the time derivatives of the total strain components by using the relations analogous to Eq. (14) for the elastic part, and Eq. (10) for the plastic part. This has in fact been done by Prandtl[35] and Reuss.[36] Two factors tend to invalidate such an equation when the stress pattern is changing under conditions where the elastic strain is comparable to the plastic strain. Firstly, the anelasticity of actual metals would render ambiguous the distinction between elastic and plastic strains. Secondly, the Bauschinger effect of actual metals is very marked for plastic strain comparable to the elastic strains, but becomes negligible for much larger plastic

[35] L. Prandtl, Proc. 1st. Int. Cong. App. Mech. p. 43 (1924).

[36] E. Reuss, Zeits. f. angew. Math. u. Mech. **10**, 266 (1936).

strains, as has been vividly demonstrated by Sachs and Shoji.[37] Prager[38] has applied the Prandtl-Reuss equation to a case of relaxation of residual stresses by deformation, the total strain being comparable to the elastic strains. Instead of placing the blame for lack of agreement of theoretical prediction with observation upon the anelastic and Bauschinger effects, Prager applied an empirical rule (which he claims is derived from the "Hencky-Nadai Theory") relating plastic strain and total strain which agreed with the experimental data. Analysis of his rule shows that it leads to different results when the plastic deformation takes place intermittently or continuously, contrary to all experience. In opposition to Prager's viewpoint, the authors believe an adequate understanding of the mechanics of small plastic deformations will be obtained only through a study of the basis of the anelastic and Bauschinger effects, not through attempting to find empirical formal relations between the stress pattern and the elastic and plastic strains.

[37] G. Sachs and H. Shoji, "Zug-Druchversuche an Messingkristallen," Zeits. f. Physik **45**, 776 (1927).
[38] W. Prager, "Exploring stress-strain relations of isotropic plastic solids," J. App. Phys. **15**, 65 (1944).

Problems in Fracture of Metals*

BY J. H. HOLLOMON AND C. ZENER

Research Division, Watertown Arsenal, Watertown, Massachusetts

In this report a review is made of the possible types of future research which might lead to an understanding of the fracture of metals, and hence to an increase of the strength level to which metals may be raised without danger of fracture. It is found that an understanding of fracture would be enhanced by research upon the following topics: 1. The effects of the following variables on the virtual fracture stress: (a) Strain; (b) strain rate; (c) temperature; (d) stress distribution; (e) structure; (f) mechanical history (i.e., fatigue). 2. A comparison of the fracture characteristics of metallic crystals with those of non-metallic crystals, such as rocksalt. 3. The hindrances of plastic deformation by sharp stress gradients. 4. The introduction of stress concentration by: (a) Non-metallic inclusions; (b) precipitates; (c) slip bands; (d) twin bands; (e) grain boundary deformation. 5. The effect of reversal of stresses upon the properties of slip bands.

I. INTRODUCTION

THE strength or hardness of our present-day metals cannot be further increased by known methods without inducing susceptibility to brittle failure. Therefore, practical increases in strength can only be accomplished through an understanding of the problems relating to fracture. Many features of the dynamics of crack propagation are imperfectly understood, such as the factors which determine the velocity and direction of propagation. An understanding of these features would not, however, lead to an improvement in the useful strength of metals, since a fractured metal member has failed, irrespective of the precise path or velocity of the crack. This paper will, therefore, be confined to the problems relating primarily to the initiation of fracture.

* The statements or opinions in this article are those of the authors and do not necessarily express the views of the Ordnance Department.

II. GROSS FEATURES OF FRACTURE

It has long been known that metals which are ductile under one set of conditions may break brittlely under other conditions. Thus metals frequently are ductile at moderate temperatures in simple tension, but are brittle at low and at high temperatures or under a more complex stress system. It would be highly desirable to have a consistent scheme by means of which, from measurements made under one set of conditions, the fracture properties under other conditions could be predicted. Such a scheme was presented by Ludwik[1] in 1909. The cardinal feature of Ludwik's contribution was the recognition that the stress at fracture of a ductile material is the fracture stress of the material after having suffered its final strain, and not of the original material. In his scheme Ludwik con-

[1] P. Ludwik, *Elemente der Technologischen Mechanik* (Berlin, 1909).

sidered two functions of strain, as represented in Fig. 1. One function is the flow stress, defined as the tensile stress necessary to produce further plastic deformation. The other function is the virtual fracture stress, defined as the tensile stress which would be required to fracture the material if further plastic deformation did not occur. A metal deforms plastically under tension as long as the flow stress is less than the virtual fracture stress. Fracture occurs at that strain at which the flow stress curve crosses the virtual fracture stress curve. The advantage of Ludwik's scheme is that it resolves the influence upon fracture of the several variables such as stress pattern, temperature, strain rate, into the influence of these variables upon the flow stress and upon the virtual fracture stress. Its success depends upon how well the reliance of these two stress functions upon the several variables may be determined. The disadvantage of Ludwik's scheme, a disdavantage which has prevented its general adoption, is that the virtual fracture stress can be measured directly only at one strain, namely the strain at fracture. Only estimates may be obtained for strains other than this final strain.

The most straightforward method of estimating the virtual fracture stress curve was used first by Davidenkov and Wittman[2] and later by the authors.[3] This method is applicable to all

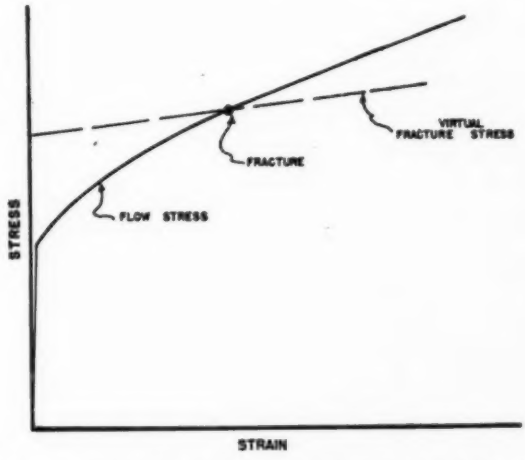

FIG. 1. Representation of fracture according to Ludwik.

[2] N. Davidenkov and F. Wittman, "Mechanical analysis of impact brittleness," Tech. Phys. U.S.S.R. **4**, 3–17 (1937).

[3] J. H. Hollomon and C. Zener, "Conditions of fracture in steel," Trans. A.I.M.E. **158**, 283 (1944).

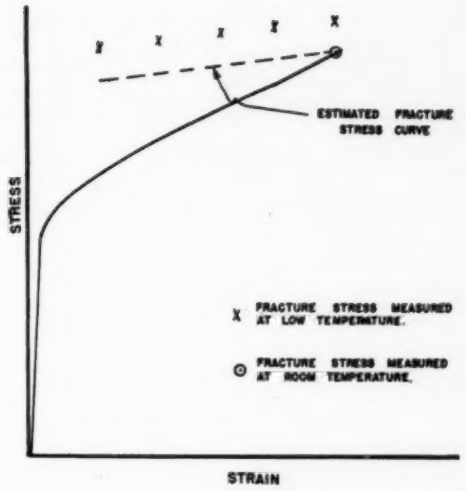
ESTIMATED FRACTURE STRESS CURVE
STRESS
X FRACTURE STRESS MEASURED AT LOW TEMPERATURE.
⊙ FRACTURE STRESS MEASURED AT ROOM TEMPERATURE.
STRAIN

FIG. 2. Alternative method of estimating fracture stress curve.

metals which deform appreciably at room temperature but which break brittlely at some low temperature. In this method specimens are deformed various amounts at room temperature, the temperature is then lowered, and they are then broken without further deformation. The fracture stress measured at the low temperature is then plotted as a function of the strain at room temperature. An estimate of the virtual fracture stress curve at room temperature is then obtained by assuming it to be parallel to the curve measured at the low temperature. The method is illustrated in Fig. 2. The method could be further improved by making the fracture measurements at a series of low temperatures, and thus at least partially justifying the undesirable assumption.

Pearlitic steels (containing lamellar carbides) and some age-hardenable alloys are brittle at low temperatures, and their virtual fracture stress curves may be obtained in this manner. Typical results for a pearlitic steel are shown as Fig. 3. All specimens deformed more than a few percent at room temperature broke with practically no further deformation at the low temperature. A specimen undeformed at room temperature, however, first exhibited an upper and lower yield point at the low temperature (Fig. 4) and actually fractured at a lower stress than it had withstood before it deformed. It can only be concluded, therefore, that at least for this type of steel* the virtual fracture stress curve has the

* Confirmatory experiments have been performed on specimens of similar steels.

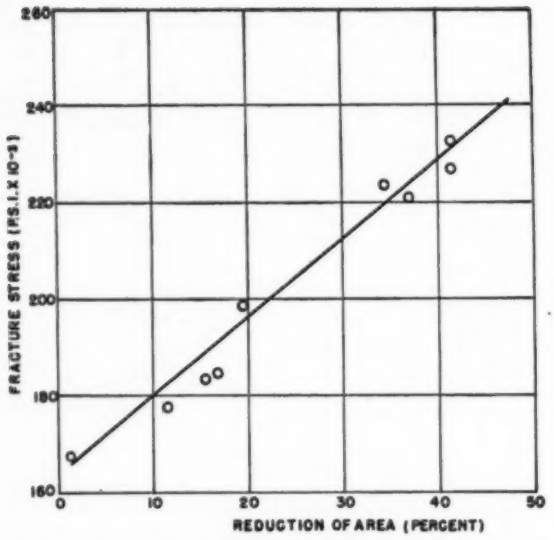

FIG. 3. Effect of prior deformation on fracture stress (at −190°C). (Pearlitic steel.)

form illustrated in Fig. 5. It is of particular interest that the estimated virtual fracture stress may be only slightly higher than the flow stress at very small strains. Any change of variables which raises the flow stress relative to the virtual fracture stress is apt to embrittle the metal.

As previously mentioned, the method described above cannot be used to estimate the virtual fracture stress curve of those metals that are not brittle at low temperatures. For such metals, one would have to utilize some other test conditions under which the metals fractured without deformation. As yet, no test conditions have been found which are as suitable in embrittling metals as is lowering the temperature (as in the case of pearlitic steels).

The virtual fracture stress curve may be highly anisotropic. The most common example of anisotropy occurs in the rolling of metal plates. The rolling of these plates raises the virtual fracture stress in the rolling direction, lowers it in the transverse direction. In an earlier paper[4] one of the authors pointed out that longitudinal fractures of certain steels could be interpreted only in terms of an anisotropic effect of deformation on the fracture stress. The tensile strain, as already pointed out, raises the tensile stress required to fracture the specimen on a plane perpendicular to the axis. In order that a tensile specimen can fracture longitudinally, the stress required to fracture a metal on a plane parallel to the axis must decrease sufficiently for the circumferential stress induced by necking to fracture the metal. Conversely, compression will lower the tensile stress required for fracture upon subsequent deformation in a direction opposite to the compression strain. Examples of such effects of compression are frequently found in bending. Thus, a specimen which has undergone a certain amount of bending, and which is capable of continued bending in the same direction, may break brittlely when an attempt is made to unbend it. The anisotropy of the virtual fracture stress may also be visibly demonstrated by pulling specimens in tension that have previously been twisted plastically. Swift[5] found that if the specimens had been sufficiently twisted prior to pulling, fracture occurred along a helical surface, rather than across the plane of maximum tensile stress, namely the transverse plane. Although many examples of anisotropic virtual fracture stress are known, no quantitative study has as yet been made of anisotropy. Thus, no measurements have been made to determine the relation between the virtual fracture stress and the reduction in cross section in rolling.

Under many conditions constraints prevent plastic deformation in one transverse direction.

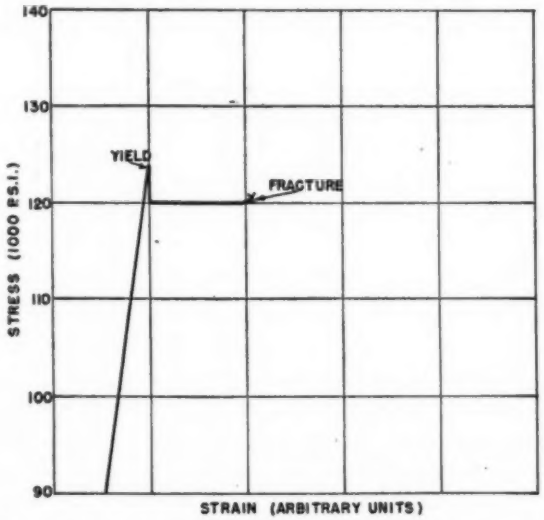

FIG. 4. Illustration of the lowering of the fracture stress by initial deformation (pearlitic steel tested at −190°C).

[4] J. H. Hollomon, "Temper-brittleness," communicated to Am. Soc. Metals.

[5] H. W. Swift, "Tensional effects of torsional overstrain in mild steel," J. Iron and Steel 140, 181 (1939).

Many experiments have been performed to determine the effects of a single transverse stress on the fracture stress. In order to interpret these experiments it is necessary to permit only the stress distribution to vary. Frequently in such tests other factors such as the strain to fracture varies as the stress distribution is changed. Suppose, for example, thin hollow tubes are loaded by means of a longitudinal tension and an internal pressure. Because of the presence of the transverse stress, the tensile stress required for plastic flow is raised and unless the virtual fracture stress curve is identically affected the strain to fracture will also change as illustrated in Fig. 6. Furthermore, as the circumferential tension in the hollow tubes becomes larger than the longitudinal tension, the fracture may change from transverse to longitudinal. Because of the anisotropy, the fracture stress may be altogether different in the new direction, and more important, it may depend differently upon strain. Experiments of Siebel and Maier[6] on tensile tests of hollow cylinders under internal pressure indicate that a single transverse stress has no effect upon the virtual fracture stress, provided the assumption is made that in their single phase materials the virtual fracture stress was independent of strain. Indirect evidence also exists that the transverse stress associated with such restraints does not influence the virtual fracture stress. Thus, the brittle failure of pearlitic steels in the notched-bar impact test can be interpreted

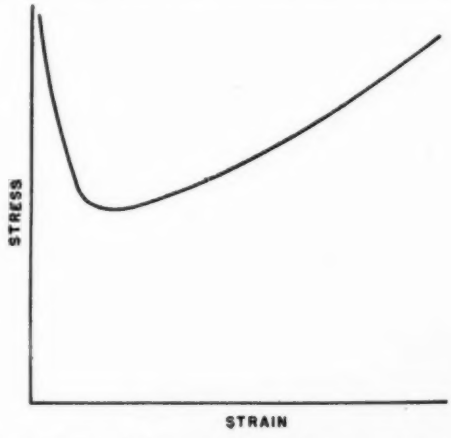

FIG. 5. Proposed shape of virtual fracture stress curve (for pearlitic steels).

[6] E. Siebel and A. Maier, "Effect of multiaxial stress states on the ductility," Zeits. f. V. D. Ing. **77**, 1345–1349 (1933).

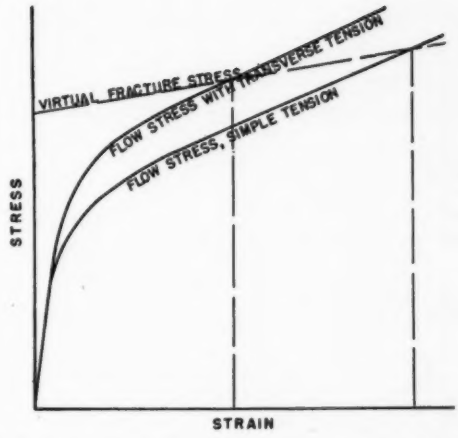

FIG. 6. Possible effect of transverse stress on flow curve and fracture strain (if virtual fracture stress is unaffected).

only by assuming that a single transverse stress has much less effect upon the virtual fracture stress than upon the flow stress.[7] It would be highly desirable to have direct evidence upon the variation of the virtual fracture stress with a single transverse stress.

Under less frequent conditions a biaxial transverse tension is present. By testing tensile specimens having circumferential notches of various depths and radii, Kuntze,[8] McAdam,[9] and Sachs[10] have attempted to evaluate the influence of a biaxial transverse tensile stress upon the virtual fracture stress, called by them the "technical cohesion strength." In their measurements the average longitudinal stress at fracture is taken as the fracture stress. The interpretation of the variation of this stress with variations in testing conditions is usually extremely difficult. As discussed by these workers, the effects of the three separate variables, strain, stress complex, and variation of stresses throughout the specimen, may be reflected by these measurements. In one case Sachs and his collaborators were able

[7] J. H. Hollomon, "Notched-bar impact test," Trans. Am. Soc. Min. Met. Eng. **158**, 298–327 (1944).

[8] W. Kuntze, for survey and bibliography, see D. J. McAdam, Trans. Am. Inst. Min. Met. Eng. **150**, 311 (1942).

[9] D. J. McAdam, "Technical cohesive strength of metals in terms of the principal stresses," Metals Tech. (December, 1944). References given to prior work.

[10] G. Sachs, J. D. Lubahn, and E. J. Ebert, "Effects of notches of varying depth on the strength of heat treated low alloy steels," Trans. Am. Soc. Metals, **34**, 517–544 (1945); G. Sachs and J. D. Lubahn, "Effect of triaxiality on the technical cohesive strength of steels," A. S. M. E. preprint, 1945.

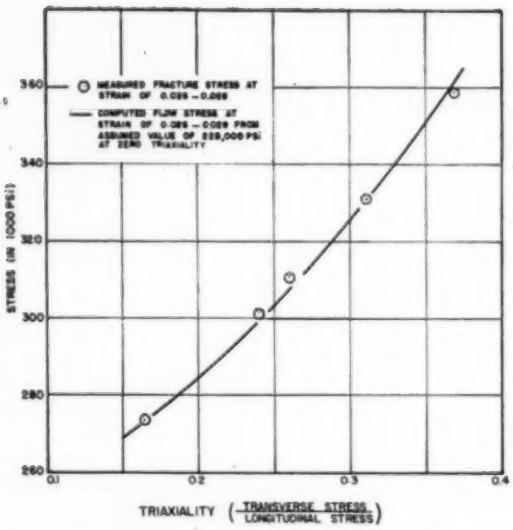

FIG. 7. Dependence of fracture stress upon biaxial tension (after data of Sachs (reference 10)).

to obtain the same strain (0.026 to 0.028) with several notch depths and notch radii. In this case the strain variable was absent. If it is assumed that the stress distribution is essentially constant throughout the unnotched region with notches of various depths and radii, then the observed change in fracture stress may be regarded as a reflection of the triaxiality of stress (ratio of transverse to longitudinal stress). Their results are reproduced as Fig. 7. The self-consistency of the data may be seen from the close agreement of the measured fracture stress with the computed flow stress at fracture. The rise of the virtual fracture stress with biaxial tension, as demonstrated in Fig. 7, confirms the earlier conclusions of McAdam and his collaborators. The constancy of the strain to fracture implies that in this particular case the virtual fracture stress rises just as rapidly with biaxial tension as does the flow stress, and hence that a biaxial tension has no embrittling effect. This conclusion is in marked disagreement with current ideas upon the influence of triaxial stresses. Investigation of the type given by Sachs should therefore be further pursued.

Fracture in steels is most apt to occur under impact conditions at low temperatures. Both a lowering of temperature and an increase in the rate of strain are known to raise the flow stress of all steels. Experiments[9] have indicated that the virtual fracture stress of all steels likewise rises with a lowering of the temperature, but not quite as rapidly as does the flow stress. It is the resulting relative rise of the flow stress with respect to the virtual fracture stress that leads to brittle failure in the case of pearlitic steels. Because of the relatively small effect of changes of strain rate obtainable with the usual type of testing machines, combined with the relatively large scatter in fracture measurements, no conclusions can as yet be drawn upon the influence of strain rate upon the virtual fracture stress.

Nearly brittle fracture of metals is also likely to occur at high temperatures under certain conditions. As was first observed by Rosenhain and Archbutt,[11] these conditions are such as to favor grain boundary slip. Under these conditions the virtual fracture stress may be considered as decreasing with time, although the accompanying strain may be negligible. This concept of the virtual fracture stress decreasing with time suggests interesting experiments which have as yet not been performed. Thus, if after the virtual fracture stress of a specimen is lowered by the application of a stress at an elevated temperature, the specimen is lowered to room temperature without removing the stress, the virtual fracture stress should stay lowered, and may thus result in brittle fracture at room temperature.

III. MECHANISM OF FRACTURE

It has long been recognized that the observed fracture stress of metals, in fact of all crystalline substances, is at least two orders of magnitude lower than the intrinsic fracture stress as computed on the basis of the forces between atoms. The only way to reconcile this divergence between observed and theoretical fracture stress is through the assumption that at any one instant the material fractures only in localized regions, regions in which the stress is much higher than the average applied stress.

Stress concentrations in localized regions were first investigated in detail by Inglis.[12] He pointed out that the tensile stress at the base of a notch

[11] W. Rosenhain and S. L. Archbutt, "On the intercrystalline fracture of metals under prolonged application of stress," Proc. Roy. Soc. **95**, 55 (1919–20).

[12] C. E. Inglis, "Stress in a plate due to the presence of cracks and sharp corners," Trans. Inst. Naval Architects **55**, Pt. 1, 219 (1913).

may be much higher than the average tensile stress throughout the specimen, the stress concentration being given by $1+2(a/\rho)^{\frac{1}{2}}$, where a is the depth of the notch, ρ the radius of curvature at the base of the notch. Joffé[13] and his collaborators have found that the discrepancy between the usually observed fracture stress of rocksalt crystals and the theoretical fracture stress may be accounted for entirely in terms of surface notches in the form of small surface cracks. By immersing these specimens in water and thereby continually dissolving away the surface, they were able to raise the actual fracture stress by a factor of 400. Under these conditions the fracture stress is in fact very nearly equal to the theoretical value.

Well-prepared metal specimens appear to be free of surface defects of the type found in dry rocksalt crystals. Their weakness with respect to fracture must be blamed upon defects within the material itself, for once deformation (in tension) has proceeded to such an extent that necking has commenced, fracture begins in the interior of the specimen and propagates outwards. That fracture should commence in the interior of the necked specimens is understandable in view of the analysis by Bridgman[14] of the stress system within a necked region. In this stress system the tensile stress is a maximum along the axis, a minimum at the surface. It would be expected that metal crystals of the same degree of purity as Joffé's rocksalt crystals would manifest the same relatively high fracture stress. As yet no experimental work has been done to check the correctness of this viewpoint.

The relatively low fracture stress of actual metals may most readily be interpreted in terms of the presence of micro-cracks within the metal itself. Starting from the observation that a crack will propagate only if the total free energy of the system is lowered by the propagation, Griffith[15] deduced that a circular crack of a given radius a will propagate only when the tensile stress normal to the crack exceeds a certain critical value S. Griffith's formula is:

$$S=(\sigma G/ca)^{\frac{1}{2}}. \qquad (1)$$

Here σ is the surface energy per unit area, G is the shear modulus, and c a constant of the order of magnitude of unity. Griffith developed his theory, and obtained experimental confirmation of it only for amorphous substances. The resistance to plastic deformation of such substances increases rapidly as the temperature is lowered, so that at sufficiently low temperatures, room temperature for ordinary glass, a crack may propagate unaccompanied by any plastic deformation. In amorphous substances, therefore, where the new surface produced by crack propagation has not undergone plastic deformation, the appropriate value of surface energy σ in Eq. (1) is very nearly the surface energy of the substance in the molten state. This surface energy may be readily measured. The situation is more complex in the case of crystalline substances. On one hand the resistance to plastic deformation of crystalline substances increases relatively slowly with temperature, so that such deformation cannot usually be eliminated entirely merely by lowering the temperature. On the other hand, the laws of plastic deformation obtained by macroscopic measurements are not applicable when the stress varies appreciably in a distance less than the linear dimensions of a single crystal. A stress greatly in excess of the macroscopic yield stress will not necessarily lead to plastic deformation if the stress is confined to a sufficiently localized region. No investigation has as yet been made to determine under what conditions a sharp crack will propagate without any attendant plastic deformation. If plastic deformation does occur, the energy associated with it must be added to the surface energy σ in order that Eq. (1) be applicable.

Although the ambiguity which now exists regarding the proper value of the surface energy σ prevents the quantitative application of Eq. (1) to metals, the qualitative aspects of Griffith's ideas may be used to correlate many diverse fracture phenomena.[16] These phenomena are associated with the reorientation and distortion of the micro-cracks by deformation. Figure 8

[13] A. Joffé, "Plastizität und Festigkeit der Kristalle," Proc. 1st Int. Cong. Ap. Mech., Delft (1924.)

[14] P. W. Bridgman, "Stress distribution at the neck of a tensile specimen," Trans. Am. Soc. Metals **32**, 553 (1944).

[15] A. A. Griffith, "Phenomena of flow and rupture in solids," Phil. Trans. Roy. Soc. **221**, 163 (1920).

[16] C. Zener and J. H. Hollomon, "Plastic flow and rupture of metals," Trans. Am. Soc. Metals **33**, 163 (1944).

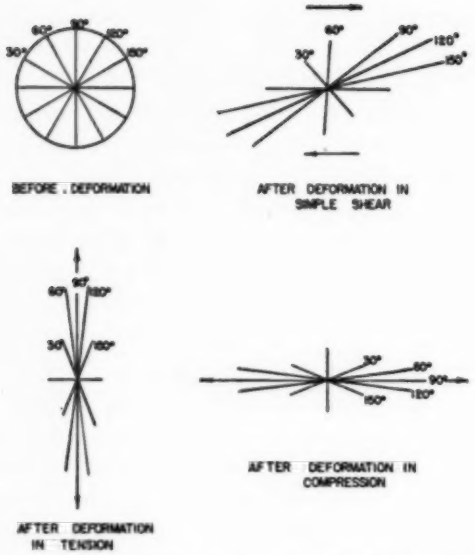

FIG. 8. Reorientation of micro-cracks by deformation.

illustrates how an initially random distribution of micro-cracks acquires a highly anisotropic distribution by deformation. Thus in tension the cracks are elongated along the tensile axis, are shortened in the transverse direction. The critical tensile stress necessary to cause some of the micro-cracks to propagate, and thus lead to rupture, is raised by deformation when the stress is longitudinal, lowered by deformation when the stress is transverse. The most common example occurs in the rolling of plate, where the fracture stress is raised in the rolling direction but reduced in the transverse direction. Another example occurs in the usual tensile tests of certain steels in which the tensile strain is found to raise the fracture stress perpendicular to the axis of the specimen but to lower it on a plane parallel to the axis. In fact, as mentioned earlier, the fracture stress with respect to transverse tension may become so low that the transverse tensile stress within the neck of a tension specimen[14] causes the specimen to rupture longitudinally rather than transversely. The most spectacular example of the influence of micro-crack reorientation upon fracture occurs when a specimen is first plastically twisted and then pulled in tension. The spiral-type crack which is observed is just of the type which one would predict from an examination of reorientation effects.[16]

Although the reorientation effects of the micro-cracks are readily understood, considerable uncertainty exists regarding the nature and origin of the micro-cracks. Inclusion of non-metallics, such as iron oxides and sulphides in steel, no doubt gives rise to stress concentration, and might, for certain purposes, be considered as the micro-cracks responsible for fracture. It is thus known that the "dirtier" the steel, i.e., the more non-metallics it contains, the worse are its fracture properties. It is also known that hot working introduces reorientation effects that are not removed by heat-treatment involving recrystallization of the matrix; reorientation effects are thus interpretable only in terms of the non-metallic inclusions. The fracture properties cannot, however, be described entirely in terms of the non-metallic distribution, for it is known that the structure of the matrix also has a marked influence upon the fracture stress. Thus, in steel, the tempered martensitic structure (spheroidal carbides) has a higher fracture stress at small strains[3] than a pearlitic structure (lamellar carbides) having the same resistance to plastic deformation; for a given type of structure the fracture stress is higher the smaller the carbide particles. The matrix itself must, therefore, contain origins for stress concentration. The stress concentration at any point within the matrix is then the product of two stress concentration factors, that arising from the dirt and that arising from the matrix itself. As yet no experimental study has been undertaken from which the relative magnitude of these two factors may be ascertained.

Considerable uncertainty exists as to the origin of the stress concentrations within the matrix itself. If the matrix contains precipitated particles, such as carbides in steel, these particles will be a source of some stress concentration. The stress concentration factor will depend upon the shape and size of the particles. Thus, as previously mentioned, plate-like particles give rise to higher stress concentrations and, therefore, lower fracture stresses than spheroidal particles. Evidence will shortly be presented by one of the authors (JHH) that the larger the size of the carbide particles, the higher the stress concentration factor associated therewith. The data are not sufficiently complete, however, that precise relations can be derived.

Quite apart from the presence of precipitated

particles, the matrix acquires stress concentrations through the very act of plastic deformation. As first pointed out by Orowan,[17] stress concentrations arise at the edges of slip bands. One of the authors[18] has cited examples of fracture that can be interpreted only through the assumption that such stress concentrations may increase with time under a constant applied stress, just as if the slip bands behaved in a viscous manner. It might be expected that such stress concentration would be larger the larger the lateral extent of the slip bands, and therefore, the larger the grain size. As yet this influence of grain size *per se* has not been demonstrated. It is generally recognized that steels of small grain size have better fracture properties than steels of large grain size. In steels, however, the grain size has a marked effect upon the manner in which the carbides precipitate, and so the direct effect of grain size cannot be determined. The stress concentration associated with plastic deformation has the unique property that it is not present until after some plastic deformation has occurred. It is thus expected that the fracture stress of well-annealed specimens would be higher before than after a slight plastic deformation. The data presented above as Figs. 4 and 7 may be regarded as further confirmation of the viewpoint that the virtual fracture stress of the undeformed material may be very high. Further corroboration that fracture stress is intimately related to plastic deformation may be found in the observation that the fracture stress varies with strain rate and with temperature in approximately the same manner as does the resistance to deformation. No experiments have so far been undertaken to determine just how large a stress an undeformed specimen would sustain without fracturing.

That stress concentrations are built up through plastic deformation itself gives rise to the possibility that the fracture properties may be modified through alterations in the conditions of test. An example has recently been described by Bridgman.[19] He found that when two identical specimens are deformed in tension by the same amount, one under atmospheric pressure and one under high pressure, the latter will suffer much more additional deformation under atmospheric pressure than the former specimen, and hence has a considerably higher fracture stress. It appears as if the high pressure prevents high stress concentrations from opening micro-cracks. Initial deformation at an elevated temperature might have the same effect provided the temperature is not so high that recovery or recrystallization occurs. At the higher temperature a smaller stress would be required to produce the same extension as at room temperature, and hence fewer micro-cracks might be formed. Experiments to demonstrate this effect of the temperature of prior deformation upon fracture properties have not yet been performed. Possibly the formation of twin bands can give rise to greater stress concentrations at their edges than the formation of slip bands, for some experiments indicate that twin bands may be associated with brittle failure.[20]

As early as 1920 Rosenhain[11] and his collaborators presented convincing evidence that grain boundaries behave in a viscous manner, and therefore that low rates of deformation and elevated temperature favor slipping at the boundaries, and that this slipping leads to premature fracture. Although not explicitly stated by Rosenhain, it is evident that the premature fracture arises from stress concentrations caused by the grain boundary slip. Unfortunately the concept of the viscous behavior of grain boundaries has not been extensively utilized by students of metals in this country. As a consequence no advance has been made during the intervening twenty-five years towards an evaluation of those factors that influence the stress concentration arising from the viscous slip at grain boundaries. Many interesting experiments which have not as yet been carried out are suggested by this concept. For example, the stress concentration induced by applying a stress at a high temperature can be frozen in by cooling to room temperature before removal of stress, and the metal thereby embrittled.

While a specimen may be able to sustain a certain stress for an indefinite time, it may fracture if the stress is alternately reversed and reapplied a large number of times. This fracture

[17] E. Orowan, "Zur Kristallplastizitat," Zeits. f. Physik **89**, 605, 614, 634 (1934).
[18] C. Zener, "Anelasticity of Metals" (in print, A.I.M.E.).
[19] P. W. Bridgman, Rev. Mod. Phys. **17**, 3 (1945).
[20] N. Davidenkov, *Dynamic Tests of Metals* (in Russian), 1936.

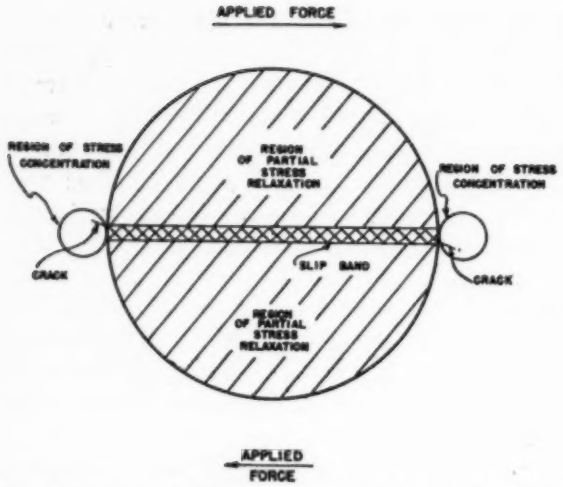

FIG. 9. Representation of stress pattern in matrix adjacent to a freshly formed slip band.

by an alternating stress, called fatigue, has been known for over 80 years. The practical importance of fatigue has led to the accumulation of a multitude of data for various metals relating the number of cycles necessary for fracture to the peak applied stress under various conditions. In this country little work has been undertaken for the purpose of finding the mechanism of fatigue failure. At the National Physical Laboratory in England, an extensive descriptive study has been made of the initiation and propagation of fatigue cracks in single crystals and in polycrystals. The early work, including the progressive changes in the hysteresis loops, has been reviewed by Moore and Kommers.[21] The descriptive work in the National Physical Laboratory initiated by Ewing[22] and collaborators, and continued by Gough and collaborators, upon the initiation of fatigue cracks, and upon their relation to slip bands, has been reviewed by Gough.[23] No attempt has been made to interpret the observed results in terms of the micro-structure, other than through the concept of attrition introduced by Ewing and Humfrey,[22] according to which the slip bands become more and more disorganized as the cyclic stressing proceeds.

A cursory analysis of the stress pattern in the neighborhood of a slip band leads to a qualitative interpretation of the salient features of fatigue. Such a stress pattern is illustrated in Fig. 9 for the case after a slip band has formed but before the applied stress is removed. The shear stress in the regions on either side of the slip bands has become partially relaxed. On the other hand, the shear stress has become highly concentrated in the region immediately adjacent to the ends of the slip bands. The high tensile stresses associated therewith lead to the formation of a small crack, as indicated in Fig. 8. This crack will not propagate outside of the zone of high stress concentration, for its size is too small to be propagated by the applied stress. Since the dimensions of the zone of the high stress concentration are comparable to the width of the slip band, the length of the crack will likewise be comparable to the width of the slip band. When the applied stress is now reversed, those regions in which the stress had formerly relaxed will now have a higher stress than the applied stress. If the original slip band is not susceptible of further deformation, the adjacent region will now slip in the opposite direction, again partially relieving shear stress in adjacent regions. Each successive alteration of stress thus increases the width of the slip band, and hence also the length of the cracks at edges of slip bands. When the cracks have attained sufficient length, the specimen fractures.

The above description of a slip band under fatigue conditions shows that the slip band must necessarily broaden. This has in fact been observed.[15] The above description also indicates that the progress of fatigue is intimately associated with residual stresses in the region surrounding the slip bands. If these stresses could be relieved by some process, the contribution to fatigue of all prior slipping could be eliminated. It appears that the harmful effects of overstressing, and their elimination by understressing, are explicable in terms of these residual stresses. The above description in fact suggests a multitude of experiments that have not as yet been undertaken. Examples are: the measurement of fracture stress before fatigue failure as a function of number of stress reversals; elimination of harmful effects of prior fatigue by application of a set of reversals of slowly decreasing amplitudes.

[21] H. F. Moore and J. B. Kommers, *The Fatigue of Metals* (McGraw-Hill Book Company, Inc., New York, 1927).

[22] J. A. Ewing and J. C. W. Humfrey, "Fracture of metals under repeated alterations of stress," Phil. Trans. Roy. Soc. **200**, A241 (1903).

[23] H. J. Gough, "Crystalline structure in relation to failure of metals—especially by fatigue," Proc. A. S. T. M. **33**, Pt. 2, 3 (1933).

Some Integral Equations of Potential Theory

BY H. BATEMAN

California Institute of Technology, Pasadena, California

1. INTRODUCTION

INTEGRAL equations arise either directly or methodically. The direct formulation of a problem by means of assumed or recognized principles frequently involves integration and may lead to an integral equation in which the unknown function has a simple physical meaning. When, for instance, use is made of the superposition of effects, one of the factors in the elementary law may be known while the other is unknown and is to be found from the equation set up. For example, one factor may be a force and the other a density.

When an integral equation arises methodically in the analysis of a problem, the unknown function or functions may be auxiliary and needed only for the ultimate expression of the physical quantities. When it happens that the auxiliary functions do have a direct physical meaning, the method gives the principles for a direct treatment. One fruitful method is to introduce all the supplementary conditions when definite integrals involving arbitrary functions are used to represent suitable types of solution of the partial differential equations of a problem.[1]

2. INVERSE PROBLEMS

In the theory of attractions either the law of force or the nature of the attracting matter may be sought from observations or field data. Progress has generally been obtained by making assumptions and analyzing their consequences in an endeavor to account for the facts. A simple consequence of the Newtonian law of attraction between particles was used, for instance, by Joseph Priestley in a deduction of the law of force between electrified particles from a known property of an electrified conductor. This is pointed out by Whittaker.[2] The effect of a conductor in modifying the action of a charged body also provided an inverse problem in which the aim was to find the induced surface distribution of electricity on the conductor which was regarded as responsible for the effect. This problem was ultimately formulated as an integral equation.

Problems in the theory of attractions relating to the figure of the earth were ultimately formulated as integral equations. For the history and terminology of these problems reference may be made to Bulletin 78 of the National Research Council and particularly to the article of W. D. Lambert.[3] When it is desired to derive the form of the geoid from the gravitational field of the earth, an integro-differential equation is derived whose solution is not unique as was noted by Brillouin[4] and other writers. Mineo[5] made the solution unique by adding certain assumptions. When these are of the type used by Stokes, the integral equation is of Fredholm's type and had been noted previously by Signorini.[6] Tables for determining the form of the geoid and its indirect effect on gravity are provided by Lambert in the chapter mentioned and in a later work in which he collaborated with F. W. Darling.[7] A Fredholm equation was found also by Idelson[8] who used the potential of a simple layer (the disturbing layer) in an equation of Helmert. For the equation of Fredholm the well-known methods of Neumann, Fredholm, Hilbert, and Schmidt are available. One good feature of these methods is that the inversion formulae generally involve integrations rather than differentiations which are hard to make accurately when data are few

[1] H. Bateman, Report, British Assoc. Adv. Sci., Sheefield, 4060407 (1910).

[2] E. T. Whittaker, *History of the Theories of Aether and Electricity* (University Press, Dublin, 1910), p. 50.

[3] See W. Lambert, *The Shape and Size of the Earth* (Nat. Acad. Sci., Washington, D. C.), Chapter IX.

[4] M. Brillouin, Comptes rendus **180**, 987–992 (1925); **181**, 749–752 (1925).

[5] C. Mineo, Palermo rendus **51**, 293–303 (1927).

[6] A. Signorini, Acc. dei Lincei [5] **20**, 154–160, 219–222 (1911). See also N. Moisseiev, Gerlands Beitr. z. Geophys. **42**, 279–290 (1934); B. Saltykov, Acad. Sci. USSR, Comptes rendus (Doklady) [2] **16**, 133–140 (1937); Jahrb. Fortschritte Math. **63**, 407 (1937).

[7] W. D. Lambert and F. W. Darling, U. S. Coast Geod. Surv., Spec. Pub. **199**, 137 (1936).

[8] N. Idelson, Gerlands Beitr. z. Geophys. **40**, 24–28 (1933).

and inexact, yet the numerical work with the inversion formulae is often very great.

3. DATA ON A VERTICAL LINE

Joachimstahl[9] in 1861 sought a law of force such that the potential of a uniform distribution of matter along a line may be an assigned function of the distance of an attracted particle from the line. His equation resembled Abel's integral equation and was solved by a known inversion formula. Beltrami[10] also made a clever use of the inversion formula for Abel's equation to solve a mixed problem of potential theory in which a symmetrical potential has given values over a circular disk and the normal derivative is zero over the part of the disk's plane outside the disk. This is really a particular case of the problem of Dirichlet—to find a potential function, regular in a region, from assigned values on the boundary of the region—the surface values assigned on the two faces of the disk being such that the desired potential function is symmetrical about the plane of the disk.

Dhar[11] discussed Joachimstahl's problem and formulated a second problem with vertical line data in which the aim was to find a rectilinear layer symmetrical about a point O on the carrying line and such that, with the Newtonian law of force, the attraction at a point P is an assigned function $f(h)$ of the distance $OP(=h)$, when OP is normal to the line. The integral equation for the linear density $F(t)$ is

$$f(h)=2h\int_0^\infty (h^2+t^2)^{-1}F(t)dt, \qquad (3.1)$$

and is of a well-known type because $\frac{1}{2}f(h)$ can be regarded as the value on the line of symmetry OP of a symmetrical potential V whose value on the plane $(z=0)$ normal to OP is $F(r)/r$, where r is the distance from O. The integral is then a special case of the integral of Poisson for the solution of the Dirichlet problem for a region bounded by a plane. The inversion formula

$$F(t)=(t/2\pi)\int_0^\pi f(it\cos a)da \qquad (3.2)$$

is sometimes useful but requires a continuation of $f(h)$ to complex values of h and, perhaps, a derivation from the data of the derivatives of the function f. A similar remark applies when use is made of power series in ascending or descending powers of h and the associated series of Legendre functions. The data must be plentiful and accurate to permit a determination of the derivatives or series.

The use of vertical line data has been developed by some members of the Gulf Research and Development Company and a partial account of some of the methods that are used by this and other companies is given in papers of Evjen[12] and Hughes.[13]

The inversion formula

$$f(h)=2\int_0^\infty e^{-hz}dz\int_0^\infty J_0(zt)F(t)dt \qquad (3.3)$$

makes the determination of $F(t)$ depend on the solution of integral equations of well-known types, $J_0(w)$ being the Bessel function of zero order. A practical method of solving the equation with exponential integral is developed in this paper.

4. IMPROVEMENTS IN OBSERVATIONAL METHODS

A description of some of the instruments used in gravity work is given in Bulletin 78 already mentioned, but the invention of instruments of

[9] F. Joachimstahl, J. reine angew. Math. **58**, 135–137 (1861).

[10] E. Beltrami, Acad. Sci. Bologna, Mem. [4] **4**, 211–246 (1882), Opere, v. 4, 45–67. An account of Beltrami's work is given in A. G. Webster, *Partial Differential Equations of Mathematical Physics*, edited by S. J. Plimpton (G. E. Stechert and Company, New York, 1933), second edition, pp. 368–375. For a good account of the theory of Abel's integral equation see M. Bôcher, *An Introduction to the Study of Integral Equations* (Cambridge University Press, New York, 1909). In the case of Joachimstahl's equation

$$f(h)=\int_h^\infty \frac{F(r)dr}{(r^2-h^2)^{\frac{1}{2}}};$$

the inversion formula,

$$F(r)=-(2/\pi)\int_h^\infty \frac{rf'(h)dh}{(h^2-r^2)^{\frac{1}{2}}},$$

is derivable from the results mentioned by Bôcher by a simple substitution. A good survey of the literature on equations resembling Abel's equation is given by H. T. Davis, "A survey of methods for the inversion of integrals of Volterra type," Indiana University Studies **14**, Nos. 76, 77 (1927).

[11] S. C. Dhar, Bull. Calcutta Math. Soc. **10**, 151–156 (1918–1919).

[12] H. M. Evjen, Geophys. **3**, 72–95 (1938).

[13] D. S. Hughes, Geophys. **7**, 169–178 (1942).

precision during the last 25 years has placed much more valuable equipment within the reach of men interested in observations of gravity. The invention by Baron Roland von Eötvös[14] of a torsion valance and of a more general apparatus permitting a determination of the curvature of the lines of force of the weight field of the earth did much to arouse interest in accurate observations and in gravity methods of geophysical prospecting for, as is remarked for instance by Roever,[15] local irregularities, such as minerals and mountains, may produce curvatures much larger than those given by the potential function whose level surface is the standard spheroid of geodesy. A brief history of the development of the gravity method of prospecting for oil is given by Eckhardt.[16] It seems that this work started in Europe about 1915 and in the United States about 1924. The subject is discussed also by Shaw and Lancaster Jones.[17] An instrument like the Eötvös balance but much smaller was used by Jones and Davies[18] for gravity measurements. It was thought that a handy instrument would facilitate observations giving valuable information concerning the shape and dimensions of buried anticlines. Many other instruments embodying pendulums or springs have been devised for measurements of gravity. An account of some of these has been given by Hoskinson.[19]

Eckhardt says that in the period 1930–1935 the torsion balance began to be superseded by the gravimeter. For the evolution of this instrument reference may be made to the papers of Skeeters,[20] Mott-Smith,[21] Hammer,[22] Neuman,[23] Bruckshaw,[24] Welch,[25] Clewell,[26] Fenwick,[27] McCollum and Brown,[28] Heiland,[29] and many others. In 1937 Stubbe and Schmidt[30] compared the gravimeter with the torsion balance and concluded that the latter was preferable, but Thyssen,[31] who can speak with some authority, disagrees. For other types of balance or observing instrument references may be made to papers of Duffield,[32] Soler,[33] Vening Meinesz,[34] Lancaster Jones,[35] Tomaschek and Schaffernicht,[36] Holweck,[37] and numerous papers by A. Schleusner, S. v. Thyssen, and others.[38]

5. HORIZONTAL LINE DATA

Although some of the inverse problems of potential theory had been stated and partially solved before 1930 when many workers became interested in geophysical prospecting, the actual use of the methods of integral equations was delayed because the data were not sufficiently accurate. With the advent of instruments of precision the situation was somewhat changed, and some members of the staff of the Gulf Research and Development Company began to study a very simple integral equation in order to acquire some skill in the solution of inverse potential problems. A solution of this guiding integral equation in the form of a double integral of Fourier type was obtained by H. M. Evjen but was not regarded as suitable for purposes of calculation. Evjen then wrote to the present author to ask if his method was new and if another method of solution was available which would involve, say, only one integration.

[14] R. von Eötvös, Konferenz der Erdmessung, Budapest **1**, 337–395 (1906). Ann. d. Physik **68**, 11–66 (1922). See also W. Haubold, Zeits. f. Geophysik **8**, 446–453 (1932).
[15] W. H. Roever, "The Weight Field of the Earth," Washington University Studies, new series, Science and Technology, No. 11 (1940).
[16] E. A. Eckhardt, Geophys. **5**, 231–242 (1940).
[17] H. Shaw and E. Lancaster Jones, Proc. Phys. Soc. London **35**, 151–166, 204–212 (1923).
[18] J. H. Jones and R. Davies, Roy. Astronom. Soc. Geophys. Suppl. **2**, 1–32 (1928).
[19] A. J. Hoskinson, Trans. Am. Geophys. Union, 44–45 (1936).
[20] W. W. Skeeters, Mines Mag. **29**, 304–309 (1939); **31**, 127–129, 472, 495 (1941).
[21] L. M. Mott-Smith and F. W. Mott-Smith, Petroleum Eng. **10**, 85–86, 89–90, 92, 94, 96–97 (1939); L. M. Mott-Smith, World Petroleum **11**, 64–67 (1940).
[22] S. Hammer, Geophys. **4**, 184–194 (1939).
[23] G. Neuman, Zeits. Bohrtechniker **58**, 33–37, 53–58 (1940).
[24] J. M. Bruckshaw, Proc. Phys. Soc. London **53**, 449–465, discussion 465–467 (1941).
[25] G. I. Welch, Rev. Sci. Inst. **12**, 179–181 (1941).
[26] D. H. Clewell, Geophys. **7**, 155–168 (1942).
[27] W. H. Fenwick, Mines Mag. **32**, 504–507, 509 (1943).
[28] E. V. McCollum and A. Brown, Geophys. **8**, 379–390 (1943).
[29] C. A. Heiland, Geophys. **8**, 119–133 (1943).
[30] G. Stubbe and K. H. Schmidt, Petroleum Eng. **8**, 137–139 (1937).
[31] S. v. Thyssen, Petroleum **23**, 34–36 (1937).
[32] W. G. Duffield, Roy. Astron. Soc. Geophys. Suppl. **1**, 161–204 (1924).
[33] E. Soler, Washington Acad. Sci. **16**, 261–266 (1926).
[34] F. A. Vening Meinesz, *Theory and Practice of Gravity Observations at Sea* (Waltman, Delft, 1929).
[35] E. Lancatser Jones, J. Sci. Inst. **9**, 341–353, 373–380 (1932).
[36] R. Tomaschek and W. Schaffernicht, Ann. d. Physik **5**, **15**, 787–824 (1932).
[37] F. Holweck, Bull. Geodesique **46**, 295–303 (1935).
[38] A. Schleusner, S. v. Thyssen, *et al.* Beitr. z. angew. Geophys. **4–6**.

As a matter of fact a solution of the desired type had been found by Chester Snow[39] in 1923. He had obtained the integral equation (with a restriction on the unknown function, which was, in his case, odd) in a spectroradiometric analysis of radio signals. Snow derived the solution also in the form of a double integral but reduced this to a single integral and extra terms by an operational method. The result was found also by means of Cauchy's theorem and some remarks were made on numerical methods.

In a reply to Evjen's letter the present author gave a method of analytical continuation which led naturally to the simple form of solution. This method seems to be of wide application in inverse potential problems in which the assigned function is analytic in the sense of Weierstrass (capable of continuation by means of power series) as it presumably is on account of the properties of a regular potential. On this account I have ventured to dedicate this description of subsequent developments to the Gulf Research and Development Company and to Dr. Evjen in particular as his letter[40] provided the stimulus which led to the development of the method now to be discussed.

6. THE GUIDING EQUATION

The integral equation mentioned in the introduction is

$$f(x)=(1/\pi)\int_{-\infty}^{\infty}\frac{yF(t)dt}{(x-t)^2+y^2}, \qquad (6.1)$$

where y is a fixed positive quantity, $f(x)$ is an analytic function supposed to be determined from observation and presumably of the right type for representation by such an expression, and $F(t)$ is the function to be determined. This function is required to be such that the integral exists and represents a potential $V(x, y)$ regular for $y>0$ which is the solution of the Dirichlet problem for the half-plane. The properties of this integral of Poisson are well known. To fix ideas we shall suppose that $F(t)$ and $F'(t)$ are finite and continuous for all real values of t, but a case in which $F(t)$ is piece-wise continuous will be considered later.

The assigned values of $f(x)$ may be used to construct a potential

$$W(x, Y)=(1/\pi)\int_{-\infty}^{\infty}\frac{(Y-y)f(t)dy}{(x-t)^2+(Y-y)^2}, \qquad (6.2)$$

which is regular for $Y>y$ and such that $W(x, y)=f(x)$. The potential $W(x, Y)$ is identical with $V(x, Y)$ for $Y>y$; but when $Y<y$, the integral on the right does not represent $V(x, Y)$ but a different potential which has the value $-f(x)$ when $Y=y$. As the particular example

$f(x)=\cos(mx)$,

$$\begin{aligned} W(x, Y)&=e^{-m(Y-y)}\cos(mx) \quad Y>y \\ W(x, Y)&=-e^{m(Y-y)}\cos(mx) \quad Y<y \end{aligned} \qquad (6.3)$$

indicates, the derivative $W_y(x, Y)$ is continuous when $Y=y$, and so the correction which must be added to $W(x, Y)$ to give $V(x, Y)$ must have a zero derivative for $Y=y$. Within the region of analyticity of this correction term

$$V(x, Y)=f(x+iY-iy)+f(x-iY+iy)+(1/\pi)\int_{-\infty}^{\infty}\frac{(Y-y)f(t)dt}{(x-t)^2+(Y-y)^2}. \qquad (6.4)$$

Since $V(x, Y)\to F(x)$ when $Y\to 0$, we have Snow's inversion formula

$$F(x)=f(x-iy)+f(x+iy)-(1/\pi)\int_{-\infty}^{\infty}\frac{yf(t)dt}{(x-t)^2+y^2}, \qquad (6.5)$$

the correctness of which may be checked by direct substitution, if a change in the order of integration is permissible. My friend Stephen O. Rice[41] of the Bell Telephone Laboratories has checked the formula with the aid of Cauchy's theorem.

7. THE CONJUGATE EQUATION

The conjugate of the guiding equation is

$$g(x)=(1/\pi)\int_{-\infty}^{\infty}\frac{(x-t)F(t)dt}{(x-t)^2+y^2}, \quad F(\pm\infty)=0. \qquad (7.1)$$

The integral on the right represents a potential function $U(x, y)$ regular for $y>0$ which is the conjugate of $V(x, y)$. In the region $Y>y$, $U(x, Y)$

[39] C. Snow, Sci. Pap. Bur. Stand. 19, 231–261, No. 477 (1923).

[40] H. M. Evjen, letter dated July 18, 1930.

[41] Stephen O. Rice, letter dated August 30, 1945.

may be represented by Poisson's integral

$$U(x, Y)=(1/\pi)\int_{-\infty}^{\infty}\frac{(Y-y)g(t)dt}{(x-t)^2+(Y-y)^2}. \quad (7.2)$$

The continuation of this into the region $Y<y$ (or that part in which the added term is analytically continuable) is

$$U(x, Y)=g(x+iY-iy)+g(x-iY+iy)+\frac{1}{\pi}\int_{-\infty}^{\infty}\frac{(Y-y)g(t)dt}{(x-t)^2+(Y-y)^2}. \quad (7.3)$$

To find $F(t)$ we write down the conjugate potential

$$V(x, Y)=ig(x+iY-iy)-ig(x-iY+iy)-\frac{1}{\pi}\int_{-\infty}^{\infty}\frac{(x-t)g(t)dt}{(x-t)^2+(Y-y)^2}, \quad (7.4)$$

zero being apparently the appropriate value of an additive constant. For $Y=0$ this gives the inversion formula

$$F(x)=ig(x-iy)-ig(x+iy)-(1/\pi)\int_{-\infty}^{\infty}\frac{(x-t)g(t)dt}{(x-t)^2+y^2}, \quad (7.5)$$

which may be tested by putting $F(t)=\sin(mt)$, $g(x)=-e^{-my}\cos(mx)$. It may be checked by direct substitution and a change in the order of integration.

8. SOLUTION BY MEANS OF ORTHOGONAL FUNCTIONS

When the function $g(x)$ is derived from $f(x)$ by means of the known formula

$$g(x)=(1/\pi)P\int_{-\infty}^{\infty}\frac{f(t)dt}{x-t}, \quad (8.1)$$

in which the P before the integral indicates that the integral has its principle value, a method of solution is possible in which use is made of the expressions for the derivatives of $f(x)$ and $g(x)$

$$f^{(n)}(x)=(n!/\pi y^n)\int_0^{\pi}F(x+y\cot a)\times\sin(n+1)a\,\sin^{n-1}a\,da, \quad (8.2)$$

$$g^{(n)}(x)=-(n!/\pi y^n)\int_0^{\pi}F(x+y\cot a)\times\cos(n+1)a\,\sin^{n-1}a\,da. \quad (8.3)$$

When linear combinations of the functions

$$u_n(a)=\sin(n+1)a\,\sin^{n-1}a,\qquad v_n(a)=\cos(n+1)a\,\sin^{n-1}a \quad (8.4)$$

are used to form the complete set of orthogonal functions,

$$1,\ \cos 2a,\ \sin 2a,\ \cos 4a,\ \sin 4a,\ \cos 6a,\ \sin 6a,\ \cdots, \quad (8.5)$$

it is seen that linear combinations of $f^{(n)}(x)$, $g^{(n)}(x)$ over various values of n will give the Fourier constants of $F(x+y\cot a)$ and so by Fejér's theorem give a practical way of determining this function whenever it is continuous over the infinite range with $F(\pm\infty)=0$. For Fejér's theorem see Whittaker and Watson.[42]

9. GENERALIZATION OF THE GUIDING EQUATION

Consider a potential $V(x, y)$ defined for the region R outside a curve C by the integral

$$V(x, y)=\int_C G_n[x, y, u(t), v(t)]F(t)dt, \quad (9.1)$$

which solves the problem of Dirichlet for the region R when V has the assigned value $F(t)$ at the point $x=u(t)$, $y=v(t)$ of the curve C. When y has a fixed positive value such that the point (x, y) is outside C for all real values of x, the equation

$$f(x)=\int_C G_n[x, y, u(t), v(t)]F(t)dt \quad (9.2)$$

may be regarded as an integral equation for the determination of $F(t)$. The potential $V(x, Y)$ may be defined for $Y<y$ and for the exterior of C by the expression (6.4) and its analytical continuation. When $x=u(T)$, $y=v(T)$ this gives the inversion formula

$$F(T)=f[u(T)+iv(T)-iy]+f[u(T)-iv(T)+iy]+(1/\pi)\int_{-\infty}^{\infty}\frac{[v(T)-y]f(t)dt}{[u(T)-t]^2+[v(T)-y]^2}. \quad (9.3)$$

A simple case in which the function G_n is known is that in which C is the circle $x^2+y^2=a^2$. Another case in which G_n is known is that in which the region R lies outside the wedge bounded by

[42] Whittaker and Watson, *Modern Analysis* (Cambridge University Press, New York), Chap. IX.

the lines $\theta=0$, $\theta=\pi+p\pi$ $(p>0)$. It should be noted that in the latter case there are two different paths of analytical continuation of the correction term. One path leads to the upper face of the wedge, the other path leads to the lower face of the wedge. This feature is particularly noticeable when the wedge reduces to a double line $y=0$, $x>0$. Generally the function $f(x)$ has different values at points with equal x but on opposite sides of the line. When, however, the two values of $f(x)$ are equal but of opposite sign, the potential $V(x, y)$ is an odd function of y and is zero for $y=0$, $x<0$. This case will be discussed by another method in Section 1.

10. OBSERVATIONS ALONG A CURVE

Conformal representation may be useful in reducing this case to that already considered but other methods are available. When the curve is the circle $r=a$ (r and θ being polar coordinates), the problem of analytical continuations may be stated as follows: A potential V, regular for $r>a$, has the value $f(\theta)$ at $x=a\cos\theta$, $y=a\sin\theta$ and is given by Poisson's integral

$$V=(1/2\pi)\int_0^{2\pi}\frac{(r^2-a^2)f(u)du}{r^2+a^2-2(x\cos u+y\sin u)a}. \quad (10.1)$$

For $r<a$ this integral represents the regular potential with the value $-f(\theta)$ at $x=a\cos\theta$, $y=a\sin\theta$. How, then, can a potential V which is regular in a region R including the whole exterior of the circle and part of its interior, including the boundary, be continued from the outside to the inside? The appropriate correction is in this case

$$C(r,\theta)=f[\theta+i\log(r/a)]+f[\theta-i\log(r/a)], \quad (10.2)$$

and is suitable for the solution of the integral equation which arises when $V(x, y)$ gives the solution of the Dirichlet problem for the region outside a curve C lying entirely within the circle $r=a$. When C is a circle, $r=b$; the integral equation and its solution can be easily written down but the result will not be given here because it may be derived by conformal representation from the solution of the guiding equation. Amerio[43] has recently given a proof, not depending on conformal representation, that a potential assuming analytical values on a segment of an analytic curve can be extended analytically across that curve. The proof depends upon the analytical character of the solution of an integral equation of Fredholm's type which gives the density of the double layer used in the representation of the potential function.

[43] L. Amerio, Portugaliae Math. **2**, 173–176 (1941).

11. GENERALIZATIONS OF THE PROBLEM OF DIRICHLET

Interest in the integral equations of potential theory was much stimulated by the work of Karl Neumann[44] on the solution by means of series of some integral equations furnished by the problem of Dirichlet and the related problems when use was made of potentials of simple or double layers for the representation of the desired potential. The introduction by Henri Poincaré[45] of a parameter λ into these problems was an important extension because it led to his surmise that the solution in series could be expressed as the ratio of two entire functions of λ, and this led Fredholm[46] to seek explicit expressions for these two functions. The work was ably continued by Plemelj[47] and others and good accounts of the progress along these lines are in books on potential theory such as those of Kellogg[48] and of Sternberg and Smith.[49] In the case of Neumann's equation and a vast number of others, the data or assigned values are at points on the line or surface carrying the distribution to be determined. When the data are "free air values," that is, at points not on covered surface, the integral equation is of the first kind, and the observed function is not arbitrary but is restricted by a large number of linear conditions which are often hard to formulate fully. When, however, the data are of the required type, the nature of the type

[44] K. Neumann, Akad. Wiss. Wien **22**, 264–326 (1870); *Untersuchungen über das logarithmische und Newton'sche Potential* (B. G. Teubner, Leipzig, 1877).
[45] H. Poincaré, *Théorie du potential Newtonien* (G. Carré et C. Naud, Paris, 1899).
[46] I. Fredholm, Acta Math. **27**, 365–390 (1903).
[47] J. Plemelj, Monats. Math. Physik **15**, 337–411 (1904); **18**, 180–210 (1907).
[48] O. D. Kellogg, *Potential Theory* (Verlagsbuchhandlung Julius Springer, Berlin, 1929).
[49] W. J. Sternberg and T. L. Smith, *The Theory of Potential and Spherical Harmonics* (The University of Toronto Press, Toronto, 1944).

of inversion formula to expect is indicated by Snow's series.

$$F(x)=2\sum_{n=0}^{\infty}[(-y^2)^n/(2n)!]f^{(2n)}(x) - (1/\pi)\int_{-\infty}^{\infty}\frac{yf(t)dt}{(x-t)^2+y^2} \quad (11.1)$$

for the solution of the guiding equation. It will be noticed that in addition to an integral involving the observed function $f(x)$ there is also a series involving $f(x)$ and its derivatives. This feature will be useful in the treatment of the problems in three dimensions.

12. THE PROBLEMS IN THREE DIMENSIONS

In space of three dimensions the guiding equation is

$$f(x, y)=(1/2\pi)\int_{-\infty}^{\infty}\int zF(s, t)dsdt/r^3, \quad (12.1)$$

where

$$r^2=z^2+(x-s)^2+(y-t)^2,$$

and z is a fixed positive quantity. The integral on the right is the well-known solution of the Dirichlet problem for the region $z>0$. It is the potential of a double layer over the plane and can also be interpreted as the z component of force due to a simple layer on the plane.

For the region $Z>z$ there is a similar integral

$$W(x, y, Z)=(1/2\pi)\int_{-\infty}^{\infty}\int (Z-z) \times f(s, t)dsdt/R^3, \quad (12.2)$$

where

$$R^2=(Z-z)^2+(x-s)^2+(y-t)^2.$$

For $Z>z$ we have $X(x, y, Z)=V(x, y, Z)$ where V is the potential regular for $Z>0$ with the value F when $Z=0$. For $Z<z$ the integral W is not equal to V and so by analogy with Snow's formula and our previous method, we introduce a correction in the form of a series and write for $0\leq Z\leq z$

$$V(x, y, Z)=2\sum_{n=0}^{\infty}[(Z-z)^{2n}/(2n)!] \times(-\nabla^2)^n f(x, y)+W(x, y, Z), \quad (12.3)$$

where $\nabla^2=\partial^2/\partial x^2+\partial^2/\partial y^2$. For $Z=0$ this gives the inversion formula

$$F(x, y)=2\sum_{n=0}^{\infty}[z^{2n}/(2n)!](-\nabla^2)^n f(x, y) - (1/2\pi)\int_{-\infty}^{\infty}\int zf(s, t)dsdt/r^3. \quad (12.4)$$

When in particular,

$$f(x, y)=\cos(my)f(x),$$
$$F(x, y)=\cos(my)F(x)$$

there is a simplification and the formula becomes

$$f(x)=(1/\pi)\int_{-\infty}^{\infty}K_1(mr)F(s)ds, \qquad r^2=z^2+(x-s)^2, \quad (12.5)$$

$$F(x)=2\sum_{n=0}^{\infty}[z^{2n}/(2n)!](m^2-D^2)^n f(x) - (1/\pi)\int_{-\infty}^{\infty}K_1(mr)f(s)ds, \quad (12.6)$$

where

$$K_0(mu)=\int_0^{\infty}\cos(mt)dt/(u^2+t^2)^{\frac{1}{2}}, \qquad K_1(x)=-DK_0(x), \quad D=d/dx. \quad (12.7)$$

It should be mentioned that S. O. Rice,[41] in the letter already mentioned, has obtained a solution of the equation corresponding to (12.5) with $K_0(mr)$ in place of $K_1(mr)$.

13. THE USE OF LAPLACIAN INTEGRALS

Let us now consider the equation

$$f(x)=(1/\pi)\int_0^{\infty}\frac{yF(u)du}{(x+u)^2+y^2}, \quad x>0, \quad y>0. \quad (13.1)$$

This differs from the guiding equation because (1) the double layer covers only half the x axis, namely the part for which $x<0$ and (2) because $f(x)$ is assigned only for positive values of x. It should be noticed that the notation is not quite the same as that of Section 6. When a change in the order of integration is valid there is an equivalent formula

$$fx=\int_0^{\infty}F(u)du\int_0^{\infty}e^{-(x+u)t}\sin(yt)dt, = \int_0^{\infty}e^{-xt}\sin(yt)dt\int_0^{\infty}e^{-ut}F(u)du, \quad (13.2)$$

which indicates that (13.1) may be replaced by two integral equations of Laplace's type

$$f(x)=\int_0^\infty e^{-xt}\sin(yt)G(t)dt,$$
$$G(t)=\int_0^\infty e^{-ut}F(u)du. \tag{13.3}$$

If $\sin(yt)G(t)$ and $F(u)$ are required to be continuous, the solutions of these equations, when existent, are unique. Lerch's theory indicates also that a knowledge of $f(x)$ for positive integral values of x or for a set of values in arithmetical progression is sufficient to determine $\sin(yt)G(t)$ and consequently the values of f for non-integral values of x. It should, then, be possible to derive these latter values directly by a formula of interpolation.

14. A FORMULA OF INTERPOLATION FOR LAPLACIAN INTEGRALS

A formula which is particularly suitable for this interpolation has been recommended by the author[50] and by Erdélyi.[51] It is

$$f(x)=\frac{c_0}{x}+\frac{c_1(1-x)}{x(1+x)}+\frac{c_2(1-x)(2-x)}{x(1+x)(2+x)}+\cdots. \tag{14.1}$$

The coefficients c_n are found by giving x the values 1, 2, 3, $\cdots$ in turn, thus $f(1)=c_0$, $f(2)=\frac{1}{2}c_0-c_1/6$, and it is found that generally

$$c_n=(2n+1)P_n(1-2E)f(1), \tag{14.2}$$

where $P_n(z)$ is the polynomial of Legendre of order n and E is an operator of a distributive nature such that E^s changes $f(1)$ into $f(s+1)$. The series found by expressing each term in the formula of interpolation as a Laplacian integral is in this case

$$(1/\pi)\sin(yt)G(t)=\sum_{n=0}^{\infty}c_nP_n(1-2e^{-t}), \tag{14.3}$$

and this can be used effectively to provide values of $G(t)$ for $t=1, 2, 3, \cdots$ with the aid of a table of $P_n(1-2e^{-t})$ for $t=1, 2, 3, \cdots$. Table I covers the ranges $n=0(1)10$, t; $1(1)20$ with $15D$, and an attempt is being made to extend it to higher values of n. The table was calculated from the tables of the exponential function of the Mathematical Tables Project of New York sponsored

TABLE I. $P_n(1-2e^{-t})$.

t \ n	1	2
1	0.26424 11176 57115	−0.39526 49476 08978
2	.72932 94335 26775	+0.29788 21339 12729
3	.90042 58632 64272	.71615 01028 52814
4	.96336 87222 22532	.89211 89424 35010
5	.98652 41060 01829	.95984 47175 84062
6	.99504 24956 46667	.98516 43522 14122
7	.99817 62360 68891	.99453 36973 78988
8	.99932 90747 44195	.99798 78994 43633
9	.99975 31803 91827	.99925 96325 55358
10	.99990 92001 40475	.99972 76127 88347
11	.99996 65965 98420	.99989 97914 68939
12	.99998 77115 75293	.99996 31349 52388
13	.99999 54793 41186	.99998 50108 31834
14	.99999 83369 42562	.99999 81645 86638
15	.99999 93881 95359	.99999 81645 86638
16	.99999 97749 29651	.99999 93247 89028
17	.99999 99172 01246	.99999 97516 03747
18	.99999 99695 40041	.99999 99086 20123
19	.99999 99887 94407	.99999 99663 83222
20	.99999 99958 77693	.99999 99876 33078

t \ n	3	4
1	−0.35023 61643 16206	0.13449 18185 76736
2	−0.12412 92757 10654	−0.38184 10855 26292
3	+0.47444 95488 03890	+0.21049 90508 35291
4	.79015 33279 25199	.66302 65464 69307
5	.92050 05158 57439	.86928 43716 52798
6	.97043 89956 51009	.95097 58060 24902
7	.98908 23471 09798	.98183 70921 66184
8	.99597 78237 65385	.99330 08703 23373
9	.99851 95392 12762	.99753 31743 53326
10	.99945 52626 75587	.99909 21868 95476
11	.99979 95879 58828	.99966 59910 88756
12	.99992 62705 84296	.99987 71191 50522
13	.99997 28762 00388	.99995 47938 71677
14	.99999 00216 76114	.99998 33694 87847
15	.99999 63291 74961	.99999 38819 62012
16	.99999 86495 78283	.99999 77492 97645
17	.99999 95032 07525	.99999 91720 12610
18	.99999 98172-40250	.99999 96954 00426
19	.99999 99327 66444	.99999 98879 44074
20	.99999 99752 66157	.99999 99587 76928

t \ n	5	6
1	0.34415 78146 74583	0.05464 80014 52797
2	−0.40197 48761 18927	−0.21928 12946 63080
3	−0.03838 98178 26693	−0.23878 90479 34199
4	+0.51760 76040 90602	+0.36166 40008 03395
5	.80722 55650 05097	.73556 67348 63206
6	.92691 92142 65318	.89844 75100 59999
7	.97281 77378 76441	.96204 89278 14871
8	.98995 97324 16840	.98595 77710 19097
9	.99630 09031 20756	.99482 31816 62974
10	.99853 09031 20756	.99809 40684 77302
11	.99949 90075 52514	.99929 86457 16643
12	.99981 56815 57053	.99974 19589 36336
13	.99993 21911 90691	.99990 50683 10682
14	.99997 50542 83629	.99996 50760 84201
15	.99999 08229 50036	.99998 71521 41840
16	.99999 66239 47428	.99999 52735 27981
17	.99999 87580 19044	.99999 82612 26878
18	.99999 95431 11656	.99999 93603 40948
19	.99999 98319 16113	.99999 97646 82563
20	.99999 99381 65392	.99999 99134 31550

[50] H. Bateman, Proc. Nat. Acad. Sci. **25**, 262–265 (1939). See also E. Hille, Compositio Math. **6**, 93–102 (1938).
[51] A. Erdélyi, J. London Math. Soc. **18**, 72–77 (1943); Phil. Mag. [7] **34**, 533–537 (1943).

by the National Bureau of Standards. It is thought that this and similar tables may be useful for the tabulation of functions defined by definite integrals which are hard to compute directly but have simple Laplace transforms.

The convergence of the Legendre series may be improved by a simple device. Thus the equation

$$G(t)=\int_0^\infty e^{-ut}F(u)du \qquad (14.4)$$

may be replaced by

$$h(t)=G(t+c)=\int_0^\infty e^{-ut}\cdot e^{-cu}F(u)du, \qquad (14.5)$$

and if c is positive the Legendre series for $e^{-cu}F(u)$ derived from $h(t)$ generally converges more rapidly than the series for $F(u)$ derived from $G(t)$. When the product $e^{-cu}F(u)$ has been derived by means of the Legendre series, the function $F(u)$ may be deduced with the aid of the table of exponential functions already cited.

TABLE I (*continued*).

$t \backslash n$	7	8
1	−0.26817 48023 26647	−0.18068 47715 50211
2	+0.04744 04893 23003	+0.25688 19941 18463
3	−0.36640 21347 36359	−0.40970 70706 13055
4	+0.20339 42382 48305	+0.05093 82503 44370
5	.65573 61016 54870	.56931 56160 02127
6	.86577 13712 05337	.82913 21271 95702
7	.94956 00489 40862	.93538 52422 93312
8	.98129 90110 20097	.97598 81367 27241
9	.99310 05569 44491	.99113 36665 21429
10	.99745 91437 72468	.99673 38012 46168
11	.99906 49156 19968	.99879 78289 73036
12	.99965 59526 47257	.99955 76642 75112
13	.99987 34254 13111	.99983 72627 20031
14	.99995 34349 14456	.99994 01308 03434
15	.99995 28695 40755	.99997 79751 50830
16	.99999 36980 39790	.99999 18974 83377
17	.99999 76816 36173	.99999 70192 47002
18	.99999 91471 21310	.99999 89034 41751
19	.99999 96862 43423	.99999 95965 98696
20	.99999 98845 75400	.99999 98515 96945

$t \backslash n$	9	10
1	0.14819 38218 87370	0.23699 54125 74554
2	0.31162 84080 67464	0.20063 77685 73120
3	−0.37146 40496 78268	−0.26611 53241 48726
4	−0.08810 26036 60170	−0.20710 75794 20539
5	+0.47800 57810 98811	+0.38358 79739 59843
6	.78879 97720 45136	.74507 07436 35930
7	.91956 30995 25272	.90213 67456 08779
8	.97003 04866 29698	.96343 20474 31386
9	.98892 32382 79290	.98647 00901 33615
10	.99591 80856 76644	.99501 21261 41743
11	.99849 73991 57471	.99816 36412 25220
12	.99944 70956 31578	.99932 42487 54669
13	.99979 65804 68941	.99975 13789 98542
14	.99992 51637 84321	.99990 85338 98542
15	.99997 24689 76435	.99996 63510 22666
16	.99998 98718 59350	.99998 76211 68393
17	.99999 62740 59447	.99999 54460 73600
18	.99999 86293 02282	.99999 83247 02917
19	.99999 94957 48383	.99999 93836 92485
20	.99999 98144 96182	.99999 97732 73114

Equation (14.3) indicates that the series on the right should have zeros at the zeros of $\sin(yt)$. When the series is convergent or summable by the Cesaro method, the equations found by putting $t=1, 2, 3, \cdots$ in turn may be regarded as included among the numerous linear conditions that $f(x)$ must satisfy in order that it may be expressible by a definite integral of the form (13.1). The relations derived from the series may be used as a check on the accuracy of the observations or may be used to check the tabular values of a function represented by an integral of type (13.1). In particular, if $F(t)=\pi$, we have $f(x)=\tan^{-1}(y/x)$ and if $y=1$ the coefficients c_n may be calculated with the aid of the table of inverse tangents published by the Mathematical Tables Project mentioned previously. When $t=\pi$ and

$$\mu=1-2e^{-\pi}=0.91357\ 21634\ 72,$$

we have

$$P_2(\mu)=0.75192\ 11468, \quad P_3(\mu)=0.53584,$$
$$P_4(\mu)=0.29273\ 5162.$$

In using such a check it is probably advisable to improve the convergence of the Legendre series by the device already mentioned. The formula of interpolation for Laplace integrals and the table of Legendre functions may be useful in some problems of geophysics in which integral equations of Laplace's type occur. It may be mentioned that one such equation was used by Keck and Colby[52] in working out a method for deriving the depth dependence of earth conductivity from surface potential data.

When the series of Legendre functions is used to solve Eq. (3.3), an equation of type

$$2F(t)=t\sum_{n=0}^{\infty}c_n\int_0^\infty P_n(1-2e^{-z})J_0(zt)dz \qquad (14.6)$$

is obtained, each term of which can be found when the expansion of the Legendre function is used.

[52] W. G. Keck and W. F. Colby, J. App. Phys. **13**, 179–188 (1942).

15. SOME PROBLEMS OF ANALYTICAL CONTINUATION

When the solution $F(u)$ of (13.1) has been found, the function $f(x)$ may be continued to negative values of x by means of the formula

$$f(-x)=(1/\pi)\int_0^\infty \frac{yF(u)du}{(x-u)^2+y^2}, \quad (15.1)$$

the formula of interpolation being unsuitable for this purpose. The function $f(-x)$ can also be found directly by solving the integral equation

$$f(x+iy)+f(x-iy)-(1/\pi)\int_0^\infty \frac{yf(u)du}{(x-u)^2+y^2}$$
$$=(1/\pi)\int_0^\infty \frac{yf(-u)du}{(x+u)+y} \quad 0<x, \quad (15.2)$$

which expresses that the function $F(x)$ derived by means of Snow's inversion formula (with an appropriate change of notation) is zero for positive values of x.

It is sometimes possible to continue a function defined by a Laplace integral to negative values of x by means of the equations

$$\int_0^\infty e^{-xt}\cos(yt)F(t)dt$$
$$=\tfrac{1}{2}\int_0^\infty \cos(xt)e^{-yt}[iF(-it)-iF(it)]dt$$
$$-\tfrac{1}{2}\int_0^\infty \sin(xt)e^{-yt}[F(it)+F(-it)]dt, \quad (15.3)$$

$$\int_0^\infty e^{-xt}\sin(yt)F(t)dt$$
$$=\tfrac{1}{2}\int_0^\infty \cos(xt)e^{-yt}[F(it)+F(-it)]dt$$
$$-\tfrac{1}{2}\int_0^\infty \sin(xt)e^{-yt}[iF(-it)-iF(it)]dt, \quad (15.4)$$

in which $F(z)$ is supposed to be an analytic function regular when the real part of z is not negative and having a suitable form at infinity. These equations are readily derived by means of Cauchy's theorem. The equation holds for positive values of x and positive values of y but whereas the integrals on the left may diverge for $x<0$, the integrals on the right may exist and give the desired analytical continuation.

16. POTENTIALS WITH AXIAL SYMMETRY

The equation

$$f(z)=\int_0^\infty [(z+a)^2+r^2]^{-\frac{1}{2}}F(a)da$$
$$=\int_0^\infty e^{-zt}J_0(rt)dt\int_0^\infty e^{-at}F(a)da, \quad z>0 \quad (16.1)$$

can, when the foregoing change in order of integration is valid, be solved with the aid of two successive inversions of a Laplace integral. For some values of r it may be possible to continue the function $f(z)$ to negative values of z and apply a method of solution to be sketched in Section 17. Some progress in the continuation of Laplacian integrals involving Bessel functions has been made elsewhere by an extension of some work of King[53] and Muskat.[54] The results are included in the general formula (extending that of Pekeris)

$$\int_0^\infty e^{-zt}J_0(rt)f(t)dt$$
$$=(1/\pi)\int_0^\infty K_0(rt)[\cos(zt)\{f(it)+f(-it)\}$$
$$+\sin(zt)\{f(it)-f(-it)\}]dt,$$
$$\text{real } (t)>0, \quad (16.2)$$

in which $f(t)$ is an analytic function regular in the half plane. This formula and those of Section 15 are included in a more general formula involving Bessel functions as indicated by the author.[55] Integrals of the present type in which there are no sources above the plane $z=0$ are of interest in aerodynamics, geophysics, and many other subjects. Reference may be made in particular to the work of Theodore von Kármán and others[56] on the distribution of pressure over an airship in which use is made of a line of sources on the axis of the ship. When the second form of

[53] L. V. King, Proc. Roy. Soc. London **A139**, 237–277 (1933).
[54] M. Muskat, Physics **4**, 129–147 (1933).
[55] H. Bateman, Monats. Math. Physik **48**, 322–328 (1939).
[56] Theodore von Kármán, Aachen Abhandlungen, No. 6 (1927). See also O. Fuhrmann, *Theoretische und experimentelle Untersuchungen an Ballonmodellen*, Diss. Göttingen (Verlagsbuchhandlung Julius Springer, Berlin, 1912); H. Föttinger, Zeits. f. tech. Physik **9**, 26–39 (1928); F. Weinig, Zeits. f. tech. Physik **9**, 39–43 (1928); H. Lerbs, Werft, Reederei, Hafen **9**, 263–266 (1928).

integral is used with a fairly general type of function $G(t)$ in place of $\int_0^\infty e^{-at}F(a)da$ there may be sources on circles with the z-axis as line of centers.

It may be of interest to form an idea of the equipotential surfaces and streamlines in the whole field of Eulerian flow round the airship though this type of flow is not applicable in the rear of the ship for the flow is useful for finding the actual flow in the boundary layer. We shall suppose, then, that observations are made in front of the ship where the flow is almost exactly of the Eulerian type. If the velocity potential ϕ and stream function ψ are given by

$$\phi = Uz + \int_0^\infty e^{-zt}J_0(rt)G(t)dt = Uz + f(z)$$

for a fixed r, (16.3)

$$\psi = \tfrac{1}{2}Ur^2 - r\int_0^\infty e^{-zt}J_1(rt)G(t)dt = \tfrac{1}{2}Ur^2 + g(z)$$

for a fixed r, (16.4)

we have two Laplacian integral equations for the determination of $G(t)$ when $f(z)$ and $g(z)$ are known. When use is made of the Legendre series for the solution, the derived values of $J_0(rt)G(t)$, $J_1(rt)G(t)$ should be zero at zeros of $J_0(rt)$, $J_1(rt)$, respectively, and so observational values of $f(z)$ and $g(z)$ may be checked.

17. INFINITE LINE OF SOURCES

When sources extend to infinity in both directions, the integral equation

$$f(z) = \int_{-\infty}^{\infty}[(z-a)^2+r^2]^{-\frac{1}{2}}F(a)da \quad (17.1)$$

is harder to solve. It is easy to write down an integral which represents a potential $V(R, z)$ having the value $f(z)$ for $R=r$ and regular for $R>r$. To continue this potential into the region $R<r$ we follow the plan of Section 10 and seek an expansion of V in powers of the quantity $s=\log(R/r)$. Writing

$$V(z, R) = \int_{-\infty}^{\infty}[(z-a)^2+r^2e^{2s}]^{-\frac{1}{2}}F(a)da, \quad (17.2)$$

the derivatives of V with respect to s can, when $s=0$, be expressed linearly in terms of the integrals

$$V = \int_{-\infty}^{\infty}[(z-a)^2+r^2]^{-n-\frac{1}{2}}F(a)da, \quad (17.3)$$

and these integrals can likewise be expressed linearly in terms of the derivatives of V with respect to s for $s=0$. Now if

$$g(z) = \int_{-\infty}^{\infty}\frac{(z-a)F(a)da}{(z-a)^2+r^2} = V_0 - \tfrac{1}{2}r^2V_1 - (r^4/8)V_2 - \cdots \quad (17.4)$$

the function $g(z)$ can be regarded as a known function of z when the series converges. The function $F(a)$ can then be derived from $g(z)$ by means of the inversion formula of Section 7.

The expression for V for $R>r$ has the form of an integral involving the function $K_0(mR) = K_0(mre^s)$, the integration being with respect to m. We need, then, an expansion of this function in powers of s. Now if $W=K_0(mre^s)$ we have

$$dW/ds = mre^sK_0'(mre^s),$$

$$d^2W/ds^2 = (mr^2e^s)^2K_0''(mre^s) + (mre^s)K_0'(mre^s),$$

$$d^nW/ds^n = p_{n-1}(R^2)W + q_{n-2}(R^2)dW/ds,$$

where $p_{n-1}(x)$, $q_{n-2}(x)$ are polynomials of degrees not exceeding $n-1$, $n-2$, respectively. These polynomials satisfy recurrence relations and can be calculated step by step so the nth derivative of W can be found when W and dW/ds are known and it follows that the nth derivative of the potential V for $R=r$ can be found from the values of V and dV/dR for $R=r$.

18. FOURIER ANALYSIS

In 1904 Tedone[57] found some integral equations of type

$$f(x) = F(x) + (1/2\pi)\int_{-\infty}^{\infty}k(t)dt \times \int_{-\infty}^{\infty}\cos[t(x-u)]F(u)du \quad (18.1)$$

in a discussion of the equilibrium of an infinitely long elastic cylinder with given surface displacements. With the abbreviation $C=\cos t(x-u)$ the

[57] O. Tedone, Acc. dei Lincei, [5] 13, 232–240 (1940).

solution used was

$$F(x)=(1/\pi)\int_{-\infty}^{\infty}H(t^2)dt\int_{-\infty}^{\infty}C\cdot f(u)du, \quad (18.2)$$

where

$$H(t^2)=\frac{1}{2+k(t)+k(-t)}. \quad (18.3)$$

With Snow's symbolical method

$$F(x)=2H(-D^2)f(x), \quad \text{where} \quad D=d/dx. \quad (18.4)$$

In the case $f(x)=M\cdot g(x)$, $k(t)=M\cdot h(t)$, where M is a large positive number, the limit $M\to\infty$ gives the solution of an integral equation of the first kind[58]

$$g(x)=(1/2\pi)\int_{-\infty}^{\infty}h(t)dt\int_{-\infty}^{\infty}C\cdot F(u)du, \quad (18.5)$$

$$F(x)=(1/\pi)\int_{-\infty}^{\infty}\frac{dt}{h(t)+h(-t)}\int_{-\infty}^{\infty}C\cdot g(u)du. \quad (18.6)$$

In particular, if

$$h(t)=e^{-y|t|}, \quad (18.7)$$

the equation becomes the guiding equation of Section 6,

$$g(x)=(1/\pi)\int_{-\infty}^{\infty}\frac{yF(u)du}{(x-u)^2+y^2}, \quad (18.8)$$

and the solution is found in the form

$$F(x)=(1/\pi)\int_{0}^{\infty}e^{y|t|}dt\int_{-\infty}^{\infty}C\cdot f(u)du \quad (18.9)$$

given by Snow and Evjen. When, moreover, use is made of the identity

$$e^{y|t|}=2ch(yt)-e^{-y|t|},$$

the integral involving the hyperbolic cosine may be evaluated by the symbolic method and the solution obtained in the form of a simple integral with additional terms.

It must be emphasized that when use is made of the Fourier analysis the function $F(u)$ must be restricted more, perhaps, than when use is made of Poisson's integral directly. Evjen, for instance, required

$$\int_{a}^{\infty}|F(u)|du \quad \text{and} \quad \int_{-\infty}^{-l}|F(u)|du$$

to be convergent but other restrictions are permissible when Lebesgue integrals are used.

[58] When this result was sent to S. O. Rice, he remarked in a letter (reference 41) that there is a slight simplification when the exponential form of Fourier's integral is used.

19. AN INTEGRAL EQUATION OF CRYSTAL THEORY

When M is kept finite and $k(t)$ has the same form as before, Tedone's equation becomes

$$f(x)=F(x)+(M/\pi)\int_{-\infty}^{\infty}\frac{yF(u)du}{(x-u)^2+y^2}, \quad (19.1)$$

and his solution takes the form

$$F(x)=(1/2\pi)\int_{-\infty}^{\infty}\frac{dt}{1+Me^{-y|t|}}\int_{-\infty}^{\infty}C\cdot f(u)du. \quad (19.2)$$

The integral equation in this case includes one used by Hulthén[59] in work on the exchange problem for crystals. To get a solution more suitable for computation we write

$$\frac{1}{1+Me^{-y|t|}}=1-\frac{Me^{-y|t|}}{1+Me^{-y|t|}}, \quad (19.3)$$

$$F(x)=f(x)-M\int_{-\infty}^{\infty}G(M,x-u,y)f(u)du, \quad (19.4)$$

where

$$G(M,x,y)=(1/\pi)\int_{0}^{\infty}\frac{e^{-yt}}{1+Me^{-yt}}\cos(xt)dt \quad y>0 \quad (19.5)$$

$$=(1/\pi y)\int_{0}^{\infty}\frac{e^{-v}}{1+Me^{-v}}\cos(xv/y)dv.$$

For sufficiently small values of (x/y) there is an expansion

$$G(M,x,y)=(1/M\pi y)[\phi(1,-M)-(x/y)^2\phi(3,-M)+(x/y)^4\phi(5,-M)-\cdots], \quad (19.6)$$

where

$$\phi(s\cdot z)=\sum_{n=1}^{\infty}n^{-s}z^n \quad (19.7)$$

is the function studied by Appell,[60] Jonquière,[61] Truesdell,[62] and others. The function has been used in geophysical work by King.[53]

[59] L. Hulthén, Arkiv Mat. Astronom. Fysik **A26**, No. 11 (1938).
[60] P. Appell, Comptes rendus **87**, 690–692, 874–878 (1878).
[61] A. Jonquière, Bull. Soc. Math. France [2] **17**, 142–152 (1889), Stockholm Acad. Öfversigt 257–268 (1889).
[62] A. Truesdell, Ann. of Math. **46**, 144–157 (1945).

Here and There

New Appointments

Dr. William A. Shurcliff of Washington has been appointed technical consultant in the Bureau of Industry of the New York State Department of Commerce.

Edmund S. Winlund is the new RCA Victor Industrial Electronics Engineer for the Pacific Region, with headquarters in Los Angeles.

C. W. Handley and P. D. Ries have been selected as technical specialists by National Carbon Company, Inc., to help expand the company's technical service facilities applying to projector carbons and other lighting carbon products.

Dr. Emilio Segrè has been appointed professor of physics at the University of California at Berkeley.

Drs. Dana P. Mitchell and Norman F. Ramsey, Jr., of Columbia University, have been promoted to the rank of associate professor of physics.

Dr. Louis B. Slichter, professor of geophysics, Massachusetts Institute of Technology, will become professor of geophysics, University of Wisconsin, with the opening of the second semester in January.

Five new vice presidents have been announced by RCA Victor Division of Radio Corporation of America: Meade Brunet, J. B. Elliott, Joseph H. McConnell, J. W. Murray, and L. W. Teegarden.

Dr. John A. Tiedeman, formerly associate professor of physics at Woman's College, University of North Carolina, has been appointed director of the Education Department of Ansco Division of General Aniline and Film Corporation.

Professor Marcel K. Newman has been appointed Associate Professor of Mechanical Engineering in the College of Applied Science, Syracuse University.

Dr. Lise Meitner, the Austrian physicist, has joined this month the faculty of the Catholic University of America, where she is visiting professor.

Back to Former Posts

Joseph Kaplan, professor of physics, University of California at Los Angeles, has returned to his post after five years of service in the Army Air Forces.

Dr. Robert S. Shankland, on leave for the past three years to the Office of Scientific Research and Development, has returned to his position as head of the Department of Physics at Case School of Applied Science, and Drs. Robert Rinehart, Charles C. Torrance, Paul Guenther, and Lewis J. Green have resumed their work in the Department of Mathematics at Case.

National Academy Appointment

Science reports that Dr. Detlev W. Bronk, professor of biophysics and director of the Eldridge R. Johnson Foundation of the University of Pennsylvania, has been appointed foreign secretary of the National Academy of Sciences. By virtue of this appointment, Dr. Bronk also becomes chairman of the Division of Foreign Relations of the National Research Council.

Michigan Society of Spectroscopy

The Michigan Society of Spectroscopy has elected new officers for the second year of its existence. New chairman is G. A. Nahstoll of the Ford Motor Company; Secretary is Virginia Sink of the Chrysler Corporation.

Nuclear Physics Program at Harvard

The president and fellows of Harvard College have voted to establish a committee to develop a program in nuclear physics at the university. The corporation has further voted to allocate the sum of $400,000 to the committee to spend within a period of five years in developing the program.

Lighting Handbook

Plans for publication of a lighting handbook, most comprehensive and informative work of its kind ever attempted, have been announced by the Illuminating Engineering Society. The handbook, long contemplated by the Society as a major post-war project, will contain five hundred pages of text prepared by outstanding authorities in their respective fields. Every phase of lighting, from the pure physics of light to specific lighting recommendations for stores, offices, homes, factories, and even for juke boxes and television studios, will be covered. The latest authoritative information on light sources, as well as on the measurement and control of light, will be included. The handbook will be released October, 1946 and will be sold and distributed through official I.E.S. channels. Robert W. McKinley, electrical engineer, has been engaged as editor.

Necrology

Dr. Eugene Cook Bingham, professor of chemistry at Lafayette College, died on November 6 at the age of 56.

National Academy Awards

Among the awards given by the National Academy of Sciences on November 16 were the following:

Cyrus B. Comstock Prize, awarded every five years for the most important discovery or investigation in electricity, magnetism, and radiant energy. Prize of $3,000 for the period 1938 to 1943 was awarded to Donald W. Kerst, Department of Physics, University of Illinois, "for his pioneer work in connection with the development of the betatron and the results which he has obtained with this new and powerful scientific tool."

The gold Public Welfare Medal, for eminence in the application of science to the public welfare, was awarded for 1945 to Vannevar Bush, Director of the Office of Scientific Research and Development, Washington, D. C., "in recognition of his outstanding service in bringing to bear the scientific and engineering talent of this country upon problems of research connected with the war effort."

Nobel Prizes

The 1945 Nobel prize in physics has been awarded to Professor Wolfgang Pauli of the Institute for Advanced Study at Princeton, New Jersey, for his work on the "exclusion principle," which deals with regulation of electrons in the outer shell of atoms and molecules. The 1944 prize in chemistry has been awarded to Professor Otto Hahn, Germany, an authority on radioactivity, for his discovery of a method of breaking the heavy atom nucleus. Artturi Wirtanen, of Finland, biochemist, has received the 1945 award in chemistry for his discoveries relating to food chemistry.

Atomic Energy Forum at Cleveland

On November 27 the Cleveland Physics Society, Case School of Applied Science, and Western Reserve University sponsored a forum on the control of atomic energy. It was attended by more than 500 scientists in the Cleveland area. Main speaker was Dr. W. H. Zinn, nuclear physicist from the University of Chicago. At the end of the meeting the following resolution was passed almost unanimously by the audience:

"RESOLVED, that the Government of the United States be urged to take rapid, effective steps to make the United Nations Atomic Energy Commission a reality. Further, that all effort be made to secure international cooperation resulting in free exchange of scientific information among all countries and unhampered inspection by United Nations experts to insure that such information is not misused. Also, that the Government of the United States be urged to take such legislative steps as will avoid compromising either atomic or nuclear research in this country or the establishment of an adequate international policy. Further, that this resolution be submitted to all government officials immediately concerned.

Revised Fulbright Bill

Hearings on the revised Fulbright Bill, S. 1248, to establish an Office of Technical Services within the Department of Commerce, consolidating several similar or related scientific agencies of the Government, began December 12. The revised bill had been drafted to conform to recommendations of various agencies of the Government and private organizations that might be affected by or interested in the proposed legislation. Among these were the Departments of Commerce and Agriculture, the Office of Scientific Research and Development, the National Inventors Council, the Smaller War Plants Corporation, and Office of Production Research and Development.

Crystallographic Society

The Crystallographic Society organized at Harvard University and Massachusetts Institute of Technology in 1939 is planning to resume its activities, which were suspended during the war. The Society concerns itself with the science of crystallography and its applications to fields such as physics, chemistry, metallurgy, ceramics, and biology and is not restricted to the classical phases of crystallography commonly associated with mineralogy. In 1940 the Society initiated the idea of launching a Journal of Crystallography. More recently, plans have been discussed by several societies for starting a new international Journal of Crystallography to replace the Zeitschrift für Kristallographie, which is no longer published. Since there is no other journal devoted exclusively to crystallography, the Society takes an active interest in this new development.

A meeting to be held at Smith College is tentatively planned for March 21–23, 1946. Those wishing to present papers are requested to send title and brief abstract to Professor M. J. Buerger, Massachusetts Institute of Technology, Cambridge 39, Massachusetts. Ten invited papers have been arranged.

All those wishing to renew membership or to become members of the Society or who desire further information may write to William Parrish, Acting Secretary-Treasurer, The Crystallographic Society, Philips Laboratories, Inc., Box 39, Irvington, New York. Membership fees have been set at $1 for 1946. A new membership list will be compiled January 31, 1946.

Society for Quality Control

On October 3 and 4, 1945, the Organizing Committee for a National Quality Control Society met at Pittsburgh, Pennsylvania, and established the Society for Quality Control. It is the intent of the Society "to serve all those interested in quality control, giving particular attention to the needs of those engaged in manufacture and inspection." The Society plans "to publish material that will be of help to quality control people everywhere, material that will help them sell and apply quality control methods."

Edward M. Schrock and Ralph E. Wareham were unanimously elected president and secretary-treasurer, respectively. Dues of the Society were set at $5, of which $3 will be returned to the local chapter. At present there are fourteen chapters. Payment of dues to the Society will make a person a member of the chapter in his geographical area. Dues should be sent to Mr. Wareham at 305 East 43d Street, New York 17, New York.

Dr. W. D. Coolidge Honored by Chile

Dr. William D. Coolidge, formerly vice president and director of research of the General Electric Company, who is now touring South America, has been awarded the "Orden al Merito" of the Chilean Government.

Division of High-Polymer Physics

The Division of High-Polymer Physics of the American Physical Society held its second regular meeting at Columbia University, New York City, January 24–26, 1946, as one of the features of the general, annual meeting of the parent society. On the program of the Division meeting were approximately 25 papers on rubbers, plastics, and other high-polymeric materials, covering both the analysis of physical behavior and experimental techniques.

The Bulletin of Mathematical Biophysics

MARCH, 1946

The Mathematical Biophysics of Some Mental Phenomena: II. Anxieties and Elations—N. RASHEVSKY

Chain Processes and Their Biophysical Applications: Part II. The Effect of Recovery—I. OPATOWSKI

A Contribution to the Mathematical Biophysics of Cell Growth and Shapes: II.—RICHARD RUNGE

A Theory of Membrane Permeability: II. Diffusion in the Presence of Water-Flow—INGRAM BLOCH

The Neural Mechanism of Logical Thinking—N. RASHEVSKY

Volume 8, Number 1—The University of Chicago Press, Chicago, Illinois.

Fellowships in Cancer Research

Fellowships in cancer research, administered by the Committee on Growth of the National Research Council, are open to citizens of the United States who possess M.D. or Ph.D. degrees. They are designed to provide opportunities for training and experience in research for men and women who are fitted for scientific investigation, basic or clinical (including research in biophysics). The fellowships are intended for recent graduates who, as a rule, are not more than thirty years of age.

Applicants for these fellowships may plan to enter any field of research pertaining broadly to the problem of cancer. Candidates will be favored who desire to obtain thorough experience in one of the basic sciences.

The annual stipends are determined by individual circumstances and by cost of living in the location of study. The usual amount is from $2000 to $3000 per annum. The fellowships are granted for one year, but they may be renewed. Fellows are usually chosen at annual meetings of the Committee on Growth in February, and applications to receive consideration at these meetings must be filed on or before January 1. During 1945–46, interim applications will be considered. Appointments may begin on any date determined by the Committee.

Further particulars concerning these fellowships may be obtained on request from Executive Secretary of the Committee on Growth, National Research Council, 2101 Constitution Avenue, Washington 25, D. C.

Radiation Laboratory Technical Series

Publication of the largest series of books on physics and electrical engineering ever undertaken in the United States has been arranged by the Massachusetts Institute of Technology for the Office of Scientific Research and Development, according to an announcement by James R. Killian, Executive Vice President of the Institute. The Radiation Laboratory Technical Series, comprising twenty-eight titles and a General Index, reports the results of five years' wartime work on radar. The purpose of the series is to make available to science, industry, and the public generally the results of the immense developments in electronics and in microwave theory and technique during the war years, which, once secret, have now widely been declassified. These will be of inestimable value in peacetime research in physics, biology, and other natural sciences, as well as providing the engineering foundation for post-war industrial developments in television, communications, and electronics.

Work reported in the series required the expenditure of about 20,000 technical man-years in the various radar research and development establishments, Dr. Killian revealed. "For the first time," he said, "the technical literature of a large subject is being created all at once, on a uniform basis. Emphasis in the series will not be on radar itself, but rather on the basic techniques which underlie many phases of electronics in addition to radar."

Publication of the series will be handled by an agreement between Massachusetts Institute of Technology, acting for the Office of Scientific Research and Development, and the McGraw-Hill Book Company, which is undertaking the publication. This arrangement is expected to serve as a model for the publication of other scientific work done with public funds under OSRD contract, now that the need for wartime secrecy no longer exists where this information is of general interest and can desirably appear in book form. Royalties on the sale of the books will be paid to the U. S. Treasury.

Plans for the series have been under way since late 1944, when it became clear that the end of the war was not far off. Intensive work has been carried on since June. Manuscript is now being prepared at the rate of nearly 400 pages per day by 187 authors under the direction of nine editors. Illustrations are being drawn by more than a hundred artists and draftsmen.

Books of the series are being written chiefly by staff members of the Radiation Laboratory, wartime radar research center maintained at the Massachusetts Institute of Technology by OSRD contract, but will include the results of work on radar done in British development establishments and in industrial laboratories both here and in England. Several British scientists have come to the Massachusetts Institute of Technology to cooperate in the preparation of the series.

Summaries of the scope and contents of the series show that it covers several fields of the greatest scientific and engineering importance. Some of these are: precise timing techniques; new methods of cathode-ray tube display; generation, transmission, and radiation of high-power microwaves; and broad-band amplifier techniques. Present titles planned for the series follow:

The generation of high power microwaves is dealt with in a book on *Microwave Magnetrons* which presents the theory of operation of these oscillators as well as practical design considerations and operating techniques. *Low Power Microwave Tubes* deals principally with the properties of reflex klystrons and lighthouse tubes when used as oscillators, amplifiers, rectifiers, and mixers. Production of accurately timed pulses having various waveforms at high and very high peak powers is treated in *Pulse Generators*. A theoretical and practical treatment of pulse transformers is also included in this book.

Transmission line and wave guide techniques are discussed exhaustively. *The Theory of Guided Waves* develops a basic theory of electromagnetic waves in wave guide. This theory draws from conventional field theory, circuit theory, and transmission line theory, but is directed to the solution

of problems of importance in the microwave region. Maximum use of engineering concepts is made. A *Waveguide Handbook* collects the analytical results given by the theory and presents all available numerical and experimental results in graphic form, chosen to be most convenient for practical circuit design. *The Principles of Microwave Circuits* develops a generalization of low frequency network theory and of the impedance concept. The properties of wave guide circuit elements and devices are developed and discussed in terms of this generalization. *Microwave Transmission Circuits* treats from a practical point of view the same general matters. Design principles for connectors, rotary joints, and other wave guide and transmission line devices will be discussed, and examples of successful designs given. *The Techniques of Microwave Measurements* describes in detail the methods for measuring power and attenuation at high and low level, standing wave measurements, means for accurate determination of wave-length and frequency, r-f spectrum and pulse shape, and other means of measurement peculiar to the microwave field.

Microwave Antenna Theory and Design provides a comprehensive survey of theory and design techniques for microwave antennas, a full discussion of antenna measurement methods, and an indication of special methods used in antenna production. *Propagation of Short Radio Waves in the Troposphere* collects and summarizes the very extensive wartime investigations of the propagation characteristics of radiation at frequencies too high to be affected by the ionosphere. The theory of atmospheric refraction, the meteorology of the refraction problem, and the experimental approach to the refraction problem will be followed by a treatment of matters which include target properties, ground and sea clutter, and molecular absorption.

Crystal Rectifiers discusses the theory, properties, manufacture, and use of the silicon and germanium point contact rectifiers which have been developed for use as microwave converters and other circuit applications. *Microwave Receiving Circuits* deals with the problem of frequency conversion and duplexing. Means of automatic frequency control for a local oscillator are discussed, and designs of mixers and duplexing assemblies are described.

A series of works on the design and application of vacuum tube circuits is opened with the *Components Handbook* which describes the properties of available wire, resistors, capacitors, inductors, instrument motors, potentiometers, and other circuit elements. Emphasis is placed on the specifications which components meet and on features of performance which are not usually given in other publications. The book includes the results of independent measurements of important properties of various types of commercial components. *Cathode Ray Tubes* describes methods for using such tubes, with emphasis on good focus, freedom from distortion, and reliable operation. It includes discussions of focusing and deflection magnets and coils, the properties of fluorescent screens, and methods of constructing auxiliary apparatus such as projectors, magnetic shields, light filters, and the like.

Two books follow which analyze the fundamental properties of basic circuits useful in the various branches of electronics. *Vacuum Tube Amplifiers* deals with circuits which can be treated theoretically by linear circuit analysis. It seeks to analyze completely many types of amplifiers, especially those of high gain, wide band pass, or large dynamic range. Constructional details of special amplifiers, and rigorous critical discussions of amplifier sensitivity will be given. *Waveforms* discusses basic circuits which include a non-linear element. These and other circuits for the generation and shaping of the form of current and voltage waves are analyzed with the help of the cathode-ray oscillograph. The wave forms described make possible radar and television displays, and permit the precise measurement of time and position. A treatment of their generation is followed by discussions of their manipulations, such as modulation, analysis, and frequency division.

Then follow those books whose object it is to present design techniques for synthesizing from the basic circuits and components just described the complex instruments required to fill various functional demands. *Electronic Instruments* deals with devices for the purpose of precision time measurement, data transmission, and mathematical computation. It emphasizes instrument function, gives details of engineered circuit designs, and recommends preferred equipment types where possible. *Cathode Ray Tube Display Circuits* shows how cathode-ray tubes may be combined with electronic circuits to provide a wide variety of measuring and precision data display devices. Applications of such devices include the precision measurement of time intervals shorter than one ten-thousandth of a microsecond, and the plotting of several functions of several variables simultaneously in any of several coordinate systems, as well as special devices suitable for radar and television use.

The use of electrical and other time-variable indications in automatic control devices is discussed in *Automatic Control Systems*. Basic principles for the design of electrical and mechanical feedbacks control systems are developed in detail, and application is then made to a series of automatic control problems, including those which have arisen in automatic radar range and angle tracking.

Microwave Receivers-describes many different types of complete receiving systems, suitable for radar, television, relay telephony, and repeat-back devices. Examples are chosen to illustrate actual design techniques. *Signal Thresholds in Interference* offers an analysis, both theoretical and experimental, of the factors affecting the perception of desired signals in the presence of various types of interference, principally receiver noise.

An outline of the general principles of design of radar systems is presented in a volume entitled, *Radar Systems Engineering*. It is intended as a basic treatise and reference book for anyone interested in making any application of radar.

The applications of radar to problems of air and sea navigation, including airport and harbor traffic control, are discussed in a volume entitled, *Radar Aids to Navigation*.

In the book, *Loran*, a comprehensive treatment is made of the principles and engineering design of this war-born long range navigational aid.

The final book is a general index providing cross references among the various books of the technical series.

Symposium on Molecular Spectroscopy and Molecular Structure

A conference on Industrial and Chemical Infra-red Spectroscopy will be held at Mendenhall Laboratory of Physics, Ohio State University in Columbus, Ohio, June 13–15, 1946. This meeting will be sponsored jointly by the Physics departments of the University of Michigan and the Ohio State University.

The conference will be a part of a larger symposium on Molecular Spectroscopy and Molecular Structure to be held at the Ohio State University beginning Monday, June 10 and extending to June 15.

More complete details on this symposium will be published in a later issue of the Journal. Inquiries concerning the infra-red conference may be directed to Professor Harald H. Nielsen, Mendenhall Laboratory or to Dr. Norman Wright, Dow Chemical Company, Midland, Michigan.

Naval Ordnance Laboratory

The Charles H. Tompkins Company, of Washington, has begun work in preparation for the construction of the main buildings of the Naval Ordnance Laboratory's new research center at White Oak, Maryland. The contract, totaling $4,813,000 was awarded the Tompkins Company for construction of a group of structures which will include the administration building, the photographic laboratory, spherical field laboratory, long field laboratory, officers' quarters, Marine barracks, and a portion of the roads which will connect the numerous units in the 938-acre area at White Oak.

A total of 50 permanent buildings is planned for the research center which the Naval Ordnance Laboratory will use for the peacetime continuance of scientific experiments in connection with underwater ordnance. More than a dozen of the smaller buildings have already been completed, and a $300,000 boiler plant—which will supply steam for heating and for process work in the main laboratory—will be ready within a few weeks. Cost of the entire project will be approximately $15,000,000.

Included in the buildings now in operation are six magnetic laboratories, which are located in a remote section of the White Oak property away from all local media of interference. They contain no properties which would tend to create disturbances during experiments, and are devoid of red brick—which contains iron oxide—and reinforced concrete—which requires the use of iron rods. Downspouts, radiators, and nails are all of copper.

One of these magnetic buildings, the Quiet Laboratory, has no electric lights, water pipes, or other ordinary facilities which could in any possible way interfere with the work of the men who will be probing into the mysteries of magnetic weapons and counterweapons. Another structure in this group has a temperature control room for producing immediate temperature variations of between minus 80 and plus 180 degrees Fahrenheit.

The new Laboratory was planned by the Navy Department's Bureau of Ordnance in collaboration with Captain W. G. Schindler, USN, Officer-in-Charge of the Naval Ordnance Laboratory, and Captain R. D. Bennett, USNR, its technical director. Captain Schindler came to the Laboratory's present headquarters, at the Navy Yard in Washington, two years ago after a brilliant career as Ordnance Officer in a carrier squadron in the South Pacific. He made numerous sorties as rear seat gunner in an SBD dive bomber, and is credited with being the first American to shoot down a Japanese plane in aerial combat. Captain Bennett, internationally known for the development of cosmic-ray measuring equipment, is a former professor of electrical engineering at Massachusetts Institute of Technology.

Most of the construction details for the gigantic laboratory were handled through the Bureau of Yards and Docks, but in NOL's own offices were prepared the unique laboratory features designed to provide the technical staff with the world's most modern equipment for the development of the various projects which the Laboratory will inherit.

Architects are Eggers and Higgins, of New York City, with Taylor and Fisher, Baltimore, associates.

Naval Ordnance Laboratory has long been the Navy's headquarters for the design and development of underwater weapons and countermeasures. It was established in 1918 as a mine laboratory, but because of the country's "peace economy" program only a skeleton staff was retained for the next two decades. When Germany introduced the magnetic mine at the beginning of World War II, the Laboratory immediately began to expand its activities to include the development of depth charges, bomb fuzes, projectile fuzes, pyrotechnics, and numerous other items as well as mines. Perfection of degaussing equipment, which was to protect our ships from lurking enemy magnetic mines, was one of the first tasks assumed by the Laboratory after the dark months of 1940.

Until the last days of Japan's resistance, most of the Laboratory's work was restricted from public attention because of security regulations. Announcement of the mining of the Inland Sea and other strategic Japanese waters first turned the spotlight on NOL, and finally the Navy announced that it was this research center that had developed all the mines which were used in the history-making blockade. In addition, the Laboratory had perfected the parachutes which eased the deadly missiles into the water from an altitude of 10,000 feet.

Another of the Naval Ordnance Laboratory's outstanding contributions which was withheld from the public until the cessation of hostilities was the development of the 40-mm fuze. Through this device the Navy's guns were able to destroy enemy aircraft with greater accuracy, and at the same time the U. S. taxpayer was given considerable help in the cost of producing the ammunition. NOL's technical experts are credited with having effected a saving of $236,820,000 in the three years that the new fuzes were in production.

More than a thousand scientists and technicians will make up the peacetime staff of the Laboratory. Nearly one hundred of the scientific personnel have already moved to the new workshops at White Oak, with others following as the various buildings are completed. The entire staff is expected to be transferred by the late summer of 1946.

Federation of Atomic Scientists

The following statement has been prepared regarding the aims of the newly formed Federation of Atomic Scientists:

We, the undersigned representatives of the Associations of Scientists who have worked on the atomic bomb, hereby agree to form a united group, to be known as "The Federation of Atomic Scientists," in order to carry out more effectively the common aims of the separate organizations.

Each of the six Associations shall retain its identity and independence of action. The Federation will provide a central office and staff for the purpose of aiding and coordinating the activities of the several member Associations.

The component organizations were founded to achieve the following aims:

(1) To study the implications to our nation and to the world of the liberation of nuclear energy.
(2) To create a realization of the dangers that this nation and all civilization will face if the tremendous destructive potential of nuclear energy is misused.
(3) To help establish an atmosphere of world security in which the beneficial possibilities of nuclear energy may be developed.
(4) To study the relation between national legislation and the establishment of an adequate international policy.

. . . and to give all possible publicity to the following convictions:

(1) That a continuing monopoly of the atomic bomb by the United States is impossible.
(2) That there can be no specific defenses against the destructive effects of the atomic bomb.
(3) That in view of the existence of the atomic bomb, no nation can, in this new age, feel secure until the problem of the control of atomic power is solved on a world level.

The council of the Federation will consist of those delegates of the component associations who are in Washington at any given time. It is intended that one such member from each association should be present in Washington at all times and two will frequently be present. There will be a central office which will act primarily as headquarters for the Associations. It will also serve as an information and speakers' bureau and will handle contacts with other groups which hold views similar to our own.

The Washington office shall be made available to all scientists' organizations in America which find it necessary to have the same information that we are to supply to the Associations. Many of these newly formed groups have the same aims and purposes as our own organization.

Signed by representatives from:

Association of Oak Ridge Scientists at Clinton Laboratories
The Atomic Scientists of Chicago
The Association of Los Alamos Scientists
The Association of Manhattan Project Scientists, New York City Area
The Atomic Production Scientists, Oak Ridge
The Atomic Engineers, Oak Ridge

The Federation of Atomic Scientists may be reached by calling National 5818, Washington, D. C. Its street address is 1621 K Street, N.W., Washington 6, D. C.

New Booklets

National Patent Council, new organization devoted to the interests of small manufacturers, is issuing an 8-page monthly bulletin called *Competitor*. It is published at Gary, Indiana. The December issue reported progress to date in enrolling new support for the campaign.

The National Research Bureau, Inc., 415 North Dearborn Street, Chicago 10, Illinois has issued for distribution a list of some of the engineering and manufacturing problems which have been solved by the Bureau. Correspondents may order copies of the Bureau's reports on any listed problems. The Bureau also offers a list of new Masters' theses which are available for distribution. Such theses will be supplied only on microfilm.

American Instrument Company, 8030 Georgia Avenue, Silver Spring, Maryland, publishes an 8-page bi-monthly paper entitled *Aminco Laboratory News*, which is "devoted to the application of scientific instruments to modern laboratory technique, engineering, materials testing, and production control."

The Senate Subcommittee on War Mobilization has issued a monograph on *Wartime Technological Developments*, a supplement to the previous volume of the same name. Like that volume, this monograph was compiled and digested by the Bureau of Labor Statistics, U. S. Department of Labor, from items published in trade and technical journals. There are 839 technical advances included in the volume.

Calendar of Meetings

February	
23	American Mathematical Society, New York, New York
25–28	American Institute of Mining and Metallurgical Engineers, Chicago, Illinois
25–28	Technical Association of the Pulp and Paper Industry, New York, New York
25–March 1	American Society for Testing Materials, Pittsburgh, Pennsylvania
March	
7– 9	Optical Society of America, Cleveland, Ohio
27–30	American Association for the Advancement of Science, St. Louis, Missouri
April	
1– 4	American Society of Mechanical Engineers, Chattanooga, Tennessee
3– 5	Society of Automotive Engineers, New York, New York
8–12	American Chemical Society, Atlantic City, New Jersey
12–13	American Physical Society, Southeastern Section, Atlanta, Georgia
17–19	American Society of Civil Engineers, Philadelphia, Pennsylvania
18–20	American Philosophical Society, Philadelphia, Pennsylvania
25–27	American Physical Society, Cambridge, Massachusetts
26–27	American Mathematical Society, Chicago, Illinois
26–27	American Mathematical Society, New York, New York
27	American Mathematical Society, West Coast
28–May 1	American Ceramic Society, Inc., Buffalo, New York
May	
6–10	Society of Motion Picture Engineers, New York, New York
10–11	Acoustical Society of America, New York, New York
27–29	American Geophysical Union, Washington, D. C.
June	
17–20	American Society of Mechanical Engineers, Detroit, Michigan
20–23	Society for the Promotion of Engineering Education, St. Louis, Missouri
24–28	American Institute of Electrical Engineers, Detroit, Michigan
24–28	American Society for Testing Materials, Buffalo, New York

Errata

On the Representation of Rigid Rotations

[J. App. Phys. **16**, 571 (October 1945)]

H. SCHWERDTFEGER

THE last line of footnote 2 must read: "*scientifiques* 649 (Paris 1938)." In line 15 of section 2, two different symbols are used for the exponential function (exp P and e^P) in one and the same formula.

On Maximum Gain-Band Width Product in Amplifiers

[J. App. Phys. **16**, 528 (September 1945)]

W. W. HANSEN

DR. Henry Wallman of M.I.T. has pointed out that there are certain contradictions in this article. Specifically, in the right column of page 529, one finds "Second, Wheeler's four-terminal result is also the best possible for a single stage." This statement, which occurs also in the conclusion, conflicts with the correct result of Bode, which is given in the abstract and on page 533.

The opportunity for this carelessness on my part arose because I did not see Bode's important work until my article was in press and, while modifying some of my statements, I failed to correct them all.

Calculation of the Output from Non-Linear Mixers

HARRY STOCKMAN
Cruft Laboratory, Harvard University, Cambridge, Massachusetts
(Received October 6, 1945)

The exact mathematical treatment of non-linear mixers of the type used in very-high frequency and ultra-high frequency superheterodynes is difficult. If, however, the non-linear element is simplified to the extent that it is fully described by a plotted current-voltage characteristic, several ways of determining the output become evident. Some of the most fundamental methods are described in the following, and their shortcomings pointed out. The methods are then tried out on a "guinea pig" characteristic and the results critically compared with respect to accuracy, amount of labor, required mathematical tools, and other factors. It is found that no "best" method exists and that all methods require simplifying assumptions and approximations that frequently lead the converter designer to consider practical measurements, or special methods, such as the one provided by the frequency conversion diagram technique.

THE conventional frequency converter has two essential parts; the non-linear element and the local oscillator. The action of the non-linear element or mixer is to combine the incoming wave e_A of angular velocity A with the local oscillator wave e_B of angular velocity B so that one or more product terms result. Each product term yields a sum and a difference component, and the output circuit is arranged to emphasize the current, voltage, or power of a selected sum or difference component, the angular velocity C of which is determined from the relation $C=|pA\pm qB|$, where p and q are any integers. The desired output current is in the following indicated i_C.

The mixer may be linear when operated with zero oscillator voltage, but if so is made non-linear by the application of the oscillator voltage. A rigorous and general mathematical treatment of the non-linear device is more difficult to carry out and apply when the operation is "Class B" or "Class C," and when the frequency is very high. To make a mathematical treatment possible a number of factors, which control the behavior of the non-linear element, must be left out of consideration. Accordingly the results of the mathematical investigation will not tell the full story, and the interpretation of the results must be done with utmost care.

FUNDAMENTAL CONSIDERATIONS

The following treatment is built upon the assumption that the non-linear element of interest is fully described by a single current-voltage or *ie*-characteristic. This *ie*-characteristic may be a tube characteristic, issued by the tube manufacturer, or a curve obtained from measurements on an available physical mixer. In both cases there will be certain errors in the current and voltage coordinates, and these errors are magnified in the readings taken from the curve. Fundamentally there are a number of mathematical methods that can be applied to find the resulting output from a given input. Some of these methods lose their meaning, however, if the primary information is too inaccurate. One way of getting around this difficulty is to assume that the plotted *ie*-characteristic is exact, i.e., entirely free from error. Several limiting curves representing various amounts of error can then be plotted, and the calculation procedure repeated for each one of them. A comparison of the results gives information about the intervals of variations that can be expected in particular variables, for example the maximum and minimum value of conversion transconductance.

One fundamental idea in the treatment of non-linear devices is to investigate the given, plotted characteristic for the purpose of obtaining its equation in the explicit form $i=f(e)$. This idea seems to leave out of consideration "Class B" and "Class C" operation, as $i=f(e)$ is an analytical function. If, however, the device is provided with a small artificial current in the non-conducting interval of the variational voltage, the non-analytical function of a "Class B" or "Class C" mixer can be transformed into an

analytical one. Such a transformation is actually of practical importance as will be shown later.

Another way of obtaining the desired output component is to make a conventional Fourier analysis of the output current wave. This method has several limitations that will be pointed out in the text. Still another method involves that the "mixer-local oscillator" combination is treated as a unit, the variational transconductance of the unit varying periodically with the oscillator frequency. When encountering this periodic transconductance the incoming voltage yields the well-known amplitude-modulation pattern in the output, indicating the generation of one or more product terms. This method is of considerable practical value.

The following methods are centered on the non-linear element itself, and apply to the types of single input low-ohmic mixers, that have recently become of importance in the very-high frequency and ultra-high-frequency field. The mixer may be considered as operating with short-circuited output, but the treatment applies as well to mixers which have a load impedance of the same value for all frequencies. The given *ie*-characteristic is then with advantage transformed into a dynamic *ie*-characteristic. The treatment given is not extended to mixer circuits with load impedances of general type, but it is well to remember that in the conventional circuit, with the load impedance existing at one frequency only, the voltage drop across this impedance may be treated as part of the applied voltage.[1,2] Another case that permits a simplified treatment is the high impedance mixer, as here the load impedance may be neglected in series with the comparatively large average value of the plate resistance.

CURVE-FITTING METHODS

Some useful methods of determining the equation $i=f(e)$ for a given *ie*-characteristic are described below. The final form of this equation depends very much upon the method employed. If this form is not explicit in the desired current component, there remains the procedure of developing such an explicit expression

$$i_C \equiv F(E_A, E_B, A, B).$$

This procedure may involve as much labor as the "curve-fitting" procedure itself.

Before going into a discussion of methods we will study an assumed *ie*-characteristic to be used later as a "guinea pig." This assumed characteristic is shown in Fig. 1 and represents a somewhat idealized diode tube. Actually we know the equation for this characteristic, which is, in milliamperes and volts,

$$i=c_1(e+b)+c_2(e+b)^2+c_3(e+b)^3, \quad (1)$$

$$=0.50(e+0.50)+0.70(e+0.50)^2+0.01(e+0.50)^3. \quad (2)$$

The variational voltage applied around the Q-point is

$$\Delta e = e_A+e_B = E_{A\max}\cos At + E_{B\max}\cos Bt, \quad (3)$$

where the maximum values are 0.10, respectively, 0.90 volts, the angular velocities $A=2\pi\ 30\ 10^6$ and $B=2\pi\ 27\ 10^6$, and the operation "Class A" with the Q-point coordinate $E_{cc}=+1.00$ volt. The fundamental operation output will then be

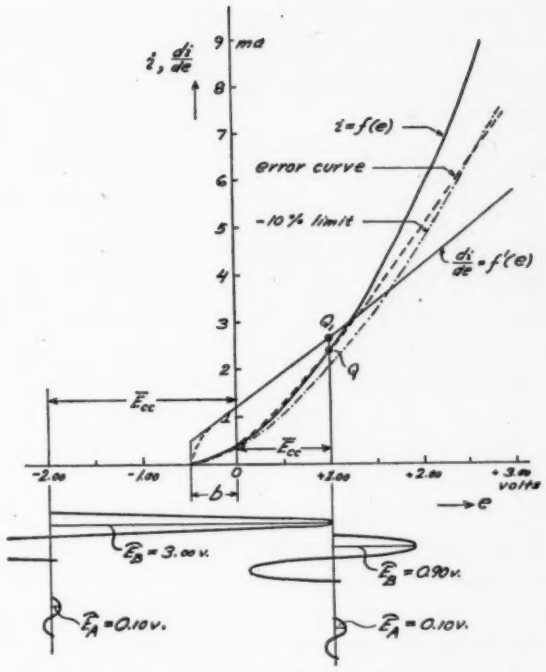

FIG. 1. The "measured" characteristic and its first derivative, illustrating operation in "Class A" and "Class C." The error curve refers to the "log-log straight line" method.

[1] E. G. James and J. E. Houldin, "Diode frequency changers," Wireless Engineer **20**, 15 (1943).

[2] E. W. Herold and L. Malter, "Some aspects of radio reception at ultra-high frequency," Proc. I.R.E. **31** (August, September, and October, 1943).

of frequency $3\,10^6$ c.p.s. Expanding the parenthesis $(\bar{E}_{cc}+\Delta e+b)$ by means of the binomial theorem and collecting proper terms, we obtain the final result

$$i_C = E_{A\max}E_{B\max}[c_2+3c_3(\bar{E}_{cc}+b)] \times\cos(A-B)t, \quad (4)$$

which yields the output current 0.0670 ma peak value. (Formula (4) may be directly obtained from the expansion in the appendix with $k_2=c_2$, $k_3=c_3$, and $k_4=0$.)

The conversion transconductance is defined as

$$g_{mc}=\frac{I_{C\max}}{E_{A\max}}\Bigg|_{E_{C\max}=0}^{\text{small values}}, \quad (5)$$

(in absolute current and voltage values) and becomes 670 μmhos. The obtained numerical values are in the following treated as being exact so that a comparison can be made between the numerical results obtained with different methods. The methods to be presented follow.

a. $i=f(e)$ Obtained on the Assumption that the Given Characteristic Follows a Square-Law, a $\frac{3}{2}$-Power Law or Similar Law, Making Possible a log-log Straight-Line Plot.

This method is mainly of interest for *ie*-characteristics without sharp bends, utilized in "Class *A*" operation. Assuming an *ie*-characteristic that extends the amount b on the negative voltage side of the origin, we may write its unknown equation in the form

$$i=f(e)=0.5K(e+b)^a.^3 \quad (6)$$

In a log-log plot this equation has the form

$$\log i = a\log(e+b)+\log 0.5K. \quad (7)$$

Reproducing the given curve in a log-log plot we may obtain an almost straight line. A substituted straight line has the intercept in the origin $\log 0.5K$ and the slope

$$a=\frac{d[\log i]}{d[\log(e+b)]}=\frac{\log i_1-\log i_2}{\log(e+b)_1-\log(e+b)_2}, \quad (8)$$

where subscripts 1 and 2 indicate points on the straight line. Thus the numerical values of K and a can be obtained and the equation $i=f(e)$ determined. The method becomes impractical in cases where $i=f(e)$ cannot be expressed by the simple form (6).

Proceeding from (6) to determine the desired output current i_C for fundamental operation we will avoid the simple case of a equal to 2 and treat the more general case of a unequal to 2. Selecting a Q-point with the positive coordinate $\bar{E}_{cc}$ we obtain for a small voltage variation Δe around the Q-point the variational current

$$\Delta i=-i_Q+0.5K(\bar{E}_{cc}+b+\Delta e)^a. \quad (9)$$

The parenthesis is then expanded by means of the binomial theorem for the variational voltage Δe given by (3), and all terms containing the product $\cos At\cos Bt$ collected. The result of these operations becomes

$$i_C=0.25Ka(a-1)E_{A\max}E_{B\max}[(\bar{E}_{cc}+b)^{a-2} +0.125(a-2)\cdot(a-3)(\bar{E}_{cc}+b)^{a-4} \times(E^2_{A\max}+E^2_{B\max})+\cdots]\cos(A-B)t. \quad (10)$$

The output current for harmonic operation is obtained in a similar way by collecting terms for the proper higher-order product term. The more terms we include in the expansion the less become the amplitudes, which indicates as a first approximation that harmonic operation is less efficient than fundamental operation.

Applying method (*a*) to our practical example, we reproduce the given *ie*-characteristic in Fig. 1 on log-log paper and obtain after rough calculation $K=2.5$ and $a=1.7$.[4] Using Eq. (10) we find the desired output current to be $I_{C\max}\doteq 0.060$ ma, and the error to be -10 percent. Repetition of the procedure will reduce the error to the more permissible value of a few percent.

We may use the same "guinea-pig" characteristic to investigate "Class *C*" operation, but in this case there is no equation available, the result of which may be used as the exact answer for determining the error in various graphical methods. For "Class *C*" operation we may locate the Q-point at the coordinate $\bar{E}_{cc}=-2.00$ volts and use an oscillator amplitude of $E_{B\max}=3.00$ volts. It is understandable that method (*a*) is not suitable for "Class *C*" operation, for even if

[3] For $a=2$ this becomes the important case of a parabola and the factor 0.5 then makes the constants identical with specified derivatives.

[4] Maximum values are in the figures indicated by means of an eyebrow above the symbol.

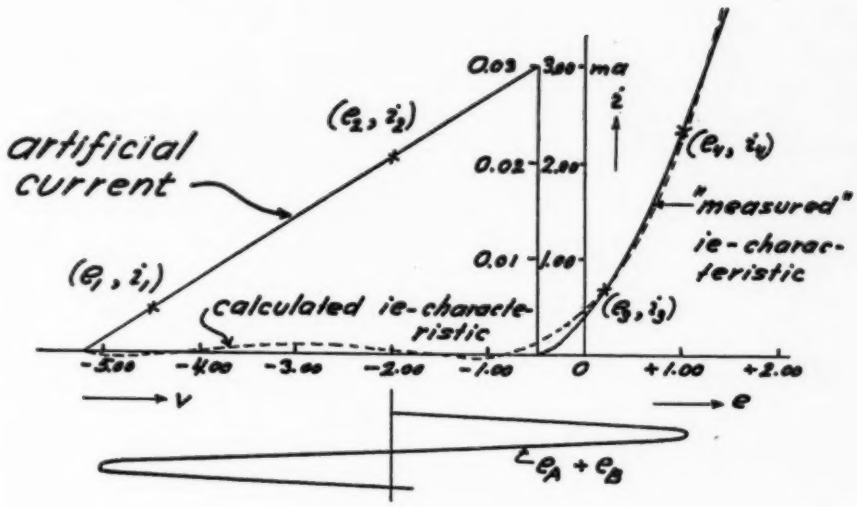

FIG. 2. Method of extending the *ie*-characteristic to make possible the application of the variable-coefficient method with four points for "Class C" operation.

we extend the characteristic into the non-conducting interval to obtain an analytical function, it would be most unlikely that the resulting curve should be of such form that it with advantage could be represented by the simple formula (6).

b. $i=f(e)$ Written as a Power Series, the Constants of Which are Determined by the Methods of Variational Coefficients.

We start out with the unknown equation, introducing for simplicity the symbol v to describe the variational coordinate measured from the cut-off point. Then in series representation

$$i=f(v)=\sum_{n=1}^{\infty} k_n v^n, \tag{11}$$

or

$$i=k_1 v+k_2 v^2+k_3 v^3+\cdots, \tag{12}$$

where k_1, k_2, k_3, $\cdots$ are the coefficients to be determined by means of the variational coefficient method. The power series method is much more general than the previous method and also handles characteristics with sharp bends. The procedure is to select on the given *ie*-characteristic a number of points, which, particularly in case of a sharp-bend curve, have to be carefully grouped—a matter of experience. An equation system is then written down with as many equations, and as many terms in each question, as there are points on the *ie*-characteristic. This provides a linear equation system in k, the i- and e-values being read off from the given curve. The solution of the equation system is generally simple, but may require accurate computation if small differences between large quantities occur. It is recommended that the calculated curve is plotted on top of the given curve so that unpermissible wiggles can be checked. The accuracy of the final result does not necessarily increase with an increased number of terms, as the equation will simultaneously become of higher order and therefore somewhat more difficult to handle, particularly with reference to small differences. It must also be realized that a vaguely known curve does not justify a large number of terms unless the previously mentioned stunt of assuming the curve free from error is made use of.

This method may also be used for the treatment of "Class *C*" operated devices, if a non-vanishing current is assumed in the non-conducting region of the variational voltage. We will study such a case with reference to the given or "measured" *ie*-characteristic reproduced to the right in Fig. 2. The *Q*-point is located at -2.00 volts. The sum-voltage e_A+e_B, with $E_{A\max}=0.10$ volts and $E_{B\max}=3.00$ volts, is applied around the *Q*-point. Choosing arbitrarily 1 percent of the maximum current as artificial current value in the cut-off point, we arrive with an assumed straight-line current distribution to the result shown, one hundred times magnified, in Fig. 2. Choosing more or less arbitrarily four points along the total *ie*-characteristics, and counting v from the new cut-off point, we can

write down the equation system,

$$\left.\begin{aligned} i_1 &= k_1v_1+k_2v_1^2+k_3v_1^3+k_4v_1^4,\\ i_2 &= k_1v_2+k_2v_2^2+k_3v_2^3+k_4v_2^4,\\ i_3 &= k_1v_3+k_2v_3^2+k_3v_3^3+k_4v_3^4,\\ i_4 &= k_1v_4+k_2v_4^2+k_3v_4^3+k_4v_4^4. \end{aligned}\right\} \quad (13)$$

From the graph we read off the *ei*-values (−4.50, 0.00447), (−2.00, 0.02040), (+0.20, 0.7000), and (+1.00, 2.36000), which are given with an accuracy justified by the assumption that the given curve is exact. As the equation system is linear in k we obtain after straightforward computation work the results $k_1=-0.130$, $k_2=+0.244$, $k_3=-0.101$, and $k_4=+0.012$. For checking purposes the resulting curve has been roughly plotted in Fig. 2, and it is seen that the agreement between the given and the computed characteristic is quite good. Thus we can accept as a working empirical equation

$$i=-0.130v+0.244v^2-0.101v^3+0.012v^4. \quad (14)$$

Introducing here

$$v=V+E_{A\max}\cos At+E_{B\max}\cos Bt, \quad (15)$$

where $V=3.20$ volts, expanding the terms in (14) and collecting and grouping terms we obtain (see Appendix with $(\bar{E}_{cc}+b)=V$)

$$i_C=E_{A\max}E_{B\max}[k_2+3k_3V$$
$$+6k_4(V^2+\tfrac{1}{4}E_{A\max}^2+\tfrac{1}{4}E_{B\max}^2)]\cos(A-B)t, \quad (16)$$

which yields the numerical value $I_{C\max}\doteq 0.052$ ma. This is the intermediate frequency output for fundamental operation, "Class *C*." The conversion transconductance is approximately 520 μmhos.

To provide figures for the table in the latter part of the discussion calculations were as well carried out for the "Class *A*" case. The result is $I_{C\max}=0.0663$ ma, the error being −1 percent.

c. $i=f(e)$ Written as a Power Series, the Constants of Which are Determined by the Method of Taylor's Series

In this method we determine the coefficients as derivatives in the *Q*-point, and it follows that if there is a sharp bend in this point or anywhere else in the interval so that the function becomes non-analytical, the derivative cannot be determined and the method breaks down. Thus the method applies to smooth curves only, and is restricted to "Class *A*" operation, as an artificially extended *ie*-characteristic for "Class *C*" operation scarcely fulfills the requirements on a smooth curve. (The extended curve in Fig. 2 would yield second and higher-order derivatives of zero value.)

Generally we may write Taylor series for a single input device

$$\Delta i=\sum_{n=1}^{\infty}\frac{1}{n!}\left(\frac{\partial}{\partial e}\Delta e\right)^n i, \quad (17)$$

where $\partial/\partial e$ operates upon i. For two variables Δe_1 and Δe_2, so applied that

$$\Delta e=\Delta e_1+\Delta e_2, \quad (18)$$

we obtain

$$\Delta i=a\Delta e_1+b\Delta e_2+c\Delta e_1^2+d\Delta e_1\Delta e_2$$
$$+f\Delta e_2^2+g\Delta e_1^3+\cdots. \quad (19)$$

The coefficients in this series have the values

$$a=\frac{\partial i}{\partial e_1}, \qquad d=\frac{\partial^2 i}{\partial e_1\partial e_2},$$
$$b=\frac{\partial i}{\partial e_2}, \qquad f=\frac{1}{2}\frac{\partial^2 i}{\partial e_2^2},$$
$$c=\frac{1}{2}\frac{\partial^2 i}{\partial e_1^2}, \qquad g=\frac{1}{6}\frac{\partial^3 i}{\partial e_1^3},$$
$$\cdots\cdots\cdots, \quad (20)$$

where several numerical identities occur as we deal with one current-voltage function only. (Partial derivatives are used unconventionally to indicate that the evaluation is made in the *Q*-point). For fundamental operation and with the variational voltage (18) expressed by (3) the useful *i-f* output becomes

$$\Delta i=\cdots+\frac{\partial^2 i}{\partial e_1\partial e_2}E_{A\max}\cos At\cdot E_{B\max}\cos Bt, \quad (21)$$

so that

$$i_C=\frac{1}{2}\frac{\partial^2 i}{\partial e_1\partial e_2}E_{A\max}E_{B\max}\cos(A-B)t. \quad (22)$$

By plotting the slope and measuring the slope of the slope of the given *ie*-characteristic in Fig. 2 we obtain $\partial^2 i/\partial e_1\partial e_2=1.50$ ma/volts^2, so that with $E_{A\max}=0.10$ volt and $E_{B\max}=0.90$ volt the result becomes $I_{C\max}=0.0675$ ma. The

error in this result is approximately +1 percent, which is better than what can generally be expected from a slope-of-the-slope method (the error may easily have amounted to 5 or 10 percent).

In more complicated applications the following treatment may prove useful. We will write the total instantaneous current, with $\partial/\partial e$ operating upon the current i,

$$i=f(e)=f(\bar{E}_{cc})+\sum_{n=1}^{\infty}\frac{1}{n!}\left(\frac{\partial}{\partial e}\Delta e\right)^n i. \qquad (23)$$

Here $f(\bar{E}_{cc})$ is the direct-current component produced in the Q-point by the bias voltage $\bar{E}_{cc}$. Rather than to expand (23) we will make use of the following transformation

$$f(e)=f(\bar{E}_{cc}+\Delta e)=e^{(\partial/\partial e)\Delta e}f(\bar{E}_{cc}), \qquad (24)$$

which can be proven by series expansion. We obtain for $\Delta e=\Delta e_1+\Delta e_2$,

$$i=e^{(\partial/\partial e_1)\Delta e_1}\cdot e^{(\partial/\partial e_2)\Delta e_2}\cdot f(\bar{E}_{cc}). \qquad (25)$$

Thus the current is generally obtained as the product of two factors, each one with an exponent which is a specified derivative of the given current-voltage function evaluated in the Q-point. As Δe_1 and Δe_2 are both cosinusoidal, the e-functions become periodical and can be expanded in Fourier series with Bessel function coefficients. These steps will not be carried through as the following method involves practically the same developments (see Eqs. (27) and (28)).[5]

d. Empirical Equation Written as an ϵ-Series and Developed in Fourier Series with Bessel-Function Coefficients

As an alternative to the previously given power series, we may use the ϵ-series

$$i=\sum_{n=1}^{\infty}A_n\epsilon^{a_n v}=A_1\epsilon^{a_1 v}+A_2\epsilon^{a_2 v}+\cdots, \qquad (26)$$

where, as before, the coordinate is counted from the cut-off point. For a smooth "Class A" characteristic of roughly exponential form this series can with advantage be utilized as equation.

[5] A. C. Bartlett, "Calculation of modulation products," Phil. Mag. **16**, 845 (1933) and **17**, 628 (1934).

Two terms involve four coefficients to be determined. Again "Class C" operation would necessitate artificial extension of the given *ie*-characteristic, only feasible in the few cases where the resulting characteristic remains essentially exponential.

It is desirable that the series in (26) be transformed into a new series, in which the product terms appear in more obvious form, so that the sum and difference frequency components can be quickly identified. The final series will be explicit in the desired current component only if the applied voltages are independent of current. The variational voltages in a modern u.h.f. diode converter circuit sometimes depend upon various current components in such a way that the problem becomes complicated beyond engineering consideration.[1,2]

If the applied voltage is of form (15) we may write down a general term m in expansion (26)

$$A_m\epsilon^{a_m v}=A_m\epsilon^{a_m V}\cdot\epsilon^{a_m E_{A\max}\cos At}\cdot\epsilon^{a_m E_{B\max}\cos Bt}. \qquad (27)$$

To expand a factor of the form $\epsilon^{k\cos\omega t}$ we may make direct use of the relation

$$\epsilon^{k\cos\omega t}=J_0\left(\frac{k}{j}\right)-2\left[J_2\left(\frac{k}{j}\right)\cos 2\omega t-J_4\left(\frac{k}{j}\right)\cos 4\omega t+\cdots\right]+2j\left[J_1\left(\frac{k}{j}\right)\cos\omega t-J_3\left(\frac{k}{j}\right)\cos 3\omega t+\cdots\right], \qquad (28)$$

where $J_0(k/j)$ is the Bessel function of the first kind and 0th order and $J_\nu(k/j)$ the Bessel function of the first kind and νth order, k/j, or rather jk with proper sign, being the argument. Using mathematical texts and tables for the Bessel functions, we proceed to express each one of the last two factors in (27) by means of (28) with $m=1$, $m=2$, etc. Carrying out these steps and grouping and collecting terms for fundamental operation, we obtain

$$i_C=I_{C\max}\cos(A-B)t, \qquad (29)$$

where

$$I_{C\max}=2[A_1\epsilon^{a_1 V}jJ_1(ja_1E_{A\max})jJ_1(ja_1E_{B\max})+A_2\epsilon^{a_2 V}jJ_1(ja_2E_{A\max})jJ_1(ja_2E_{B\max})]. \qquad (30)$$

Applying this method to our practical example

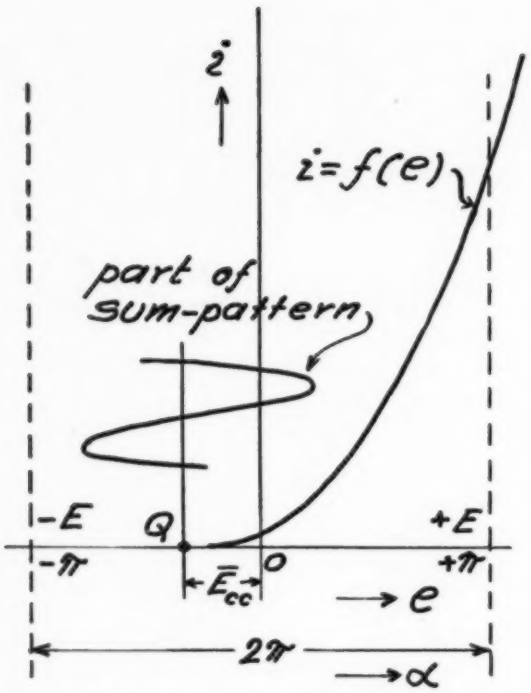

FIG. 3. Obtaining an empirical equation for a measured *ie*-characteristic by means of single period Fourier analysis in terms of voltage.

we will find that if all factors are known the procedure mainly simplifies to the use of tables of Bessel functions. We may, however, run into considerable difficulties when trying to determine the coefficients A_1, A_2, $\cdots a_1$, a_2, $\cdots$. Limiting ourselves to two terms in the practical example we will here employ a graphical method for determining the four coefficients by replotting the given *ie*-characteristic with logarithmic current axis. If this construction is carried out it is found that the resulting curve bends downwards so that if we approximate its initial part with a straight line of the form

$$\log i_1 = 0.4343 a_1 v + \log A_1, \tag{31}$$

we shall have to subtract the ordinates for a second similar line, covering the upper part of the given characteristic. Carrying out the graphical work and reading off the constants for the two straight lines we obtain for the given practical application the approximate values

$A_1 \doteq 0.40$, $a_1 \doteq 1.35$, $A_2 \doteq -0.04$, and $a_2 \doteq 1.97$.

Using formulas (29) and (30) we obtain $I_{C\max} \doteq 0.05$ ma. The error in the answer is -25 percent and is representative for the inaccuracy that can be expected in applications where the given *ie*-characteristic is not essentially of exponential form.

e. $i=f(e)$ Obtained by Means of the Trigonometric Polynomial Method

Let us consider the given characteristic in Fig. 3 for the general case of "Class B" or "Class C" operation. Applying the sum-pattern e_A+e_B around a chosen Q-point we may select a voltage interval $-E$ to $+E$ and treat this interval as a single period of a repeated wave.[6] By means of "single period" Fourier treatment we can then determine the equation for the extended *ie*-characteristic, or rather the path of operation between $-E$ and $+E$, and thus obtain, with the voltage coordinate e expressed by $\alpha=(\pi/E)e$,

$$i=f(\alpha)=b_0+\sum_{n=1}^{\infty}(b_n\cos n\alpha+a_n\sin n\alpha). \tag{32}$$

Here

$$b_n=\frac{1}{\pi}\int_{-\pi}^{+\pi} f(\alpha)\cos n\alpha d\alpha, \tag{33}$$

$$a_n=\frac{1}{\pi}\int_{-\pi}^{+\pi} f(\alpha)\sin n\alpha d\alpha. \tag{34}$$

Making use of the relation $\alpha=(\pi/E)e$, where

$$e=\bar{E}_{cc}+E_{A\max}\cos At+E_{B\max}\cos Bt, \tag{35}$$

(with $\bar{E}_{cc}$ indicating the bias voltage), we may solve for i in (32) and write out a series expansion with terms of type cos (amplitude·cos argument) or sin (amplitude·sin argument), so that we with advantages can use Bessel functions for the amplitudes. Thus the desired product term can be quickly determined by means of a table of Bessel functions, and the work involved is actually less than what would at first be surmised from (32).

The reason why a comparatively large number of terms must be employed is the sudden jumps in the curve, causing oscillations in the empirical curve. Professor W. L. Barrow has shown a method[7] by means of which the number of terms

[6] A. Preisman, *Graphical Constructions for Vacuum Tube Circuits* (McGraw-Hill Book Company, Inc., New York, 1943).

[7] W. L. Barrow, "Contribution to the theory of nonlinear circuits with large applied voltages," Proc. I.R.E. 22, 981 (August, 1943).

can be reduced. He extends the *ie*-characteristic to become part of an artificial, smooth characteristic that approaches a sine wave or cosine wave in shape, and then utilizes only the part of the curve covered by the variational voltage. No computation work with reference to the trigonometric polynomial method has been carried out, as reference (7) contains extensive calculations that closely resemble the ones we should have to go through in such a treatment.

OTHER METHODS

f. Conventional Fourier Analysis of the Total Output Current, the Function $i=f(e)$ Remaining Unknown

If we project the sum-pattern $E_{A\max}\cos At+E_{B\max}\cos Bt$ on a given *ie*-characteristic, we obtain a distorted sum-pattern, such as the one shown to the right in Fig. 4. It is assumed that A and B are related in such a way that $(A-B)$, A, B, and $(A+B)$ are all component values in one and the same harmonic series, $(A-B)$ being the fundamental. Only in special cases would practical A and B values fulfill such a requirement. This means that $(A-B)$ is generally not the fundamental, so that Fourier analysis performed with $(A-B)$ as fundamental becomes erroneous. The true fundamental is in the general case some component $|pA\pm qB|$ with particular numerical values for the integers p and q. As an example assume that A and B are related by an irrational number such as $\sqrt{2}$. Performing the stunt of approximating $\sqrt{2}$ to 1.4 we may transform the problem and write $10A=14B$, meaning that the cycle will close after 14 cycles of A (or 10 cycles of B), so that a repeating wave is obtained that can be analyzed in conventional way. Such a transformation may, however, increase the amount of labor beyond engineering considerations. In other applications we may be able to change the numerical value of A or B until a repetition cycle of small enough period is produced.

When the method applies, the output current is of the form

$$i(t)=b_0+\sum_{n=1}^{\infty}(b_n\cos n\omega t+a_n\sin n\omega t), \quad (36)$$

where a coefficient such as b_n is conventionally

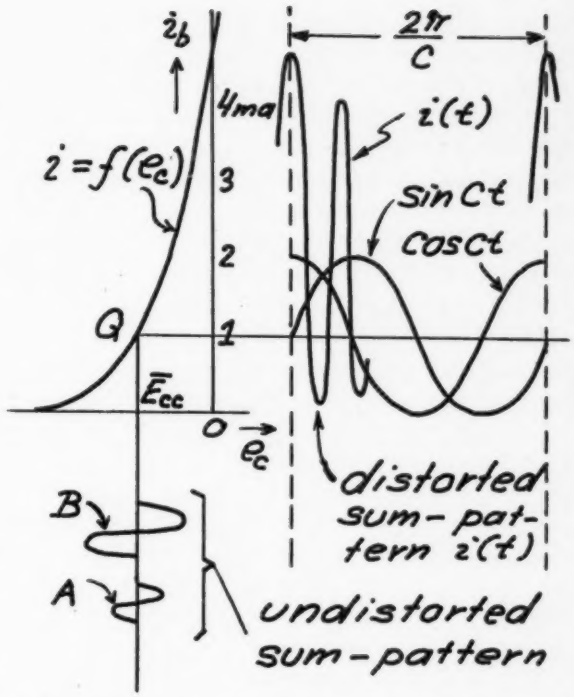

FIG. 4. Sum-pattern e_A+e_B impressed on a measured *ie*-characteristic with the resulting current variation shown to the right. This is a special case, suitable for Fourier analysis.

written

$$b_n=\frac{2}{T}\int_{-T/2}^{+T/2}i(t)\cos n\omega t dt. \quad (37)$$

To determine such a component we may, for example, perform a graphical integration. For the simple case of fundamental operation with $A-B=C$, (37) takes the form

$$b_1=\frac{2}{T}\int_{-T/2}^{+T/2}i(t)\cos Ctdt. \quad (38)$$

Superimposing a unit amplitude cosine way, and employing a planimeter or counting squares, we obtain the integral above in agreement with Fig. 4, and thus find $b_1=2y$, where y is the height of a rectangle of the same area as is indicated by the planimeter. The coefficient a_1 is obtained in a similar way (or is conveniently arranged to have zero value), whereafter $I_{C\max}=(b_1^2+a_1^2)^{\frac{1}{2}}$.

Theoretically at least the Fourier analysis can be applied directly to the *ie*-characteristic without the necessity of plotting the output wave. This harmonic analysis procedure, so practical when applied to sine-wave driven

power amplifier tubes,[8,9,10] seems not very attractive for sum-pattern operated converters.

Using conventional Fourier analysis in the practical example, "Class A" operation, we obtain $I_{C\max}=0.09$ ma. The error in this value is very high, +35 percent, because of the approximative nature of the graphical integration. An accurate value is hard to obtain in this example, as we deal with a small difference between large plus and minus areas.

g. Treatment When the A-Wave Only is Applied to the Non-Linear Element, the ie-Characteristic of Which is Replaced by a B-Wave Controlled Instantaneous Characteristic

A frequency converter may be defined as a device with periodically varying transadmittance, the periodicity of the variation determining the frequency of each possible output component. Neglecting the out-of-phase component we may develop the transadmittance as the transconductance $g_m(t)$ in a Fourier series with the fundamental frequency $B/2\pi$, the local oscillator voltage being

$$e_B=E_{B\max}\cos Bt. \tag{39}$$

Thus

$$g_m(t)=b_0+\sum_{n=1}^{\infty}(b_n\cos nBt+a_n\sin nBt). \tag{40}$$

The transconductance $g_m(t)$ will contain harmonics even if the applied oscillator voltage, as in (39), is free from harmonics. The coefficients in this series are defined in conventional manner.

Applying this method to our practical example, we obtain for "Class A" operation, with the Q-point at plus one volt and $E_{B\max}=0.90$ volt, a slope $(g_{m1})_{\max}=1.33$ ma/v. As the slope curve happens to be almost a straight line, there will be a negligible amount of harmonics in the variational conductance. Thus, with $b_0=g_{m0}$ in (40),

$$g_m(t)=g_{m0}+(g_{m1})_{\max}\cos Bt. \tag{41}$$

Fundamentally the resulting variational current is obtained as the product of the variational conductance and the applied variational voltage, so that, leaving any existing bias voltage out of consideration, we obtain

$$\begin{aligned}\Delta i&=g_m(t)\cdot\Delta e_A\\&=(g_{m0}+(g_{m1})_{\max}\cos Bt)E_{A\max}\cos At,\end{aligned} \tag{42}$$

which yields the difference frequency term

$$i_C=\tfrac{1}{2}(g_{m1})_{\max}E_{A\max}\cos(A-B)t. \tag{43}$$

With an A-wave amplitude of 0.10 volt, formula (43) yields $I_{C\max}=0.0665$ ma. The error here is less than −1 percent, which is a permissible value.

"Class C" operation requires a more elaborate analysis. The slope curve is now discontinuous and again we employ Fourier analysis to find the desired conductance harmonic (counting the fundamental as the first harmonic). The graphical integration method described under Section (f) may be used, or we may employ conventional schedule analysis. Using the Chaffee harmonic analysis 9-point method[9,10] we obtain for fundamental operation

$$(g_{m1})_{\max}=\tfrac{1}{6}[S_1+3S_2+S_4], \tag{44}$$

where the ordinates S_1, S_2, and S_4 have the respective values 2.12, 2.67, and 0 ma. Using formulas (42) and (43) we then obtain $I_{C\max}=0.056$ ma. (The graphical integration method gave the answer 0.057 ma, and proved to be the slower method of the two.)

CONCLUSIONS

There are other methods and combination of methods that could be considered but the presented material is sufficient to shed light on the questions of interest. Table I gives the computation results obtained with the various methods.

TABLE I.

Method	$I_{C\max}$ in ma	Error in percent
a. log-log straight-line plot	0.060	−10
b. variational coefficients	0.0663	−1
c. Taylor series coefficients	0.0675	+1
d. e-series, Bessel coefficients	0.05	−25
f. Fourier analysis of output	0.09	+35
g. variational conductance	0.0665	−1

The error values have been calculated with

[8] E. L. Chaffee, *Theory of Thermionic Vacuum Tubes* (McGraw-Hill Book Company, Inc., New York, 1933).
[9] E. L. Chaffee, "The operating characteristics of power tubes," J. App. Phys. 9, 471 (June, 1938).
[10] E. L. Chaffee, "Power tube characteristics," Electronics 11, No. 6 (June, 1938).

0.0670 ma as the correct value, obtained for the test or "guinea pig" characteristic from Eq. (2).

When comparing the results, the writer concludes that the natural form of the unknown mathematical expression for the studied characteristic and the actual shape of this characteristic favors certain methods and handicaps others. To make this point more clear, suppose we started out to investigate a characteristic that happens to be fairly exponential in its form. Two ϵ-terms would then describe this characteristic with good accuracy, and method *d* gives an error of only a few percent, while some of the other methods with tabulated errors of the order of one percent may give very large errors. As another example, assume that the form of the characteristic, in amplitude and frequency values, was very suitable for investigation by means of Fourier analysis. Then method *f* may give an error of only a few percent, while (if the input voltage effects the transconductance variation) a method like *g* may give a large error. More enlightening examples could be brought up if we extended the discussion to the treatment of discontinuities, such as sharp bends.

The judgment of the proper method becomes still more difficult if the discussion is extended to harmonic operation and to problems concerning loading conditions (to the extent we can cope with such problems). Further, there is no sharp definition of what is meant by the "best method," for there are many factors that enter into the comparison, for example accuracy of final result, amount of labor involved, level of required skill, type of required skill, type of computation equipment required, possibilities of extending the method, etc. It follows that a successful comparison of different methods can only be made if the scope of the work, and the nature of the judgment, is clearly specified from the beginning, and in addition the computation work is carried far outside the limits indicated by this paper. A number of "guinea pig" characteristics must be employed and a number of operating conditions must be studied. Actually, the serious investigator must be prepared to have at hand a computation office to take care of the landslide of calculations that result from a general approach to the problem.

The above discussion concerns mainly "Class *A*" operation. The extension of the treatment to "Class *B*" and "Class *C*" operation brings up a number of additional questions. The computation work for one analytical method, the variational coefficient method, and one graphical method, the variational conductance method, has here been carried out. The former gives a fundamental operation output current of 0.052 ma and the latter for the same quantity 0.057 ma. The error in one, considering the other correct, is only 5 percent, which is a good result, considering the straightforward manner of computation. Some of the presented methods may not apply at all to "Class *C*" problems, while others can be made to apply, for example by means of the mathematical stunt of adding an artificial current in the non-conducting region. (A comparison of "Class *A*" and "Class *C*" operation from the computation values in the practical example would not be fair as we are not making the most of the "Class *C*" operation.)

To summarize the most important points, there does not exist any one particular method to determine *i-f* output current and conversion transconductance, which method is general, quick, accurate and reliable. This is particularly true as most converters operate in "Class *B*" or "Class *C*." There are, however, certain methods, such as the variational conductance method, which for many applications yield a fairly accurate answer in a short time, and such a method is therefore used more frequently than other methods. The bottleneck in the use of the various methods is that we in complicated cases are forced to deal with so strongly simplified conditions that the close connection between our computation results and the true characteristics of the physical device are obscured. There are many factors, which have a bearing on the result, and if all these factors were included in our calculations, the problem would become too complicated for a straightforward theoretical treatment.

It is therefore natural that direct measurement methods are sometimes preferred for computation methods, and the experienced converter designer frequently finds himself involved in extensive practical measurements, in which mathematical investigations of the type presented in

this paper are coming in here and there merely as aids in the development work.

It is at this point the Chaffee Conversion Diagram Method calls for attention, as this method may be worth consideration between all-out calculations and all-out measurements. The conversion diagrams encourage systematic investigation and describe important relations under practical operating conditions for the nonlinear element. Thus some of the resistive and reactive properties of the nonlinear element, which are very difficult to take into account in calculations, may be automatically taken into account by a conversion diagram. Useful curves, such as the *i-f* output power as function of the oscillator voltage, can be directly plotted from the diagrams. The writer will not in this connection carry the discussion of the conversion diagram method further. For an estimation of its value as a tool for the converter designer the reader is referred to the references.[11–14]

ACKNOWLEDGMENT

This paper provides the introductory part of a thesis for doctor's degree at Harvard University, and the author wishes to thank the Director of Cruft Laboratory, Professor E. L. Chaffee, for having made this work possible.

[11] H. Stockman, "A treatment of non-linear devices based upon the theory of related linear functions," J. App. Phys. **14**, 645 (1943).

[12] H. Stockman, "Use of frequency conversion diagrams," Proc. I.R.E. **32**, 679 (November, 1944).

[13] H. Stockman, "UHF converter analysis," Electronics **18**, 140 (February 1945), and Proc. Nat. Electronics Conference, Chicago, **1**, 242 (1944).

[14] H. Stockman, "Frequency conversion diagrams for triode tube mixers," J. App. Phys. **16**, 639 (October, 1945).

APPENDIX

Obtain the desired product term from the power series expansion in (12).

The given expansion is of the form

$$i=\sum_{n=1}^{\infty} k_n v^n = k_1 v + k_2 v^2 + k_3 v^3 + k_4 v^4 + \cdots, \quad (12)$$

where we will neglect higher order terms. Introducing $v=(e+b)$ we obtain the series

$$i = M_0 + M_1 e + M_2 e^2 + M_3 e^3 + M_4 e^4 + \cdots, \quad (12.1)$$

where

$$M_0 = k_1 b + k_2 b^2,\ k_3 b^3 + k_4 b^4 + \cdots,$$

$$M_1 = k_1 + 2k_2 b + 3k_3 b^2 + 4k_4 b^3 + \cdots, \text{ etc.}$$

Introducing

$$e = \bar{E}_{cc} + E_{A\max} \cos At + E_{B\max} \cos Bt \quad (12.2)$$

in (12.1) we obtain, among other terms,

$$i = \cdots + E_{A\max} E_{B\max} [M_2 + 3M_3 \bar{E}_{cc} + 6M_4 (\bar{E}_{cc}^2 + \tfrac{1}{4} E_{A\max}^2 + \tfrac{1}{4} E_{B\max}^2)] \times \cos (A-B)t, \quad (12.3)$$

so that the desired difference-frequency current becomes, with the M-coefficients expressed in k and b,

$$i_C = E_{A\max} E_{B\max} [k_2 + 3k_3 (\bar{E}_{cc} + b) + 6k_4 \{(\bar{E}_{cc} + b)^2 + \tfrac{1}{4} E_{A\max}^2 + \tfrac{1}{4} E_{B\max}^2\}] \times \cos (A-B)t. \quad (16)$$

This final expression is made use of in different ways in the text.

Filmless Sample Mounting for the Electron Microscope

JOHN H. L. WATSON*
Shawinigan Chemicals Limited, Shawinigan Falls, Quebec
(Received November 15, 1945)

A method is described for supporting airborne particles upon thin glass fibers where they build up in chains and may be examined in the electron microscope. With no supporting membrane, the contrast and resolution are increased in the micrographs. The specimens are particularly useful for stereoscopic studies. A special reference is made to the study of carbon particles mounted in this fashion. The carbons examined are formed by pyrolysis of acetylene and occur naturally in pronounced chains. Reproducible particle size data for the carbons can be secured by measurements made on individual particles at ×200,000. Evidence for the crystalline nature of this carbon is rendered visible in the micrographs.

THE thin supporting film upon which electron microscope samples are mounted for examination in the instrument causes some scattering of the electrons. This scattering in the film results in lowered contrast and less than optimum resolution in the image. If it is possible to eliminate the supporting film in some cases and to mount the samples directly in the vacuum, the possible contrast and the practical resolution can be increased.[1] This is especially important when dealing with particularly minute particles of low atomic weight where the amount of scattering in the specimen itself may be of the same order as that in the film. This present discussion is the result of experiments designed to support such samples in free space. The methods have already proved useful in several problems and may suggest applications to others working with electron microscopes.

The first step in the method consists in supporting several fine fibers across the mouth of the usual electron microscope specimen holder. These can be cemented in place with rubber cement or metallic paint, or they can be held mechanically by the pressure of the cap. Fibrous materials which have been found useful for the purpose are glass, rubber, and asbestos. Glass wool fibers of a range of sizes down to one micron diameter are obtainable. Rubber fibers of even smaller diameter can be made by drawing out rubber cement.** The production of tough resinous fibers of cross-sectional diameter less than one micron may provide a source of the finest fibers usable in the mounting process here outlined.

The holder with the fibers attached is plugged into a rubber tube leading to the source of the fine particles which are to be mounted upon the fibers. The source material, which may be a dry powder, a suspension, or a true solution is atomized to form an aerosol which is drawn past the fiber by a suitable pumping arrangement. As the airborne particles go past, many of them are caught and a deposit, usually in a chain-like form, begins to build up. It is interesting to note that the 'new fibers' composed of the collected particles, themselves, act as very efficient and perhaps more efficient collectors than the original fibers. The obvious tendency of the particles mounted in this way to form chains can be seen

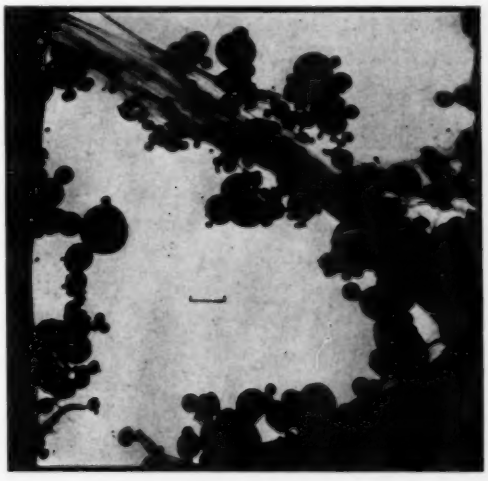

FIG. 1. Particles from a dispersion of methylene blue caught upon the fibers of a thin piece of lens paper. ×4,700 (University of Toronto).

* The method described was noted first when the author was with the electron microscope laboratory of the University of Toronto.

[1] James Hillier, A.S.T.M. Symposium on new methods for particle size determination in the subsieve range, p. 91 (1941).

** Dunlop rubber cement.

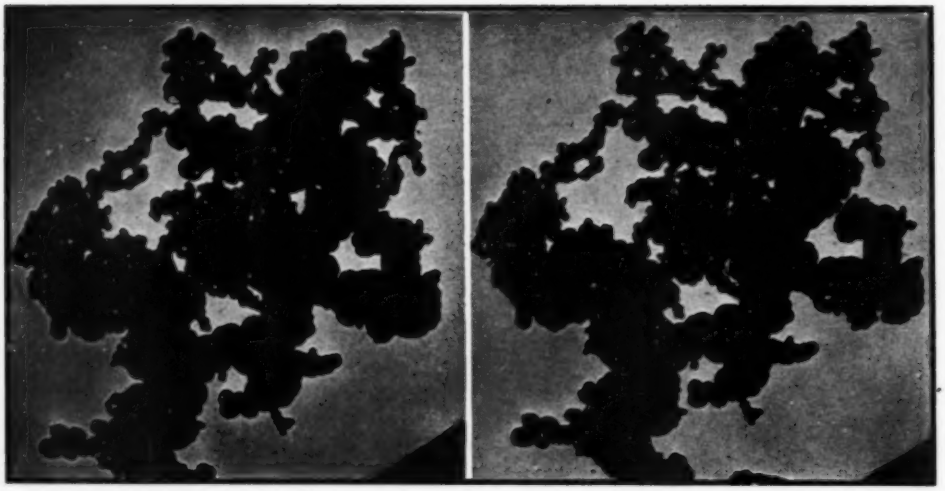

FIG. 2. A stereoscopic pair of a dispersion of Shawinigan carbon black supported in free space. ×22,000 (Shawinigan Chemicals Ltd.).

in Figs. 1 and 3. The speed past the fiber, the collecting period, and the size of the fiber affect the density of the deposit.

Many variations of this general method can be employed. The author has used thin lens paper (rice paper) for mounting particulate samples by drawing the aerosols through the paper, Fig. 1. The particles caught in the lens paper are of methylene blue which were atomized from a true solution in water. Thin asbestos paper will also serve.

The mounting obtained by the above methods has been found to be remarkably stable during mechanical handling if ordinary care is exercised and may be used for all electron microscope techniques without harmful effects to the specimen. Electrical charging of a specimen so supported is sometimes a problem. Usually, quite sufficient intensity and contrast for focusing can be achieved without any charge effect being noticed. If charge 'bulges' do appear, or if specimen deterioration does take place, a 200-mesh specimen screen (without a film) put either under or over the fibers before or after the mounting of the sample will dissipate the charge almost completely. It is wise in general to start with low beam and condenser current and to raise each carefully for focusing.

Much can be learned with this method of the actual way in which the particles build up the

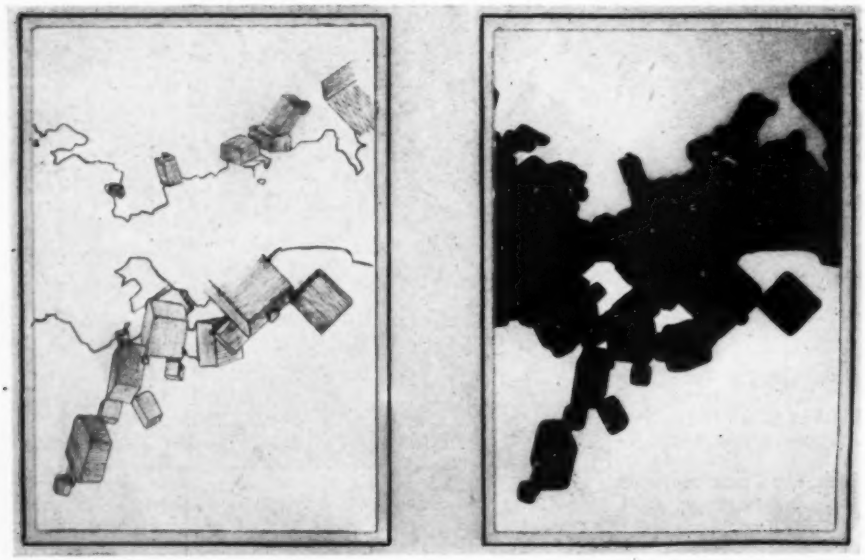

FIG. 3. Electron micrograph and diagrammatic representation of sodium chloride crystals caught upon a rubber fiber. ×2,300 (University of Toronto).

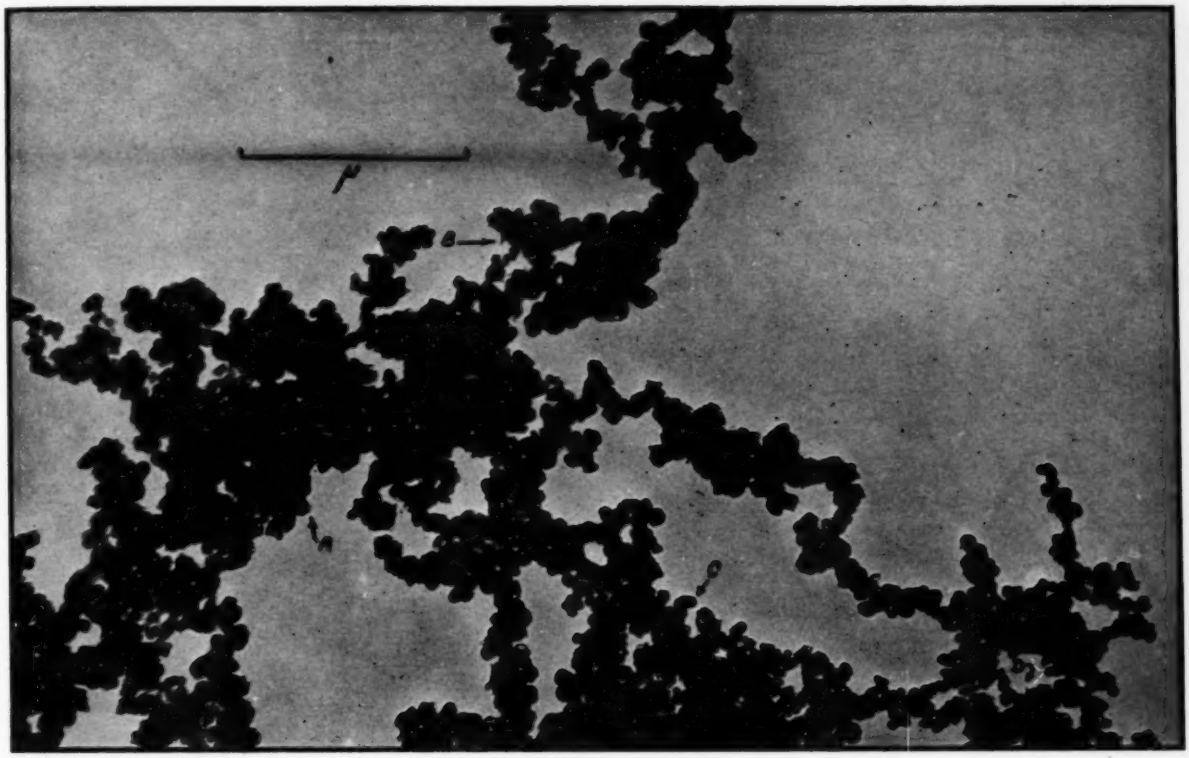

FIG. 4. Shawinigan carbon black. ×30,000 (Shawinigan Chemicals Ltd.).

one upon the other. The amount of depth in the object is much greater than that present in a sample mounted upon a film and excellent stereoscopic micrograph pairs can be obtained. Figure 2 is a stereoscopic view of carbon particles supported in free space. The tendency of the material to charge up electrically is useful for studying it three dimensionally, because different sections of the specimen can be made to move relatively to each other by slight variations of intensity. The structure of apparent aggregates can thus be studied visually at first hand on the screen of the microscope.

Figure 3 shows a deposit of small crystals of sodium chloride caught upon a rubber fiber; a diagrammatic representation is also shown of how these crystals when caught build up into a chain.[2]

THE USE OF THIS METHOD WITH COLLOIDAL CARBON SPECIMENS

Carbon micrographs often lack contrast and sufficient resolution. Indeed, the finer carbon blacks are extreme tests for the electron microscope. In order to achieve sufficient image contrast with them, it is often necessary to use an objective diaphragm. No diaphragm was used in obtaining any of the micrographs presented here. The Shawinigan carbon black has a well-known chain structure, a property important for its use in battery manufacture and in the production of thermally and electrically conductive rubbers. This structure is illustrated in Figs. 4 and 5. The chains are stretched out in space from the supporting fiber with contrast and resolution which allow a very accurate measure of particle size distribution to be made, where it might not otherwise be possible to do so. Of course only those particles projecting beyond the edge of the fiber can be counted. A sufficient number of particles can be counted in the chains, and those caught immediately at the fiber can be disregarded. It will be observed that both large and small particles are caught and there is little likelihood of sampling taking place. The plates are projected upon a screen at

[2] E. F. Burton, Nature **152**, 540 (1943).

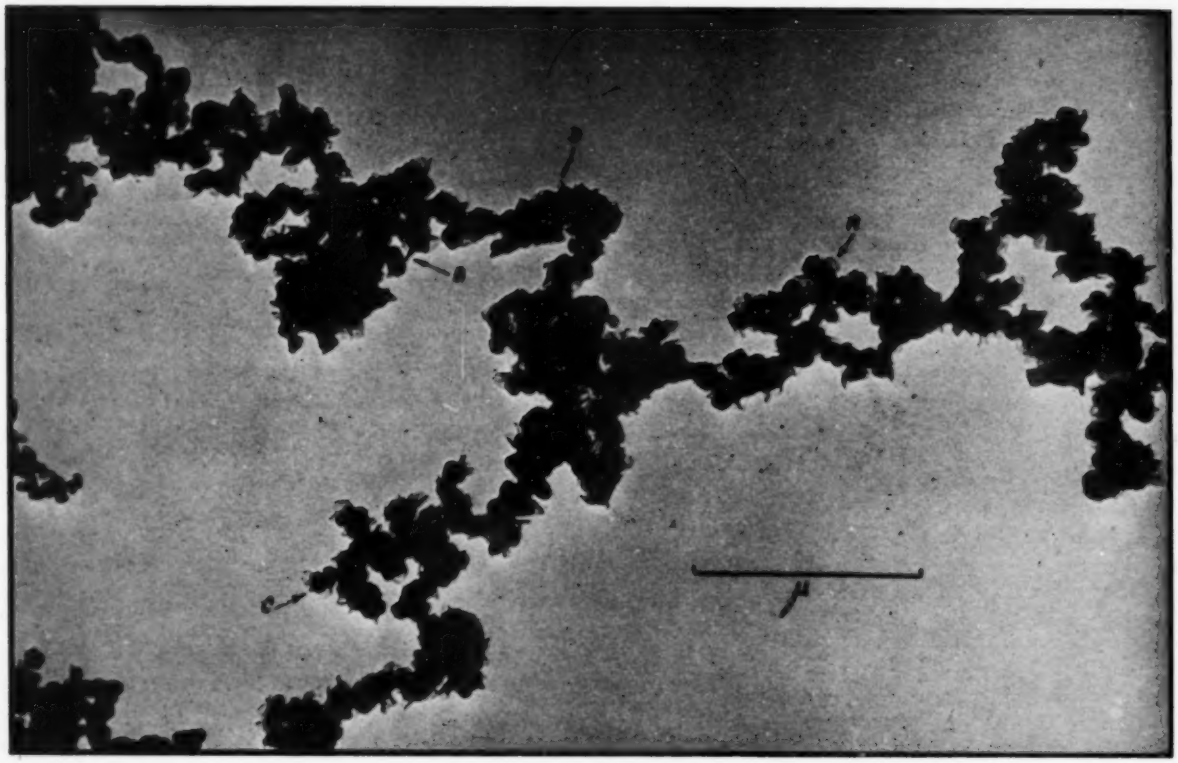

FIG. 5. Shawinigan carbon black. ×30,000 (Shawinigan Chemicals Ltd.).

×200,000, and the carbon particles are classified, as they are counted, into ranges of 50A. With the electron microscope, it is not feasible to count all the particles along the whole fiber but a number of fields give a satisfactory result. It has been found that ten good exposures taken at random of two preparations of the same sample give reproducible results for that sample.

Figures 4 and 5 are both micrographs of colloidal carbon black produced by the pyrolysis of acetylene. The most definite evidence for the crystalline nature of carbon black has come from x-ray and electron diffraction studies which have suggested that a single acetylene carbon black *particle* consists of a cluster of *pseudocrystals* (or parallel layer groups) some 40 to 50A in length and 20 to 30A in height, these in turn being composed of thin carbon *platelets* (or ultimate graphite layers) lying parallel to and equidistant from each other but randomly oriented about the perpendicular to their surfaces.[3]

[3] J. N. Mrgudich and R. C. Clock, Electrochem. Soc. 29, 329 (1944).

In these electron micrographs the crystalline nature of the carbon is made manifest. At locations *A* there are crystals which appear to be thin platelets, lying in a "flat" position, i.e., with their flat faces approximately perpendicular to the direction of the electron beam. At locations marked *B* the crystals appear to be "edge-on" to the beam. Over the micrographs positions of the crystals intermediate to these two extremes can be noted. Figures 6 and 7 are enlargements of portions of Figs. 4 and 5, respectively. Those few locations marked are representative of many such crystalline occurrences. The high chemical purity of the black leaves little doubt that these crystals are actually carbon.

The edge-on position provides an effectively thicker sample to scatter the electrons, and consequently the apparent "rods" in the micrographs have good contrast. In the flat position however the crystals offer much less scattering power and the contrast is less. From measurements made on the rods the crystal thicknesses are anywhere from 30 to 100A. Therefore the

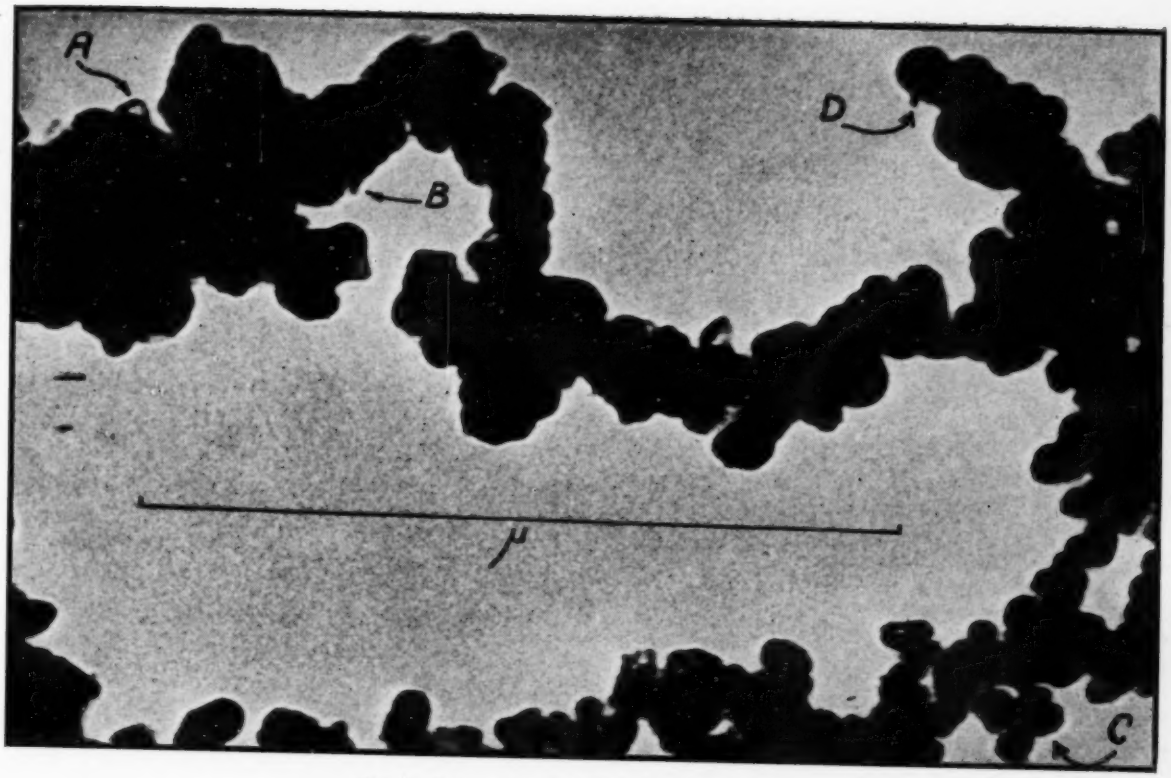

FIG. 6. Enlarged portion of Fig. 4. ×100,000.

FIG. 7. Enlarged portion of Fig. 5. ×100,000.

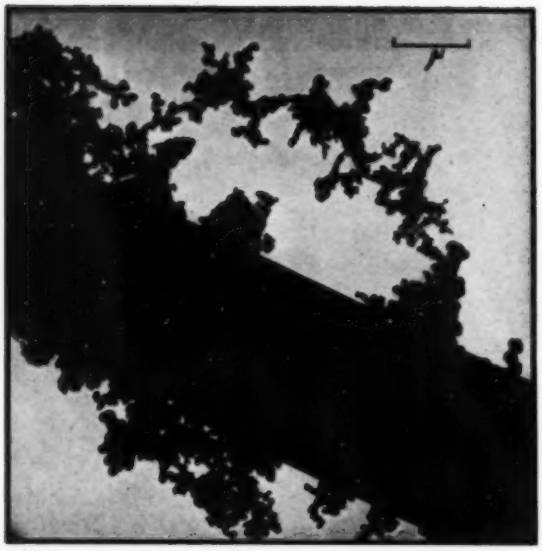

FIG. 8. Glass fiber supporting carbon black. ×10,000 (Shawinigan Chemicals Ltd.).

scattering in these thin crystals is probably of the same order or less than that in the usual thin collodion or Formvar film. Thus, if a specimen of the carbon were mounted upon a film in the usual way, the crystals in the flat position would be practically invisible for lack of contrast. In addition their corners would be rounded off sufficiently to appear as curves owing to lack of resolution. The crystalline appearance would accordingly be lost.

Several observations can be made on the appearance of the carbon specimen in the micrographs. The first is the occurrence of very thin crystal forms at *A* and *B* mentioned above. The second is the presence of much thicker particles than those at *A* or *B* which possess hexagonal shape as at *C*, and the fact that many of these thicker particles have straight-line rather than curve boundaries. Thirdly, it is to be observed that in general the particles have diverse shapes which appear to be oval or spherical as well as angular. As a fourth observation it is to be noted that many of the edge-on crystal formations present a curved appearance as at *D*. Fifthly the average longest dimension of the particles in this sample is about 500±25A, and in some cases their thickness may be as low as 30A.

In order to offer an explanation for the first observation it seems that a slight difference between the particle structure as observed here and that suggested by Biscoe and Warren[4] must be advanced. There may be piles of the carbon platelets which are oriented in a symmetric rather than a random fashion about the common perpendicular to the surfaces. This will not only be true of the thinnest particles as at *A* and *B* but will be true of thicker particles as at *C*.

To account for the second observation it is necessary to conclude that quite large, hexagonal carbon platelets (and consequently pseudo-crystals) can occur frequently. If the platelets are arranged symmetrically in the pseudo-crystal and one such pseudo-crystal makes up a particle, then the particle will appear to be hexagonal. On the other hand several such pseudo-crystals arranged at random would give a particle with random shape. This would explain the occurrence of straight-line edges on some of the particles and the general lack of definite particle shape. Lack of resolution would obscure many of these observations and the particles would appear to be spherical or oval. At times a thin pile of platelets projecting from the main mass can be noted and the crystalline nature recognized.

The fourth observation would suggest that the carbon scales piling up to form the pseudo-crystal do not always build up to the same depth over the whole surface. The resolution however is not such as to render the carbon "steps" visible, and a curved appearance results.

These observations tend to support the contentions of Schoon and Koch[5] and Von Otto Ruff.[6] They also follow to a large extent the conclusions of Biscoe and Warren and offer a picture of carbon particle structure which is more compatible with x-ray and electron diffraction evidence than the idea of carbon black as a pure sphere or oval.

This crystalline appearance has been noted so far only in *acetylene* carbon blacks and to the greatest extent in those produced by a method of thermal decomposition. The occurrence of this

---

[4] J. Biscoe and B. E. Warren, J. App. Phys. **13**, 364 (1942).

[5] Th. Schoon and H. W. Koch, Kautschuk (January, 1941).

[6] Von Otto Ruff, Zeits. f. Elektrochem. angew. physik. Chem. **44**, 333 (1938).

crystalline habit may account not only for the higher conductivity of the acetylene blacks but may be a factor also in the formation of their strong structure. However, it is to be noted here that all acetylene blacks, produced by different processes, do not have the same appearance in electron micrographs nor are they at all identical in other properties. Acetylene black as such has been compared with blacks formed from other raw products. Such comparisons have little meaning unless the method of preparation of the acetylene black is clearly specified.

It is hoped that this mounting technique or adaptations of it will prove useful in further investigations of this and other carbon blacks. The author is indebted to the Plant Research Department of the Shawinigan Chemicals Limited and to the Physics Department of the University of Toronto for permission to reproduce the micrographs.

Investigation of Secondary Phases in Alloys by Electron Diffraction and the Electron Microscope

R. D. Heidenreich,* L. Sturkey, and H. L. Woods
The Dow Chemical Company, Midland, Michigan

(Received October 15, 1945)

The application of electron diffraction reflection methods and the electron microscope to investigations of metallurgical structures is reported. It is shown that these instruments can yield valuable information concerning very small amounts of secondary phases and impurities in metals. Thus, for example, when martensite decomposes at 200°C, the slow etching component is highly dispersed Fe_3N. The decomposition at 400°C yields the usual Fe_3C. Further, the Fe_3N formed at 200°C transforms to Fe_3C when annealed at 350°C. Other examples are presented. The successful application of these instruments is dependent upon the production of clean, etched surfaces. Surface preparation is discussed and a satisfactory technique for rinsing etched surfaces is described. In some alloy systems, the etching reaction may result in the redeposition of a component onto the etched surface. In the case of a β-brass containing 0.0005–0.001 percent silver, the silver is deposited in the form of spherical particles about 1000A in diameter. Aluminum alloys appear to offer a serious problem in discovering satisfactory etchants due to the position of aluminum in the electromotive series relative to copper, silver, etc.

INTRODUCTION

THE physical and chemical properties of metallic alloys are well known to be in a large measure dependent upon the distribution and nature of a secondary constituent in the crystals of the base metal. The detection and identification of these secondary phases and structures is often difficult and tedious using x-ray and light microscopic methods and in many instances is nearly impossible when the concentration of such phases is very small.

In x-ray studies of alloys where information concerning precipitated phases is desired, the energy diffracted by the minor phase may constitute only a small fraction of that diffracted by the matrix crystals. If this precipitate is very highly dispersed or amounts to less than about 5 percent of the total diffracting material it may not contribute to the final pattern.

It has been found that by using the electron microscope and a refined electron diffraction reflection method in close conjunction, information concerning very small amounts of secondary phases and impurities can be readily obtained. If an alloy is etched so that the minor constituents are left protruding above the matrix crystals (provided no extraneous material is deposited on the surface), a very small amount of included material can yield a strong electron diffraction pattern without an interfering pattern of the matrix.

In the past, electron diffraction has been

* Now at Bell Telephone Laboratories, Inc., Murray Hill, New Jersey.

applied chiefly to studies of polishing and grinding and to the structure of corrosion films, etc. There is reason to believe that with suitable surface preparation methods, electron diffraction techniques may be of great value in investigations where a minor phase plays an important role.

The success of this method of investigation of metallurgical structures is dependent upon the production of clean, etched surfaces. The usual metallographic techniques result in surfaces that bear oxide or hydroxide films or reaction products remaining on the surface after etching.

The first part of this paper will be concerned with obtaining satisfactory surfaces while the remainder will deal with some of the results obtained with several alloys.

SURFACE PREPARATION

In preparing metal surfaces for combined investigation by electron diffraction and electron microscopy several considerations are of major importance:

(1) The removal of all distorted and fragmented metal in the surface layers produced during grinding and polishing.

(2) The reduction of the quantity of corrosion products remaining on the etched surface below the minimum necessary to produce appreciable electron scattering.

(3) Selectivity of the etchant for the various metallic constituents so that minor phases are left standing in relief on the surface.

The distortion of the surface regions by the usual metallographic preparations has been investigated by means of x-ray[1] and electron diffraction studies.[2] Electron microscope evidence[3] in the case of rocksalt is consistent with the assumption of fragmentation and of the formation of a polish or Beilby layer during mechanical polishing. Optical investigations[4] with polished copper likewise bear out these conclusions. In view of these phenomena it was concluded that mechanical grinding and polishing introduced grave complications in this type of investigation if sufficient metal were not removed chemically during etching. This objection is readily overcome by the use of electrolytic polishing methods.

As a result, the procedure consisted in abrading the metal specimens through 4/0 metallographic paper and then electrolytically polishing with no further mechanical disturbance. Electrolytes and conditions for most metals have been published.[5] Electrolytically polished surfaces often tend to be wavy and not very satisfactory for light microscopy. For electron microscopy, however, such surfaces are quite acceptable due to the great depth of focus of the electron microscope and the fact that the area of the field viewed is small compared to the ripples that may occur in the polished surface.

After polishing, the metal surface is etched by a selective chemical reagent. The type and rate of attack of a metal crystal are determined by several factors such as the reagent used, temperature, concentration, phases present, and the behavior of the reaction products. The deposition or adsorption of reaction products or of a specific material present in the reagent may greatly alter the type of attack.[6,7]

The most critical step in obtaining clean surfaces is that of immediate rinsing after removal of the specimen from the etching solution. A sequence of rinses has been worked out whereby the etching solution is finally displaced by an inert liquid without deposition of foreign materials. For several alloys, the following sequence yields clean surfaces after etching:

Etchant
↓
Rinse I — 50:50 methanol acetone with ½ to 1 percent formic acid
↓
Rinse II — Methanol-acetone
↓
Rinse III — Clean, dry benzene. Dry in blast of clean, warm air.

The success of the rinsing procedure for various metals depends upon the use of rinses in which

[1] H. C. Vacher, J. Research Nat. Bur. Stand. **29**, 177 (1942).
[2] G. P. Thomson and W. Cockrane, *Theory and Practice of Electron Diffraction* (The Macmillan Company, New York, 1939), Chap. XIII, see also, Reference 9.
[3] R. D. Heidenreich, J. Opt. Soc. Am. **35**, 139 (1945).
[4] H. Lowry, H. Wilkonson, and D. L. Smare, Phil. Mag. **22**, 769 (1936).
[5] For a review see O. Smeckal, Metal Progress, 729 (April, 1945).
[6] C. H. Desch, *Chemistry of Solids* (Cornell University Press, Ithaca, 1934), Chap. V.
[7] H. Mahl and I. N. Stranski, Zeits. f. physik. Chemie **51**, 319 (1942).

any metallic compounds formed are soluble and are hence not precipitated onto the surface. In all cases, clean, freshly distilled solvents should be employed.

The results are not independent of the etching reagent used. Reagents which stain the surfaces are to be avoided as well as those which tend to passivate or form insoluble films. For example, in the case of steel specimens, nitric acid is not satisfactory probably due to a thin film (amorphous) formed during etching which partially obscures the underlying metal and yields poor diffraction patterns. Ferric chloride in hydrochloric acid, on the other hand, gives excellent results.

It will be found that some alloy systems will require considerable investigation in order to discover the proper etching reagent since the common reagents may result in one or more of the constituents being dissolved and then redeposited on the surface in a different form.[8] This is particularly true of aluminum-copper alloys and impurities in several copper alloys as will be shown.

EXAMINATION OF SURFACES

The electron microscope examination of the etched surfaces was carried out using the polystyrene-silica replica method after electron diffraction reflection patterns had been obtained from the surfaces.[3] The necessity of employing a replica is a disadvantage but, nevertheless, the replicas and electron diffraction patterns make it possible to deduce considerable information concerning the surface structures. All micrographs were taken with an RCA, Type B electron microscope. The electron diffraction apparatus employed in this work had a 75-cm plate-specimen distance and a well-collimated, parallel incident beam of 40 kv electrons.

The relation between the electron diffraction patterns and the electron micrographs is of immediate interest. The diffraction patterns are determined by the crystal structure and orientation of those surface protuberances which exhibit a thickness normal to the incident beam sufficiently small to allow transmission. Thus, corners, edges, and thin peaks that can be seen in the electron micrographs are to be considered as possible diffracting regions of the surface. Figure 1 illustrates the approximate relation between the image and the diffraction pattern based on the topography of an etched surface.

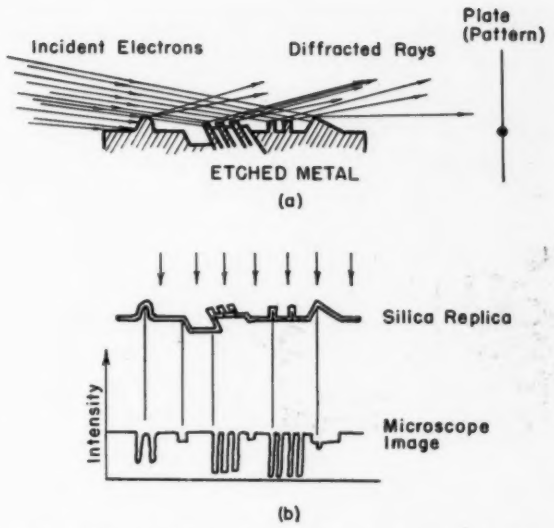

FIG. 1. Effect of surface contours on an electron diffraction reflection pattern (a) and electron microscope image of a surface replica (b). Only the diffracted beams are shown leaving the surface in (a).

The interpretation[9] of electron diffraction patterns which, on the basis of x-ray experience, would indicate preferred orientation is to be made with particular caution. In many cases, the crystallographic etch attack results in certain crystal faces having a topography such that they do not contribute to the diffraction pattern. This point has been discussed by Johnson and Gram[10] for etched tungsten and molybdenum and is thought by the authors to be a general consideration in the case of pure metals. Two-phase systems are not so likely to give difficulty.

EXAMPLES

Several alloy systems to which the surface preparation methods outlined have been applied will serve as examples of the kind of information that can be obtained. The illustrations each con-

[8] Cf. J. H. Hollomon and J. Wulff, Trans. A.I.M.E. **143**, 93 (1941).

[9] Cf. general discussion on "Structure of metallic coatings, films and surfaces," Trans. Faraday Soc. **31**, 1043 (1935).

[10] R. P. Johnson and W. R. Gram, Phys. Rev. **62**, 77 (1942).

FIG. 2. Electron micrograph and diffraction pattern from magnesium single crystal containing 1.5 percent manganese. The manganese particles are plate-shaped and are preferentially oriented in the magnesium crystal.

sist of an electron micrograph (silica replica) and sometimes an electron diffraction reflection pattern from the same surface. Reflection patterns are often difficult to reproduce so that the rings are easily visible. Measurements of the radii of the diffraction rings are made on the original negatives and in some instances tables of d_{hkl} values are included for comparison with x-ray standards. Identification is generally accomplished by such a comparison.

MAGNESIUM ALLOYS

Although this work was initiated by research with magnesium alloys, the etching methods and results will not be included here. The technique for magnesium is sufficiently unique and the results extensive enough to warrant a full paper devoted to this subject alone which will appear elsewhere. One example will suffice.

Figure 2 shows an electron micrograph and electron diffraction reflection pattern from an etched single crystal of magnesium containing 1.5 percent manganese. The manganese is in the form of plate-shaped particles precipitated along certain crystallographic planes* of the crystal. The individual particles cannot be resolved with a good light microscope and hence their shape and arrangement cannot be determined. The electron diffraction pattern in Fig. 2 is that for α-Mn with preferred orientation. The preferred orientation indicated by this pattern is not a result of preferential etching but is indicative of the relation between the particles and the matrix crystal.

STEEL

The results obtained with a plain carbon steel have been briefly reported.[11] They are of considerable interest and value both from a theoretical and practical viewpoint. The additional information obtainable by combined electron diffraction and electron microscope studies on properly prepared surfaces is clearly illustrated.

The steel employed in this series of heat treatments analyzed 0.9 percent C, 0.15 percent Si, and 0.0056 percent N for the major constituents. The surfaces were prepared by abrading through 4/0 metallographic paper, electrolytically polishing in sulfuric-phosphoric acids,[12] and then etching in a methanol solution containing 2 percent HCl and 1 percent $FeCl_3$. The etching times were 30 sec. for pearlitic structures and 60–90 sec. for martensitic specimens. The standard sequence of rinses enumerated in a previous section were employed. As stated, nitric acid etchants are not recommended and the use of picric acid is questionable.

The results for this steel when heat treated to produce fine pearlite are seen in Fig. 3.

The micrograph shows the usual lamellar structure and the electron diffraction pattern is that for polycrystalline, orthorhombic Fe_3C. The pattern for Fe_3C is to be expected since the

* The etched surface is the basal plane and the particles are oriented along the three principle directions.

[11] R. D. Heidenreich, L. Sturkey, and H. L. Woods, Nature (in press).

[12] R. I. Imboden and R. S. Sibley, Metal Finishing, 592 (November, 1942).

etchant attacks the α-Fe more rapidly, leaving the cementite lamellae standing in relief. For the sake of completeness, Table I lists the d_{hkl} values for Fe_3C compared with values obtained from measurements on the electron diffraction pattern.

The structure of pearlite is much better understood than is that of martensite and for that reason martensite is of greater interest here. Martensite is the body-centered tetragonal product obtained when austenite transforms at low temperatures and is produced by quenching the steel from 850°C into ice water. Martensite is quite unstable and decomposes at temperatures as low as 100°C. The decomposition products are of special interest since they apparently are dependent upon the temperature at which the reaction proceeds.[13] It was generally thought that decomposition below 300°C yielded a highly dispersed carbide phase, the particles of which were sufficiently strained by the stresses set up during precipitation that no satisfactory x-ray pattern could be obtained.[14] Above 300°C, the product was established to be Fe_3C by x-ray methods.

The surface of martensite, etched and rinsed as described, is seen in Fig. 4. The appearance

FIG. 3. Electron micrograph for fine pearlite in a 0.9 percent carbon steel etched in HCl—$FeCl_3$. Rockwell C.....29.

TABLE I. Comparison of electron diffraction results from sample of Fig. 3 with x-ray standard of Fe_3C.

	d-values		Relative intensities	
{*hkl*}	x-ray[a]	ED	x-ray	ED[b]
112	2.39	2.41	medium	
200	2.265		weak	
121	2.115		medium	
210	2.07		medium	
022	*2.04*	*2.08*	*strong*	very strong
211	1.98	1.99	medium	
113	*1.875*	*1.86*	*strong*	*strong*
212	1.766		weak	
004	1.69		weak	
221	1.645		very weak	
130	1.593	1.595	weak	
131	1.55		very weak	
114	1.512		weak	
311	1.415		weak	
231	1.335	1.34	medium	medium strong
015	1.31		very weak	
232	1.262		very weak	
140	1.23		medium	
313	1.22	1.22	medium	
233	1.165	1.16	*strong*	strong
142	1.156		strong	
400	1.133		strong	
006	1.127	1.125	strong	
331, 240	1.112	1.102	strong	
242	1.058		medium	
413	0.995		medium	
(150, 216)	0.987	0.980	strong	

[a] X-ray values taken from A. Westgren and G. Phragmen, J. Iron Steel Inst. **105**, 241 (1922).
[b] ED = Electron diffraction reflection.

seems to be consistent with the present theory of martensite formation.[15] The dark regions in the micrograph of Fig. 4 should appear down and are probably due to untransformed austenite. The diffraction pattern is not only weak, but the rings are broader and more diffuse than generally found by x-ray diffraction.[16] This can be taken to indicate a crystal with heterogeneous internal stresses exhibiting no sharply defined lattice spacings but, rather, *d*-values fluctuating about an average. (See Table II.)

When the specimen of Fig. 4 is annealed ½ hr. at 200°C, the martensite plates decompose into the colloidal mixture seen in Fig. 5. The slow-etching component is not Fe_3C as often assumed but is clearly identified with hexagonal Fe_3N from the reflection pattern. Table III lists the d_{hkl} values. Further heating for 4 hr. at 200°C does not change the appearance, diffraction pattern, or hardness.

[13] M. Arbusow and G. Kurdjumow, J. Phys. U.S.S.R. **5**, 2–3, 101 (1941).
[14] C. S. Barrett, *Structure of Metals* (McGraw-Hill Book Company, Inc., New York, 1943), p. 479 (further references will be found here).
[15] Reference 14, p. 483.
[16] E. Öhman, J. Iron Steel Inst. **123**, 445 (1931).

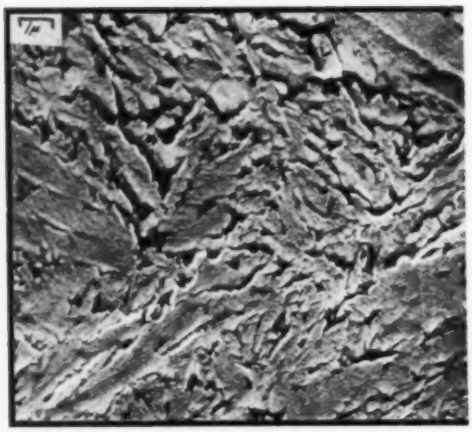

FIG. 4. Results on the same steel as Fig. 3 after heating at 850°C and quenching into ice water where the transformation austenite→martensite occurs. The diffraction pattern is weak and diffuse but is characteristic of martensite. Etched in HCl−$FeCl_3$. Rockwell C.....64.

TABLE II. Electron diffraction results from etched martensite compared with x-ray standard of α-Fe.

	d_{hkl}		Relative intensity	
(hkl)	x-ray	ED	x-ray	ED
110	2.01A	2.0–2.1A	40	Broad, diffuse rings
200	1.425	1.4–1.5	8	
211	1.164	1.1–1.2	15	
220	1.508		4	
310	0.902	0.9	2	
222	0.823		1	
321	0.763		3	
411	0.677		1	

* ED = Electron diffraction reflection.

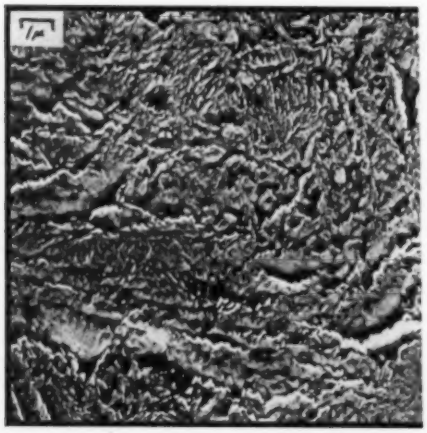

FIG. 5. Decomposition of martensite by annealing ½ hour at 200°C. The slow etching phase is Fe_3N (or isomorphous with Fe_3N). Etched in HCl−$FeCl_3$. Rockwell C.....58.

TABLE III. Electron diffraction results from sample of Fig. 5 compared with x-ray standard of Fe_3N.

	d_{hkl}		Relative intensity	
(hkl)	x-ray	ED*	x-ray	ED
020, 110	2.38A		8	
002	2.19	2.18A	10	Strong
111, 021	2.09	2.09	40	Very strong
112, 022	1.61	1.61	10	Strong
130, 200	1.375	1.38	10	Strong
	1.240	1.23	10	Strong
	1.160	1.157	8	Strong
	1.140		4	Weak
	1.095	1.10	1	Weak

* ED = Electron diffraction reflection.

The decomposition reaction at 200°C has been suggested[11] to be

$$\overbrace{Fe+C_{soln.}+N_{soln.}}^{\text{martensite}} \xrightarrow{200°C} Fe_3N+C_{soln.}$$

The nitrogen analysis gives some idea as to the small amount of the nitride phase that would be present. The greater part of the carbon must reside in α-Fe, probably as solid solution.

If the specimen of Fig. 4 is annealed ½ hr. at 400°C, the result is that of Fig. 6. A colloidal mixture is again produced but the slow etching component is now Fe_3C as ascertained by electron diffraction. When the specimen of Fig. 5 is further heated ½ hr. at 350°C, the patterns indicate that a mixture of Fe_3N and Fe_3C is produced. The appearance is illustrated in Fig. 7.

The decomposition reaction at 400°C is suggested to be

$$\overbrace{Fe+C_{soln.}+N_{soln.}}^{\text{martensite}} \xrightarrow{400°C} Fe_3C+N_{soln.}$$

Figure 7 indicates that the following reaction also may occur

$$Fe_3N+C_{soln.} \xrightarrow{350°C} Fe_3C+N_{soln.}$$

It appears from these preliminary results that the observations of Arbusow and Kurdjumow[13] are accounted for by the formation of Fe_3C above 300°C and the formation of Fe_3N below 300°C. The behavior of steel specimens from which the nitrogen has been thoroughly removed would be of great interest. The possibility of a

carbide phase isomorphous with Fe_3N should not be ignored.

The hardness of this series of specimens was determined and the values can be crudely correlated with the dimensions of the "particles" or "blocks" formed in the decomposition. The hardness is plotted against "block size" in Fig. 8 although caution should be used in drawing any general conclusions from the data. The result does seem to be consistent with the observations of Barrett[17] and may bear an interesting relation to W. L. Bragg's[18] theory of the strength of metals.

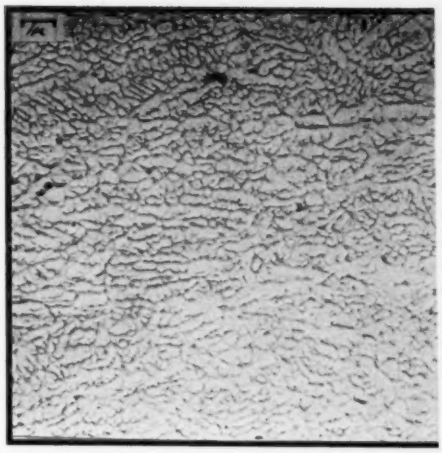

FIG. 7. Transformation of Fe_2N (formed by heating martensite ½ hour at 200°C) to Fe_3C by further heating ½ hour at 350°C. Etched in HCl—$FeCl_3$. Rockwell C.....52.

ALUMINUM ALLOYS

Preliminary experiments on the etching of an aluminum-copper alloy indicate that considerable work may be required in order to find a suitable etchant. Pure aluminum can be etched in hydrochloric acid and rinsed as with magnesium or steel and will yield good diffraction patterns for Al. An aluminum-copper alloy, however, when etched with the common reagents (HCl, HF, HNO_3, and mixtures) does not produce the desired result. In all cases the diffraction pattern obtained was that for polycrystalline copper with sometimes a trace of CuO. It seems likely that as both the aluminum and copper dissolved in the reagent the copper was redeposited as a result of the relative positions of the two metals in the electromotive series. This behavior produces a surface which may have little or no resemblance to the structure of the bulk metal and so makes the combined diffraction and microscopic technique of little value from a strictly metallurgical viewpoint. From the standpoint of corrosion studies and film formation, numerous experiments suggest themselves wherein information can be obtained using these methods.

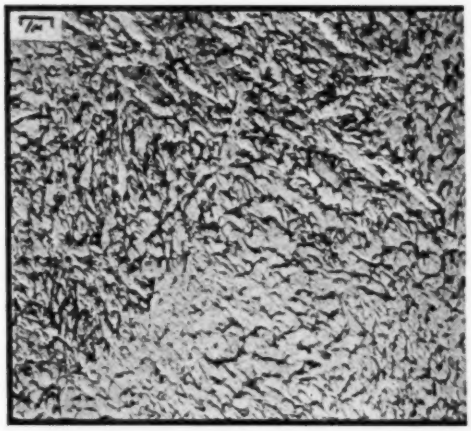

FIG. 6. Decomposition of martensite by annealing ½ hr. at 400°C. The slow etching phase is now the usual Fe_3C. Etched in HCl—$FeCl_3$. Rockwell C.....47.

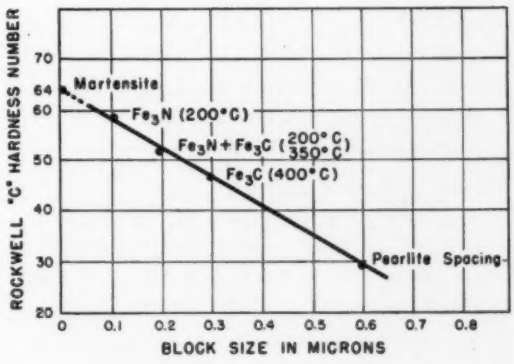

FIG. 8. Rough correlation between "particle" or "block" dimensions in heat treated steel with Rockwell C hardness values.

[17] C. S. Barrett, Metals Tech. **10** (Sept. 1943).
[18] W. L. Bragg, Nature **149**, 511 (1942).

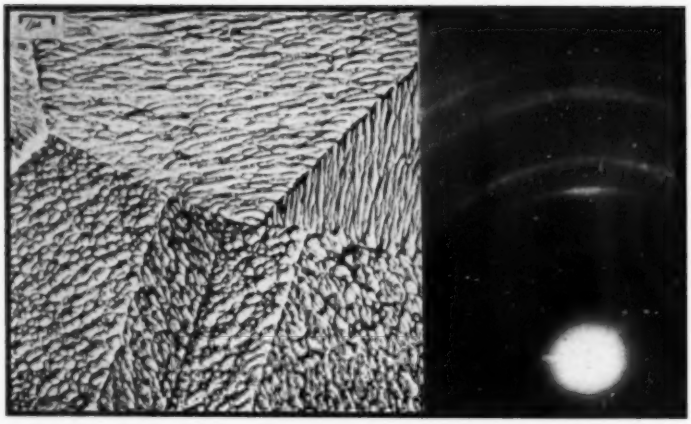

FIG. 9. Electron micrograph and diffraction pattern from commercial copper sheet etched in ammonium persulfate. The pattern is that for pure copper and exhibits arcing. The arcing is attributed to the etch attack rather than the orientation of the sheet.

COPPER ALLOYS

Inasmuch as the electron microscope and electron diffraction constitute sensitive techniques of investigating minute amounts of new phases, it would seem natural to apply them to studies of age-hardening alloys. Beryllium copper is an excellent example of an age-hardening alloy, and the work on copper was pointed toward an investigation of this system. Only the first experiments have been carried out, however.

There are several common etchants for copper and its alloys. Ammonium persulfate is satisfactory for pure copper and produces surfaces that yield strong diffraction patterns. The preparation for the commercial sheet shown in Fig. 9 consisted in electrolytically polishing in a phosphoric acid electrolyte, etching in a 10 percent solution of ammonium persulfate in distilled water, rinsing in distilled water and then through rinses I, II, and III. This surface is very rough on a micro-scale and for this reason possesses many sharp peaks that serve as diffracting centers. The reason for the etch structure of Fig. 9 has been briefly discussed by Barrett.[19] It would appear that the copper grains consist of a mosaic of rods about one micron long and a few tenths of a micron in diameter. It is evident that the orientation of the rods is related to specific directions in the copper crystal. The dimensions of the "etch blocks" are not independent of the etchant employed and therefore should be viewed cautiously until the matter has been well investigated.

The diffraction pattern of Fig. 9 shows the rings breaking into spots due to the grain size of the sample. In addition, there is arcing of the rings which was first thought to indicate preferred orientation as might be expected in rolled sheet. When this same sheet was deformed and cold

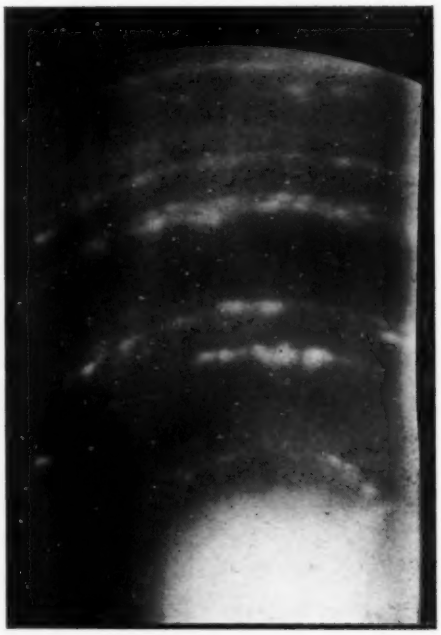

FIG. 10. Electron diffraction pattern of the same copper sheet as Fig. 9 after cold working and annealing. The grain size has increased but the arcing is still about the same as in Fig. 9.

[19] C. S. Barrett, *Structure of Metals* (McGraw-Hill Book Company, Inc., New York, 1943), p. 223.

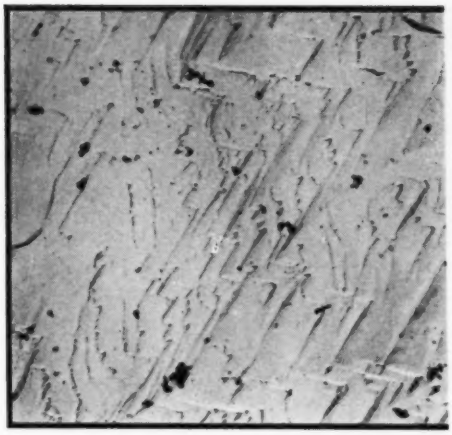

FIG. 11. Results for β-brass containing 0.0005–0.001 percent silver. The pattern obtained is that for polycrystalline silver, the particles of which can be seen in the micrograph as a result of being transferred to the silica replica. Etched in acetic-nitric reagent from which zinc displaces silver.

worked and then annealed, the pattern of Fig. 10 was obtained. The grain size has increased but the arcing is about the same as in Fig. 9. It appears that the etch attack is the chief factor in determining the arcing of the rings as previously discussed.

With certain reagents, metallic impurities in copper and brass may be deposited on the surface as shown by Holomon and Wulff.[8] An example of this is the β-brass of Fig. 11. This sample was electrolytically polished, etched in glacial acetic-nitric acids (5:2), rinsed in dilute ammonium hydroxide, distilled water, and then the usual rinses. This etchant was employed because it did not tend to stain the surfaces. The diffraction pattern from the etched surface was that for metallic silver, however. When the silica replica was examined it was found to be contaminated with black particles which had been transferred from the original surface to the replica. A spectroscopic analysis of the original sample indicated 0.0005 to 0.001 percent Ag from which it was concluded that, during etching, colloidal silver particles about 1000A in diameter had been deposited on the surface. A subsequent β-brass made from electrolytic copper and high purity zinc did not present this difficulty but gave a good pattern for body-centered brass. The transfer of foreign particles from a metal. surface to the silica replica has been observed many times.

The final example, beryllium copper, has not been subjected to a systematic investigation due to two difficulties. The first of these is the deposition of an impurity metal (less than 0.01 percent) during etching in the acetic-nitric reagent. This problem is not encountered in the use of ammonium persulfate but the type of etch structure makes it difficult to follow the aging process. The second difficulty has been the failure to produce a complete solid solution of beryllium in copper. A Cu-2 percent Be alloy was chill cast and then solution heat treated 100 hr. at 820°C and quenched.* The diffrac-

* Specimens $\frac{1}{2}$" in diameter and $\frac{3}{16}$" thick.

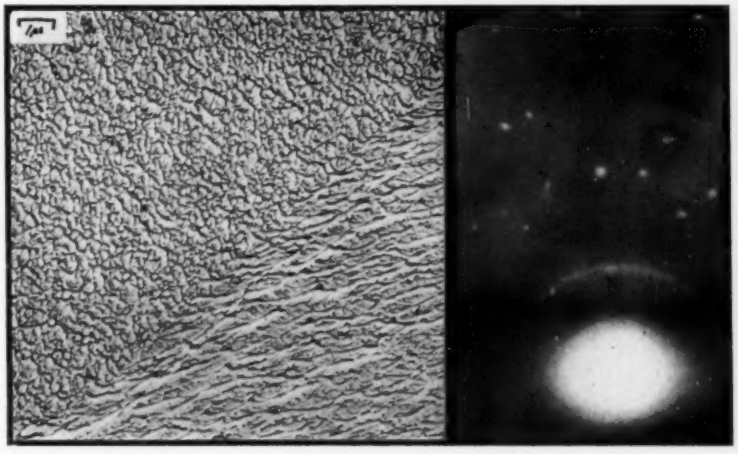

FIG. 12. Electron micrograph and diffraction pattern for beryllium copper (2 percent Be) quenched after 100 hours at 820°C. The spots are due to the copper solid solution while the rings are ascribed to both Cu and the intermetallic compound, CuBe, which has not entirely dissolved upon solution heat treatment. Etched in ammonium persulfate.

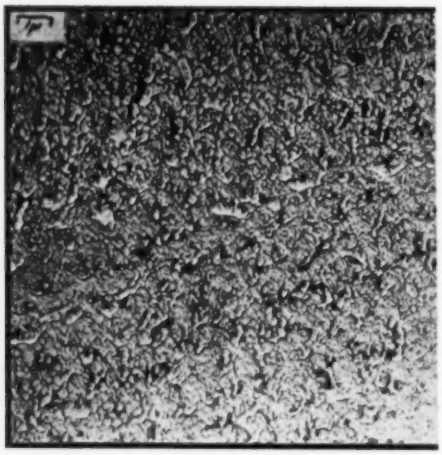

FIG. 13. Results for the same specimen as Fig. 12 after annealing 24 hours at 300°C. The compound is now densely precipitated and its diffraction pattern is that for CuBe with a trace of copper due to the matrix.

tion patterns from the surface etched with ammonium persulfate show not only the expected pattern (spots) for copper but also several rings due to the compound CuBe. Fig. 12 shows the micrograph and diffraction pattern.

If the specimen that yielded the results of Fig. 12 is aged 24 hr. at 300°C in order to heavily precipitate the compound, the result is that of Fig. 13. The particles of CuBe are evident in the micrograph. The pattern is that for polycrystalline CuBe with a trace of copper, as would be expected. The mechanism of age hardening[20] in this alloy cannot be studied, however, until a solid solution completely free of CuBe is attained. When such a solid solution is produced, a sequence of samples annealed for various lengths of time should yield some valuable information on which to base a theoretical study of age hardening.

---

[20] See, A. Guinier and P. Jacquet, Nature **155**, 695 (1945).